

# รายงานวิจัยฉบับสมบูรณ์

# โครงการ อิทธิพลของปัจจัยในกระบวนการเตรียมต่อการ เกิดเฟส โครงสร้างจุลภาคและสมบัติไดอิเล็กตริกของสาร เซรามิก PBZT-PMNT

โดย รองศาสตราจารย์ ดร. สุพล อนันตา

# รายงานวิจัยฉบับสมบูรณ์

โครงการ อิทธิพลของปัจจัยในกระบวนการเตรียมต่อการ เกิดเฟส โครงสร้างจุลภาคและสมบัติไดอิเล็กตริกของสาร เซรามิก PBZT-PMNT

> รองศาสตราจารย์ ดร. สุพล อนันตา ภาควิชาฟิสิกส์ คณะวิทยาศาสตร์ มหาวิทยาลัยเชียงใหม่

สนับสนุนโดยสำนักงานกองทุนสนับสนุนการวิจัย

(ความเห็นในรายงานนี้เป็นของผู้วิจัย สกว.ไม่จำเป็นต้องเห็นด้วยเสมอไป)

# กิตติกรรมประกาศ

ขอขอบพระคุณสำนักงานกองทุนสนับสนุนการวิจัย (สกว.) ที่ได้ให้โอกาส และ ให้การ สนับสนุนทุนวิจัยในครั้งนี้ ขอขอบคุณ ภาควิชาฟิสิกส์และบุคลากรห้องปฏิบัติการวิจัยอิเล็กโทร เซรามิกส์ คณะวิทยาศาสตร์ มหาวิทยาลัยเชียงใหม่ ที่อำนวยความสะดวกในการใช้เครื่องมือ อุปกรณ์ และสถานที่ รวมทั้งความช่วยเหลือต่างๆ ขอขอบคุณทีมงานผู้ร่วมวิจัยทุกท่าน ทั้ง คณาจารย์และนักศึกษา ที่มีส่วนสำคัญในการทำงานวิจัยโครงการนี้ จนทำให้สามารถผลิตผล งานวิจัยออกมาได้ดั่งใจอย่างต่อเนื่อง โดยเฉพาะอย่างยิ่ง ผู้ช่วยศาสตราจารย์ ดร. รัตติกร ยิ้มนิ รัญ ผู้ช่วยศาสตราจารย์ ดร. อภินภัส รุจิวัตร์ ดร. ยงยุทธ เหล่าศิริถาวร ดร. พิทักษ์ เหล่ารัตนกุล ดร. อรวรรณ อุดมพร ดร. รุ่งนภา ทิพากรฐิติกุล ดร. วรรณวิลัย ไชยสาร คุณเรวดี วงศ์มณีรุ่ง และคุณอรวรรณ คำมั่น สุดท้ายนี้ ขอขอบคุณ ละอองนวล ศรีสมบัติ พ่อแม่และน้องสาวสำหรับ ความรักความเข้าใจ รวมถึงกำลังใจที่มีให้ตลอดมา

(รศ.ดร. สุพล อนันตา) หัวหน้าโครงการฯ

# สารบาญ

	หน้า
ปกใน	1
กิตติกรรมประกาศ	2
Abstract	4
บทคัดย่อ	6
Executive Summary	8
Output ที่ได้จากโครงการ	9
ภาคผนวก	18

### **Abstract**

Project Code: RSA4680017

Project Title: Effect of Processing Parameter on the Phase Formation, Microstructure

and Dielectric Property of PBZT-PMNT Ceramics

Investigator: Assoc. Prof. Dr. Supon Ananta

E-mail Address: suponananta@yahoo.com

Project Period: 15 August 2003 to 14 August 2006

### Objectives:

Two major aspects (powder and ceramic processing) have been carried out in order to investigate the effect of processing parameter on the phase formation, microstructure and dielectric property of PBZT-PMNT ceramics.

### **Experimental procedures, Results and Discussion:**

(I) Powders in the PBZT-PMNT system have been synthesized by a solid-state reaction via a rapid vibro-milling technique. Selected compositions were prepared by using either conventional ball-milling or wet-chemical processing routes. Phase formation, morphology and particle size evolution of the calcined powders have been investigated as a function of calcination conditions. It has been found that the unreacted precursors and secondary phases tend to form together with the desired phase, depending on calcination conditions. The starting precursor, firing temperature and dwell time have been found to have a pronounced effect on the phase formation and morphology of the calcined powders. The milling time influences not only on the development of the solid-state reaction of the desired phase but also the particle size and morphology. Moreover, production of a single-phase nanopowder can be successfully achieved by employing a combination of appropriated milling time and calcination conditions.

(II) Ceramics in the PBZT-PMNT system have been fabricated by using conventional single-stage sintering method. Selected compositions were fabricated by employing a two-stage sintering method. Attention has been focused on relationships between chemical compositions, sintering conditions, phase formation, densification, microstructure and dielectric properties of the sintered products. It has been observed that conformable perovskite ceramics with high density were successfully fabricated by

means of carefully controlled processing parameters that include sintering temperature,

dwell time and heating/cooling rates. It is clear that PbO deficiency of these Pb-based

ceramics can result in an excessive amount of secondary phases which cause poor

densification and dielectric properties for the final product.

**Conclusions:** 

A combination of simple mixed oxide synthetic route and a rapid vibro-milling technique

has been developed for the production of single-phase powders in the PBZT-PMNT

system. Optimisation of processing parameters especially the calcination conditions and

the milling time can lead to single-phase powders of the desired compositions and

particle size range. This study clearly shows the influences of the processing parameters

on the variation of the phase formation characteristic, the microstructural evolution and

the dielectric properties of PBZT-PMNT ceramics. Under suitable two-stage sintering

conditions, the dense perovskite ceramics can be successfully achieved with better

dielectric properties than those of ceramics from a single-stage sintering technique.

Suggestion for further work:

(I) Further investigation is required for the control and optimization of the desired phase

formation. Studies on the effect of milling parameters and particle size distribution on

phase formation kinetics would be useful for the particle size control. In case of the

vibro-milling technique, other factors such as the milling speed, milling scale and type of

milling media also need be taken into account.

(II) Some improvement may be achieved by increasing the density of the samples in this

study by using higher technology such as sintering in oxygen atmosphere or hot isostatic

pressing. However, the costs of sophisticated processing and manufacturing would need

to be considered.

(III) Further work on the electrical characterization especially the piezoelectric and

electromechanical measurements of these materials would facilitate a deeper

understanding of perovskite ferroelectrics in general.

Keywords: Electroceramics, Vibro-milling, Calcination, Sintering, Dielectric properties

5

# บทคัดย่อ

รหัสโครงการ: RSA4680017

**ชื่อโครงการ:** อิทธิพลของปัจจัยในกระบวนการเตรียมต่อการเกิดเฟส โครงสร้างจุลภาคและ

สมบัติไดอิเล็กตริกของสารเซรามิก PBZT-PMNT ชื่อนักวิจัย: รองศาสตราจารย์ ดร. สุพล อนันตา

E-mail Address: suponananta@yahoo.com

ระยะเวลาโครงการ: 15 สิงหาคม 2546 ถึง 14 สิงหาคม 2549

# วัตถุประสงค์:

ทำการวิจัยในสองประเด็นหลัก (กระบวนการเตรียมผงและเซรามิก) เพื่อศึกษาถึงอิทธิพลของ ปัจจัยในกระบวนการเตรียมต่อการเกิดเฟส โครงสร้างจุลภาคและสมบัติไดอิเล็กตริกของสาร เซรามิก PBZT-PMNT

### วิธีทดลอง ผลการทดลองและวิจารณ์ผลการทดลอง

- (I) ทำการสังเคราะห์ผงสารในระบบ PBZT-PMNT ด้วยวิธี solid-state reaction โดยอาศัย เทคนิคการบดย่อยแบบสั่นกระแทกอย่างรวดเร็ว นอกจากนี้ยังได้เลือกทำการสังเคราะห์สารบาง สูตรโดยใช้เทคนิคการบดย่อยด้วยลูกบดแบบตั้งเดิมหรือไม่ก็ใช้เทคนิคการเตรียมทางเคมีแบบ เปียก ทำการตรวจสอบการก่อเกิดเฟส สัณฐานและการเปลี่ยนแปลงขนาดอนุภาคของผงที่ผ่าน การเผาแคลไซน์ด้วยเงื่อนไขต่างๆ ซึ่งจากผลการทดลองพบว่า มักจะมีสารตั้งต้นและสารแปลก ปลอมปะปนอยู่กับเฟสที่ต้องการทั้งนี้ขึ้นอยู่กับเงื่อนไขที่ใช้ในการเผาแคลไซน์ สารตั้งต้น อุณหภูมิที่ใช้เผาและระยะเวลาเผาแช่ล้วนแต่เป็นปัจจัยสำคัญที่มีอิทธิพลต่อการเกิดเฟสและ สัณฐานของผงที่ผ่านการเผาแคลไซน์ สำหรับระยะเวลาในการบดย่อยสารนั้น นอกจากจะมีผล ต่อกระบวนการเกิดปฏิกิริยาสถานะของแข็งของเฟสที่ต้องการแล้วก็ยังมีผลต่อขนาดอนุภาคและ สัณฐานของผงที่เตรียมได้อีกด้วย ยิ่งไปกว่านั้น ยังได้ค้นพบอีกว่าวิธีการเหล่านี้สามารถใช้ในการ เตรียมอนุภาคผงนาโนที่มีความบริสุทธิ์ได้ด้วย ถ้าหากว่ามีการเลือกใช้ระยะเวลาในการบดย่อย และเงื่อนใขในการเผาแคลไซน์ที่เหมาะสม
- (II) ทำการประดิษฐ์สารเซรามิกในระบบ PBZT-PMNT ด้วยวิธีการเผาซินเทอร์ครั้งเดียวแบบ ดั้งเดิม นอกจากนี้ยังได้เลือกทำการประดิษฐ์สารเซรามิกบางสูตรโดยใช้เทคนิคการเผาซินเทอร์ แบบสองขั้นตอน แล้วศึกษาความสัมพันธ์ระหว่างองค์ประกอบทางเคมี เงื่อนไขในการเผาซิน เทอร์ การก่อเกิดเฟส การแน่นตัว โครงสร้างจุลภาค และสมบัติไดอิเล็กตริกของผลิตภัณฑ์ที่ได้ จากการเผา ซึ่งจากผลการทดลองพบว่า สามารถทำการประดิษฐ์สารเซรามิกกลุ่มเพอรอพสไกด์ ที่มีความหนาแน่นสูงได้สำเร็จ ถ้าหากว่ามีการควบคุมเงื่อนไขในการเผาซินเทอร์เป็นอย่างดี โดย เฉพาะอย่างยิ่ง อุณหภูมิซินเทอร์ ระยะเวลาเผาแช่ และอัตราการขึ้นลงอุณหภูมิ เป็นที่ชัดเจนว่า

การสูญเสียออกไซด์ของตะกั่วในสารเซรามิกกลุ่มที่มีตะกั่วเป็นองค์ประกอบหลักเหล่านี้สามารถ ส่งผลทำให้มีเฟสแปลกปลอมเกิดขึ้นมาในระบบอย่างเด่นชัดซึ่งสิ่งเหล่านี้จะไปบั่นทอนพฤติ กรรมการแน่นตัวและสมบัติไดอิเล็กตริกของผลิตภัณฑ์ให้แย่ลง

### สรุปผล

โครงการวิจัยนี้ได้พัฒนากระบวนการเตรียมผงเฟสบริสุทธิ์ของสารสูตรต่างๆในระบบ PBZT-PMNT ขึ้นมาโดยอาศัยวิธีผสมผสานกระบวนการเตรียมสารแบบ mixed oxide อย่างง่ายๆเข้า กับเทคนิคการบดย่อยแบบสั่นกระแทกอย่างรวดเร็ว การเตรียมผงบริสุทธิ์ของสารที่มีองค์ ประกอบและช่วงขนาดอนุภาคตามต้องการนั้นสามารถกระทำได้โดยอาศัยวิธีการควบคุมปัจจัย ในกระบวนการเตรียมให้มีความเหมาะสม โดยเฉพาะอย่างยิ่ง เงื่อนไขในการเผาแคลไซน์และ ระยะเวลาในการบดย่อย ซึ่งโครงการนี้ได้แสดงให้เห็นถึงอิทธิพลของปัจจัยในกระบวนการเตรียม ที่มีต่อลักษณะเฉพาะของการก่อเกิดเฟส พัฒนาการของโครงสร้างจุลภาคและสมบัติไดอิเล็กตริก ของสารเซรามิกในระบบ PBZT-PMNT อย่างชัดเจน นอกจากนี้ยังได้คันพบวิธีการประดิษฐ์สาร เซรามิกกลุ่มเพอรอพสไกด์ที่มีความหนาแน่นสูงและมีสมบัติไดอิเล็กตริกดีกว่าเดิมโดยอาศัย เทคนิคการเผาซินเทอร์แบบสองขั้นตอนภายใต้เงื่อนไขที่เหมาะสม

### ข้อเสนอแนะสำหรับงานวิจัยในอนาคต

- (I) การศึกษาวิจัยเพื่อหาวิธีการควบคุมพฤติกรรมในการก่อเกิดเฟสของสารเหล่านี้ที่เหมาะสม เป็นสิ่งที่น่าสนใจมากสำหรับการวิจัยในอนาคต การศึกษาถึงอิทธิพลของปัจจัยในกระบวนการ บดย่อยและการกระจายตัวของขนาดอนุภาคที่มีต่อจลนศาสตร์ของการก่อเกิดเฟสน่าจะมี ประโยชน์ต่อการควบคุมขนาดอนุภาคของสารให้เป็นไปตามที่ต้องการได้ ซึ่งในกรณีของเทคนิค การบดย่อยแบบสั่นกระแทกนั้น ควรจะพิจารณาถึงปัจจัยอื่นๆเพิ่มเติมด้วย อาทิเช่น ความเร็วใน การบดย่อย ขนาดของชุดบดย่อย และชนิดของลูกบดที่ใช้ เป็นต้น
- (II) การปรับปรุงคุณภาพของชิ้นงานอาจกระทำได้โดยการเลือกใช้เทคโนโลยีที่สูงขึ้นในการเพิ่ม ความหนาแน่นของผลิตภัณฑ์ อย่างเช่น การเผาชิ้นงานภายใต้บรรยากาศของออกซิเจน หรือ การใช้เทคนิคการกดร้อนแบบความดันเท่ากันทุกทิศทาง แต่ก็ควรจะต้องพิจารณาถึงความ เหมาะสมของค่าใช้จ่ายในกระบวนการผลิตด้วยวิธีการเหล่านี้ด้วย
- (III) งานวิจัยในอนาคตที่มุ่งเน้นเรื่องการตรวจสอบสมบัติทางไฟฟ้าของวัสดุเหล่านี้ โดยเฉพาะ อย่างยิ่ง สมบัติทางพิโซอิเล็กตริกและสมบัติทางไฟฟ้าเชิงกล น่าจะช่วยเสริมสร้างความรู้ความ เข้าใจในเรื่องของสารเฟร์โรอิเล็กตริกกลุ่มเพอรอพสไกด์ให้มีความลึกซึ้งมากยิ่งขึ้น

**คำหลัก:** อิเล็กโทรเซรามิก, การบดย่อยแบบสั่นกระแทก, การเผาแคลไซน์, การเผาซินเทอร์, สมบัติไดอิเล็กตริก

### **Executive Summary**

ในโครงการวิจัยนี้ ผู้วิจัยได้ทำการศึกษาถึงอิทธิพลของปัจจัยต่าง ๆในกระบวนการผลิตที่ มีต่อพฤติกรรมการก่อเกิดเฟส โครงสร้างจุลภาคและสมบัติไดอิเล็กตริกของสารเซรามิกในระบบ PBZT-PMNT โดยสามารถสรุปเนื้อหาของงานวิจัยสองส่วนหลัก คือ การศึกษาถึงอิทธิพลของ ปัจจัยในขั้นตอนการเตรียมผงและในขั้นตอนการประดิษฐ์เซรามิก ได้ดังนี้

ในส่วนแรกนั้น ทางผู้วิจัยได้ดำเนินการศึกษาวิจัยถึงกระบวนการสังเคราะห์ผงสูตรต่างๆ ในระบบ PBZT-PMNT ได้แก่ PbTiO<sub>3</sub> (PT), BaTiO<sub>3</sub> (BT), PbZrO<sub>3</sub> (PZ), MgNb<sub>2</sub>O<sub>6</sub> (columbite-MN), Mg<sub>4</sub>Nb<sub>2</sub>O<sub>9</sub> (corundum-MN), Pb(Mg<sub>1/3</sub>Nb<sub>2/3</sub>)O<sub>3</sub> (PMN), Pb(Zr<sub>0.52</sub>Ti<sub>0.48</sub>)O<sub>3</sub> (PZT), PMN-PZT, PMN-PT, PZT-BT และ PBZT-PMNT ด้วยการใช้เทคนิค solid-state reaction ทั้งแบบดั้งเดิมและแบบดัดแปลง เป็นหลัก พร้อมทั้งทำการศึกษาความสัมพันธ์ระหว่าง ปัจจัยในกระบวนการเตรียม ได้แก่ สารตั้งต้น วิธีการบดย่อย ระยะเวลาในการบดย่อย อุณหภูมิที่ ใช้ในการเผา ระยะเวลาเผาแช่ อัตราการขึ้นและลงของอุณหภูมิ กับพฤติกรรมการก่อเกิดเฟส สัณฐาน การแจกแจงของขนาดอนุภาคผงที่ได้ ซึ่งจากผลการศึกษาวิจัยพบว่า สามารถทำการ พัฒนากระบวนการสังเคราะห์ผงสารสูตรต่างๆเหล่านี้ให้มีความบริสุทธิ์สูงได้เป็นผลสำเร็จด้วย การเลือกใช้เงื่อนไขในการเผาแคลไซน์ที่เหมาะสม และยังสามารถทำช้ำใหม่ได้ดีอย่างแม่นยำ นอกจากนี้ยังสามารถทำการพัฒนาเทคนิคการสังเคราะห์อนุภาคผงนาโนของสารเหล่านี้ใน ปริมาณมากๆโดยใช้เทคนิคการบดย่อยแบบสั่นกระแทกซึ่งมีทั้งความง่ายในการใช้งานและมีค่า ใช้จ่ายน้อยกว่าวิธีการแบบอื่นๆที่มีอยู่ในปัจจุบันได้เป็นผลสำเร็จอีกด้วย

สำหรับในส่วนที่สอง ทางผู้วิจัยได้ดำเนินการศึกษาวิจัยถึงกระบวนการประดิษฐ์สารเซรา มิกจากการใช้ผงสูตรต่าง ๆในระบบ PBZT-PMNT ที่เตรียมได้จากการศึกษาวิจัยในส่วนแรก ด้วย การใช้เทคนิคการเผาซินเทอร์แบบดั้งเดิมและแบบดัดแปลง พร้อมทั้งทำการศึกษาความสัมพันธ์ ระหว่างปัจจัยในกระบวนการเตรียม ได้แก่ อุณหภูมิที่ใช้ในการเผา ระยะเวลาเผาแช่ อัตราการ ขึ้นและลงของอุณหภูมิ กับพฤติกรรมการก่อเกิดเฟส การแน่นตัว โครงสร้างจุลภาค และสมบัติ ใดอิเล็กตริกของสารเซรามิกที่ได้ ซึ่งจากผลการศึกษาวิจัยพบว่า สามารถทำการพัฒนากระบวน การประดิษฐ์สารเซรามิกสูตรต่าง ๆเหล่านี้ให้มีความหนาแน่นและมีความบริสุทธิ์สูงได้เป็นผล สำเร็จ ด้วยการเลือกใช้เงื่อนไขในการเผาซินเทอร์ที่เหมาะสม และยังสามารถทำช้ำใหม่ได้ดี อย่างแม่นยำ ซึ่งสารเซรามิกเหล่านี้สามารถแสดงพฤติกรรมของความเป็นเฟร์โรอิเล็กตริก ที่มี สมบัติใดอิเล็กตริกเปลี่ยนแปลงไปตามปริมาณสัดส่วนขององค์ประกอบทางเคมี นอกจากนี้ยัง สามารถทำการพัฒนาเทคนิคการประดิษฐ์สารเซรามิกนาโนคอมโพสิตชนิดที่มีเกรนขนาดเล็กใน ระดับนาโนเมตรยึดเกาะอยู่กับเกรนขนาดปกติในระดับไมโครเมตร ของระบบ PBZT-PMNT ที่ สามารถแสดงสมบัติทางไฟฟ้าแตกต่างออกไปจากกรณีทั่ว ๆไปที่เป็นแบบ solid-solution ได้ด้วย การใช้เทคการเผาซินเทอร์แบบสองขั้นตอนที่พัฒนาขึ้นมาโดยผู้วิจัยเองได้เป็นผลสำเร็จ ซึ่งจะก่อ ให้เกิดความหลากหลายในการนำวัสดุเหล่านี้ไปประยุกต์ใช้งานต่อไป

# Output ที่ได้จากโครงการ

- 1. ผลงานตีพิมพ์ในวารสารวิชาการนานาชาติ จำนวนทั้งสิ้น 30 (+ 6) เรื่อง ได้แก่
- 1.1 ผลงานวิจัยที่ได้ตีพิมพ์เสร็จเรียบร้อยแล้ว 22 เรื่อง
  - (1) **S. Ananta**, "Synthesis, formation and characterization of Mg<sub>4</sub>Nb<sub>2</sub>O<sub>9</sub> powders," *Materials Letters*. 2004; **58**: 2530-2536. มี Impact factor 1.299
  - (2) **S. Ananta**, "Phase and morphology evolution of magnesium niobate powders synthesized by solid-state reaction," *Materials Letters*. 2004; **58**: 2781-2786. រឺរ Impact factor 1.299
  - (3) **S. Ananta**, "Effects of starting precursor and calcination condition on phase formation characteristics of Mg<sub>4</sub>Nb<sub>2</sub>O<sub>9</sub> powders," *Materials Letters*. 2004; **58**: 2834-2841. រីរ Impact factor 1.299
  - (4) R. Tipakontitikul and **S. Ananta**, "A modified two-stage mixed oxide synthetic route to lead zirconate titanate powders," *Materials Letters*. 2004; **58**: 449-454. រឹរ Impact factor 1.299
  - (5) L. Srisombat, S. Ananta and S. Phanichphant, "Chemical synthesis of magnesium niobate powders," Materials Letters. 2004; 58: 853-858. มี Impact factor 1.299
  - (6) A. Udomporn and **S. Ananta**, "The phase formation of lead titanate powders prepared by solid-state reaction," *Current Applied Physics*. 2004; **4**: 186-188. រឹl Impact factor 1.0
  - (7) A. Udomporn and **S. Ananta**, "Effect of calcination condition on phase formation and particle size of lead titanate powders synthesized by the solid-state reaction," *Materials Letters*. 2004; **58**: 1154-1159. រឺរ Impact factor 1.299
  - (8) A. Udomporn, K. Pengpat and S. Ananta, "Highly dense lead titanate ceramics from refined processing," Journal of The European Ceramic Society. 2004; 24: 185-188. มี Impact factor 1.567
  - (9) R. Yimnirun, **S. Ananta**, E. Meechoowas, S. Wongsaenmai, "Effects of uniaxial stress on dielectric properties of lead magnesium niobate-lead zirconate titanate ceramics," *Journal of Physics D: Applied Physics*. 2003; **36**: 1615-1619. រឺរ Impact factor 1.957
  - (10) R. Yimnirun, **S. Ananta** and P. Laoratanakul, "Effects of Pb(Mg<sub>1/3</sub>Nb<sub>2/3</sub>)O<sub>3</sub> mixed-oxide modification on dielectric properties of Pb(Zr<sub>0.52</sub>Ti<sub>0.48</sub>)O<sub>3</sub> ceramics," *Materials Science and Engineering B.* 2004; **112**: 79-86. 

    Impact factor 1.281

- (11) R. Yimnirun, **S. Ananta** and P. Laoratanakul, "Dielectric and ferroelectric properties of lead magnesium niobate-lead zirconate titanate ceramics prepared by mixed-oxide method," *Journal of The European Ceramic Society*. 2005; **25**: 3235-3242. J Impact factor 1.567
- (12) A. Rujiwatra, J. Jongphiphan and **S. Ananta**, "Stoichiometric synthesis of tetragonal phase pure lead titanate under mild chemical conditions employing NaOH and KOH," *Materials Letters*. 2005; **59**: 1871-1875. រឺ Impact factor 1.299
- (13) R. Yimnirun, **S. Ananta**, A. Ngamjarurojana and S. Wongsaenmai, "Uniaxial stress dependence of ferroelectric properties of xPMN-(1-x)PZT ceramic systems," *Applied Physics A: Materials Science & Processing*. 2005; **81**: 1227-1231. រឿ Impact factor 1.99
- (14) W. Chaisan, R. Yimnirun, **S. Ananta** and D.P. Cann, "Dielectric properties of solid solutions in the lead zirconate titanate-barium titanate system prepared by a modified mixed-oxide method," *Materials Letters*. 2005; **59**: 3732-3737. มี Impact factor 1.299
- (15) S. Wongsaenmai, Y. Laosiritaworn, **S. Ananta** and R. Yimnirun, "Improving ferroelectric properties of Pb(Zr<sub>0.44</sub>Ti<sub>0.56</sub>)O<sub>3</sub> ceramics by Pb(Mg<sub>1/3</sub>Nb<sub>2/3</sub>)O<sub>3</sub> addition," *Materials Science and Engineering B.* 2006; **128**: 83-88. រឺl Impact factor 1.281
- (16) A. Rujiwatra, N. Thammajak, T. Sarakonsri, R. Wongmaneerung and **S. Ananta**, "Influence of alkali reagents on phase formation and crystal morphology of hydrothermally derived lead titanate," *Journal of Crystal Growth*. 2006; **289**: 224-230. มี Impact factor 1.681
- (17) R. Wongmaneerung, R. Yimnirun and **S. Ananta**, "Effect of vibro-milling time on phase formation and particle size of lead titanate nanopowders," *Materials Letters*. 2006; **60**: 1447-1452. រឺ Impact factor 1.299
- (18) R. Yimnirun, S. Wongsaenmai, A. Ngamjarurojana and **S. Ananta**, "Effects of uniaxial stress on dielectric properties of ferroelectric ceramics," *Current Applied Physics* 2006; **6**: 520-524. มี Impact factor 1.0
- (19) R. Tipakontitikul, **S. Ananta** and R. Yimnirun, "Phase formation and transitions in the lead magnesium niobate-lead zirconate titanate system," *Current Applied Physics* 2006; **6**: 307-311. มี Impact factor 1.0
- (20) R. Yimnirun, R. Tipakontitikul, and **S. Ananta** "Effect of sintering temperature on densification and dielectric properties of Pb(Zr<sub>0.44</sub>Ti<sub>0.56</sub>)O<sub>3</sub> ceramics," *International Journal of Modern Physics B* 2006; **20**: 2415-2424. រឺl Impact factor 0.381

- (21) R. Wongmaneerung, R. Yimnirun and **S. Ananta**, "Effect of milling time and calcination condition on phase formation and particle size of lead titanate nanopowders prepared by vibro-milling," *Materials Letters* (2006); **60**: 2666-2671. มี Impact factor 1.299
- (22) R. Yimnirun, M. Unruan, Y. Laosiritaworn and **S. Ananta**, "Change of dielectric properties of ceramics in lead magnesium niobate-lead titanate system with compressive stress," *Journal of Physics D: Applied Physics* 2006; **39**: 3097-3102. 
  រីរ Impact factor 1.957

# 1.2 ผลงานวิจัยที่มีการตอบรับแล้วและอยู่ระหว่างการตีพิมพ์ 8 เรื่อง

- (1) R. Wongmaneerung, O. Khamman, R. Yimnirun and **S. Ananta**, "Fabrication of lead titanate ceramics by a two-stage sintering technique," *Journal of Electroceramics* (2006) *in press*. រីរ Impact factor 0.816
- (2) N. Triamnak, M. Unruan, S. Ananta and R. Yimnirun, "Effects of uniaxial stress on dielectric properties of 0.9PMN-0.1PT ceramics," Journal of Electroceramics (2006) in press. มี Impact factor 0.816
- (3) S. Wongsaenmai, O. Khamman, **S. Ananta** and R. Yimnirun, "Synthesis, formation and characterization of lead indium niobate-lead titanate powders," *Journal of Electroceramics* (2006) *in press*. រីរ Impact factor 0.816
- (4) A. Ngamjarurojana, O. Khamman, **S. Ananta** and R. Yimnirun, "Synthesis, formation and characterization of lead zinc niobate-lead zirconate titanate powders via a rapid vibro-milling method," *Journal of Electroceramics* (2006) *in press*. រីរ Impact factor 0.816
- (5) A. Rujiwatra, S. Tapala, S. Luachan, O. Khamman and **S. Ananta**, "One-pot hydrothermal synthesis of highly dispersed, phase-pure and stoichiometric lead zirconate," *Materials Letters* (2006) *in press*. រ្វី Impact factor 1.299
- (6) W. Chaisan, R. Yimnirun, **S. Ananta** and D.P. Cann, "Phase development and dielectric properties of (1-x)Pb(Zr<sub>0.52</sub>Ti<sub>0.48</sub>)O<sub>3</sub>-xBaTiO<sub>3</sub> ceramics," *Materials* Science and Engineering B (2006) in press. 

  il Impact factor 1.281
- (7) W. Chaisan, R. Yimnirun and **S. Ananta**, "Two-stage sintering of barium titanate ceramic and resulting characteristics," *Ferroelectrics* (2006) *in press*. រឹ Impact factor 0.459

(8) W. Chaisan, O. Khamman, R. Yimnirun and **S. Ananta**, "Effects of calcination condition on phase and morphology evolution of lead zirconate powders synthesized by solid-state reaction," *Journal of Materials Science* (2006) *in press*. มี Impact factor 0.901

# 1.3 ผลงานวิจัยที่ส่งออกไปเพื่อรับการพิจารณาตีพิมพ์ 6 เรื่อง

- (1) R. Yimnirun, M. Unruan, R. Wongmaneerung, O. Khamman, W. Chaisan and S. Ananta, "Dielectric properties of complex perovskite PZBT-PMNT ceramic under compressive stress," submitted to *International Journal of Modern Physics B.* រឹរ Impact factor 0.381
- (2) R. Yimnirun, **S. Ananta**, and S. Chamunglap, "Dielectric properties of (*1-x*)PZT-*x*BT ceramics under uniaxial compressive pre-stress," submitted to *Materials Chemistry and Physics*. 

  □ Impact factor 1.136
- (3) R. Wongmaneerung, R. Yimnirun and **S. Ananta**, "Effects of sintering condition on phase formation, microstructure and dielectric properties of lead titanate ceramics," submitted to *Applied Physics A.* រឺ Impact factor 1.99
- (4) O. Khamman, R. Yimnirun and **S. Ananta**, "Effect of vibro-milling time on phase formation and particle size of lead zirconate nanopowders," submitted to *Materials Letters*. រីរ Impact factor 1.299
- (5) R. Yimnirun, Y. Laosiritaworn, S. Wongsaenmai and **S. Ananta**, "Scaling behavior of dynamic hysteresis in soft PZT bulk ceramics," submitted to *Applied Physics Letters*. រ្ Impact factor 4.127
- (6) R. Yimnirun, S. Wongsaenmai, **S. Ananta** and Y. Laosiritaworn, "Stress-dependent scaling behavior of dynamic hysteresis in soft PZT bulk ceramics," submitted to *Journal of Applied Physics*. រ្វី Impact factor 2.498

### 2. การนำผลงานวิจัยไปใช้ประโยชน์

### 2.1 เชิงพาณิชย์

โครงการวิจัยนี้ได้สร้างองค์ความรู้ใหม่ในการสังเคราะห์สารเฟร์โรอิเล็กตริกสูตรใหม่ ๆ และได้พัฒนาเทคนิคการผลิตอนุภาคผงนาโนและสารเซรามิกเฟร์โรอิเล็กตริกแบบต้นทุนต่ำ ซึ่ง สามารถนำไปประยุกต์ใช้ในการต่อยอดงานวิจัยในสาขาอื่น ๆที่เกี่ยวข้องและการผลิตในเชิงอุต สาหกรรม นอกจากนี้ ยังเป็นการผลิตวัสดุเฟร์โรอิเล็กตริกที่มีราคาแพงใช้เองในกลุ่มวิจัยช่วยลด การนำเข้าจากต่างประเทศได้อีกทางหนึ่ง

### 2.2 เชิงนโยบาย

ผลการวิจัยที่ได้จากโครงการนี้ได้ถูกนำไปใช้ในการวางแผนเพื่อกำหนดแผนและทิศทาง การวิจัยแบบต่อยอดของทีมผู้ร่วมวิจัย เพื่อขอรับทุนจากแหล่งต่างๆ อย่างต่อเนื่อง และยังใช้เป็น หลักในการกำหนดหัวข้อวิจัยของนักศึกษาในระดับชั้นต่างๆ ซึ่งเป็นการส่งเสริมให้เกิดกลุ่มวิจัย แบบมีทิศทางมากขึ้น

### 2.3 เชิงสาธารณะ

โครงการวิจัยนี้ได้ก่อให้เกิดเครือข่ายความร่วมมือในการวิจัยระหว่างนักวิจัยทั้งในและ นอกประเทศ อาทิเช่น กับ ผศ. ดร. รัตติกร ยิ้มนิรัญ และ ดร. ยงยุทธ เหล่าศิริถาวร สังกัดภาค วิชาฟิสิกส์ คณะวิทยาศาสตร์ มหาวิทยาลัยเชียงใหม่ ในการศึกษาสมบัติทางไฟฟ้าร่วมกับการ ศึกษากลไกทางเทอร์โมไดนามิกส์ของกระบวนการ solid-state reaction ความร่วมมือกับผศ. ดร. อภินภัส รุจิวัตร์ และ ดร. ฐปนีย์ สาครศรี สังกัดภาควิชาเคมี คณะวิทยาศาสตร์ มหาวิทยาลัยเชียงใหม่ ในการศึกษาการสังเคราะห์สารโดยใช้เทคนิคไฮโดรเทอร์มอล การ วิเคราะห์โครงสร้างเฟสด้วยเทคนิคจุลทรรศน์อิเล็กตรอน นอกจากนี้ยังมีความร่วมมือกับนักวิจัย ในต่างประเทศ คือ Prof. David Cann และ Prof. Xiaoli Tan แห่ง Iowa State University Prof. Kenji Uchino และ Prof. A.S. Bhalla แห่ง Pennsylvania State University สหรัฐอเมริกา

# 2.4 เชิงวิชาการ (พัฒนาการเรียนการสอน/สร้างนักวิจัยใหม่)

ผลงานที่ได้ถูกนำไปใช้ประกอบการเรียนการสอนในกระบวนวิชาวัสดุศาสตร์ เช่น MATS 210743 Electroceramics, MATS 210741 Physics of Advanced Ceramics, MATS 210701 Characterization and Properties of Materials และ MATS 210703 Fabrication Processes of Materials นอกจากประโยชน์โดยตรงที่เกิดกับการสร้างทีมของผู้วิจัยเองแล้ว โครงการนี้ยังมีส่วนสำคัญในการฝึกฝน ทักษะ ประสบการณ์ในการทำวิจัยและเผยแพร่ผลงานให้ กับนักศึกษา ในฐานะผู้ช่วยวิจัยร่วมกับหัวหน้าโครงการ และผลงานวิจัยที่ได้ก็สามารถนำไปดี พิมพ์เผยแพร่ในวารสารทางวิชาการทั้งในและต่างประเทศ รวมทั้งการนำเสนอผลงานในที่ ประชุมทางวิชาการระดับต่างๆ ซึ่งยังผลให้เกิดมีดุษฎีบัณฑิตสาขาวัสดุศาสตร์และการพัฒนานัก วิจัยรุ่นใหม่ขึ้นมาเป็นจำนวนมาก

# 3. อื่น ๆ (ผลงานตีพิมพ์ในวารสารวิชาการในประเทศ การเสนอผลงานในที่ประชุม วิชาการ หนังสือ การจดสิทธิบัตร)

# 3.1 ผลงานตีพิมพ์ในวารสารวิชาการในประเทศ จำนวนทั้งสิ้น 19 เรื่อง คือ

- (1) **S. Ananta**, "Effect of calcination condition on phase formation characteristic of magnesium niobate powders synthesized by the solid-state reaction," *Chiang Mai University Journal*. 2003; **2(2)**: 79-87.
- (2) S. Wongsaenmai, **S. Ananta**, E. Meechoowas and R. Yimnirun, "Uniaxial stress dependence of dielectric properties of poled ceramics in lead magnesium niobate-lead zirconate titanate system," *Chiang Mai Journal of Science*. 2003; **30(2)**: 81-93.
- (3) S. Wongsaenmai, **S. Ananta** and R. Yimnirun, "Effects of uniaxial stress on dielectric properties of ceramics in PMN-PZT system," *Songkhanakarin Journal of Science and Technology*, 2003, **25(5)**, 629-636.
- (4) S. Wongsaenmai, **S. Ananta** and R. Yimnirun, "Effects of uniaxial stress on dielectric properties of lead zirconate titanate ceramics," *Suranaree Journal of Science and Technology*, 2003, **10**, 206-209.
- (5) S. Wongsaenmai, **S. Ananta** and R. Yimnirun, "Effects of uniaxial stress on dielectric properties of unpoled ceramics in PMN-PZT system," *Journal of Science Khon Kaen University*, 2003, **31(2)**, 73-84.
- (6) S. Wongsaenmai, **S. Ananta**, E. Meechoowas and R. Yimnirun, "Uniaxial stress dependence of dielectric properties of poled ceramics in lead magnesium niobate-lead zirconate titanate system," *Chiang Mai Journal of Science*, 2003, **30(2)**, 81-93.
- (7) S. Wongsaenmai, P. Moonrat, T. Silawongsawat, **S. Ananta** and R. Yimnirun, "Study of hysteresis properties of lead zirconate titanate (PZT) ceramic by sawyer-tower circuit," *Naresuan University Journal*, 2003, **11(3)**, 21-27.
- (8) S. Wongsaenmai, **S. Ananta** and R. Yimnirun, "Dielectric properties of unpoled lead magnesium niobate-lead zirconate titanate ceramics under uniaxial stress," *Chiang Mai Journal of Science*. 2004; **31(1)**: 11-15.
- (9) R. Yimnirun, E. Meechoowas, **S. Ananta** and T. Tunkasiri, "Mechanical Properties of *x*PMN-(*1-x*)PZT Ceramic Systems," *Chiang Mai University Journal*, 2004, **3(2)**, 147-154.

- (10) R. Yimnirun, **S. Ananta** and P. Laoratanakul, "Ferroelectric properties of ceramics in lead zirconate titanate-lead magnesium niobate system," *Chiang Mai University Journal*, 2004, **3(1)**, 53-58.
- (11) R. Yimnirun, **S. Ananta** and P. Laoratanakul, "Dielectric properties in lead zirconate titanate-lead magnesium niobate system," *Songkhanakarin Journal of Science and Technology*, 2004, **26(4)**, 529-536.
- (12)A. Ngamjarurojana, S. Wongsaenmai, R. Tipakontitikul, **S. Ananta** and R. Yimnirun, "Effect of uniaxial stress on hysteresis properties of 0.1PMN-0.9PZT ceramic," *Chiang Mai University Journal*, 2005, **4(2)**, 129-135.
- (13) R. Tipakontitikul, **S. Ananta** and R. Yimnirun, "Effect of sintering conditions on densification and dielectric properties of PZT ceramics," *Chiang Mai Journal of Science* 2005; **32(3)**: 323-329.
- (14) S. Chamunglap, **S. Ananta** and R. Yimnirun, "Uniaxial stress dependence of dielectric properties of PZT and 0.95PZT-0.05BT ceramics," *Chiang Mai Journal of Science* 2005; **32(3)**: 337-342.
- (15) S. Wongsaenmai, A. Ngamjarurojana, R. Tipakontitikul, **S. Ananta** and R. Yimnirun, "Hysteresis properties of 0.1PMN-0.9PZT ceramic under different poling fields," *Chiang Mai Journal of Science* 2005; **32(3)**: 351-354.
- (16) A. Ngamjarurojana, S. Wongsaenmai, O. Khamman, **S. Ananta** and R. Yimnirun, "Hysteresis properties of lead zirconate titanate ceramic under uniaxial compressive pre-stress," *Chiang Mai Journal of Science* 2005; **32(3)**: 355-359.
- (17) R. Wongmaneerung, R. Yimnirun and **S. Ananta**, "Synthesis and characterizations of lead titanate nano-sized powders prepared via a rapid vibro-milling," *Chiang Mai Journal of Science* 2005; **32(3)**: 399-404.
- (18) R. Wongmaneerung, R. Yimnirun, **S. Ananta** and Y. Laosiritaworn, "Monte Carlo simulations of nano-powders from mechanical milling," *Chiang Mai University Journal* 2005; **4(1)**: 169-175.
- (19) S. Wongsaenmai, A. Ngamjarurojana, R. Tipakontitikul, **S. Ananta** and R. Yimnirun, "Effect of poling conditions on hysteresis properties of lead magnesium niobate-lead zirconate titanate ceramics," *Naresuan University Journal*, 2006, **2(2)**: 131-138.

# 3.2 การเสนอผลงานในที่ประชุมวิชาการนานาชาติ จำนวนทั้งสิ้น 15 เรื่อง คือ

- (1) R. Yimnirun, P. Laorattanakul, and **S. Ananta**, "Synthesis and dielectric properties of lead magnesium niobate-lead zirconate titanate solid solutions", presented at the 2<sup>nd</sup> International Conference on Materials for Advanced Technologies 2003 (ICMAT-2003), December 7-12, 2003, Singapore
- (2) S. Wongsaenmai, **S. Ananta** and R. Yimnirun, "Effect of uniaxial stress on dielectric properties of lead zirconate titanate-lead magnesium niobate ceramics", presented at the 2<sup>nd</sup> International Conference on Materials for Advanced Technologies 2003 (ICMAT-2003), December 7-12, 2003, Singapore
- (3) A. Ngamjarurojana, S. Wongsaenmai, S. Ananta, D. Cann, X. Tan and R. Yimnirun, "Dielectric properties of lead zirconate titanate-lead magnesium niobate ceramics under uniaxial stress", presented at the 106<sup>th</sup> Annual Meeting of the American Ceramics Society (ACERS-2004), April 18-21, 2004, Indianapolis, USA
- (4) W. Chaisan, R. Yimnirun, D. Cann, X. Tan and S. Ananta, "Relationships between compositions and mechanical properties of lead zirconate titanate-barium titanate ceramics," presented at the 106<sup>th</sup> Annual Meeting & Exposition of the American Ceramic Society, 1-3 April 2004, Indianapolis, USA.
- (5) R. Tipakontitikul, **S. Ananta** and R. Yimnirun, "Effect of sintering conditions on densification and dielectric properties of PZT ceramics," presented at *the International Conference on Smart Materials (SmartMat-* '04), 1-3 December 2004, Chiang Mai, Thailand.
- (6) A. Ngamjarurojana, S. Wongsaenmai, R. Tipakontitikul, S. Ananta and R. Yimnirun, "Effect of uniaxial stress on hysteresis properties of 0.1PMN-0.9PZT ceramic," presented at the International Conference on Smart Materials (SmartMat-'04), 1-3 December 2004, Chiang Mai, Thailand.
- (7) R. Wongmaneerung, R. Yimnirun and S. Ananta, "Synthesis and characterizations of lead titanate nano-sized powders prepared via a rapid vibro-milling," presented at *the International Conference on Smart Materials (SmartMat-'04)*, 1-3 December 2004, Chiang Mai, Thailand.

- (8) **S. Ananta**, R. Tipakontitikul and R. Yimnirun, "Phase formation and transitions in the lead magnesium niobate-lead zirconate titanate system," presented at the 2<sup>nd</sup> International Conference on Advanced Materials and Nanotechnology (AMN-2), 6-11 Feb. 2005, Queenstown, New Zealand.
- (9) R. Yimnirun, S. Wongsaenmai, A. Ngamjarurojana and S. Ananta, "Effect of uniaxial stress on dielectric properties of ferroelectric ceramics," presented at the 2<sup>nd</sup> International Conference on Advanced Materials and Nanotechnology (AMN-2), 6-11 Feb. 2005, Queenstown, New Zealand.
- (10) S. Chamunglap, S. Ananta and R. Yimnirun, "Dielectric properties of lead zirconate titanate-barium titanate ceramics under uniaxial stress," presented at the 4<sup>th</sup> Asian Meeting on Electroceramics (AMEC-4), 27-30 June 2005, Hangzhou, China.
- (11) N. Thammajak, T. Sarakonsri, **S. Ananta** and A. Rujiwatra, "Influences of alkali reagents on phase-purity and crystal morphology of lead titanate synthesized under mild hydrothermal conditions", presented at *the 11*<sup>th</sup> Asian Chemical Congress (ACC), 24-26 August 2005, Seoul, Korea.
- (12) W. Chaisan, R. Yimnirun and **S. Ananta**, "Synthesis, dielectric and ferroelectric characteristics of barium titanate ceramics prepared by a solid-state reaction," presented at *the KMITL International Conference on Science and Applied Science*, 8-10 March 2006, Bangkok, Thailand.
- (13) W. Chaisan, R. Yimnirun and **S. Ananta**, "Fabrication, microstructural characterization and electrical properties of PZT-BT nanocomposites," presented at *the International Symposium on the Applications of Ferroelectrics (ISAF)*, 29 July-2 August 2006, North Carolina, USA.
- (14) R. Wongmaneerung, R. Guo, A. Bhalla, R. Yimnirun and **S. Ananta**, "Effect of sintering temperature on dielectric properties of PbTiO<sub>3</sub> ceramics," presented at *the International Symposium on the Applications* of Ferroelectrics (ISAF), 29 July-2 August 2006, North Carolina, USA.
- (15) R. Yimnirun, Y. Laosiritaworn, **S. Ananta** and S. Wongsaenmai, "Uniaxial stress dependence and scaling behavior of dynamic hysteresis response in soft PZT ceramics" presented at *the International Symposium* on the Applications of Ferroelectrics (ISAF), 29 July-2 August 2006, North Carolina, USA.

### ภาคผนวก ก

# **Reprints & Menuscripts**

(Part I: Powders in the PBZT-PMNT System)







materials letters

Materials Letters 58 (2004) 2530-2536

www.elsevier.com/locate/matlet

# Synthesis, formation and characterization of Mg<sub>4</sub>Nb<sub>2</sub>O<sub>9</sub> powders

S. Ananta\*

Department of Physics, Faculty of Science, Chiang Mai University, Chiang Mai 50200, Thailand

Received 2 October 2003; accepted 8 March 2004 Available online 10 May 2004

#### Abstract

Magnesium niobate  $(Mg_4Nb_2O_9)$  powders have been prepared and characterized by thermogravimetric and differential thermal analysis (TG-DTA), X-ray diffraction (XRD), scanning electron microscopy (SEM) and energy-dispersive X-ray (EDX) techniques. The effect of calcination temperature, dwell time and heating/cooling rates on phase formation, morphology and chemical composition of the powders are examined. The calcination temperature and dwell time have been found to have a pronounced effect on the phase formation and morphology of the calcined magnesium niobate powders. It has been found that the minor phases of nano-sized MgO inclusion and the columbite-type  $MgNb_2O_6$  phase tend to form together with the corundum-type  $Mg_4Nb_2O_9$  phase, depending on calcination conditions. It is seen that optimisation of calcination conditions can lead to a single-phase  $Mg_4Nb_2O_9$  in a hexagonal phase.

© 2004 Elsevier B.V. All rights reserved.

Keywords: Magnesium niobate; Mg<sub>4</sub>Nb<sub>2</sub>O<sub>9</sub>; Powder synthesis; Phase formation; Calcination; X-ray diffraction

### 1. Introduction

The corundum-like phase of magnesium niobate (Mg<sub>4</sub> Nb<sub>2</sub>O<sub>9</sub>; MN) has attracted interest for many years, with current attention tending to focus on its use in the synthesis of low loss microwave dielectric resonator applications [1,2]. It is also a room temperature photoluminescent material and a suitable buffer layer material for fabricating ferroelectric memory devices [3,4]. Recently, Lu and Yang [5] have shown that Mg<sub>4</sub>Nb<sub>2</sub>O<sub>9</sub> is a better precursor than the columbite MgNb<sub>2</sub>O<sub>6</sub> [6] for the successful preparation of single phase perovskite lead magnesium niobate, Pb(Mg<sub>1/3</sub>Nb<sub>2/3</sub>)O<sub>3</sub>, which is becoming increasingly important for multilayer ceramic capacitor, electrostrictor and actuator applications [7,8].

To date, four possible magnesium—niobium oxides have been identified: MgNb<sub>2</sub>O<sub>6</sub>, Mg<sub>4</sub>Nb<sub>2</sub>O<sub>9</sub>, Mg<sub>5</sub>Nb<sub>4</sub>O<sub>15</sub> and Mg<sub>2/3</sub>Nb<sub>11(1/3)</sub>O<sub>29</sub> [9]. You et al. [10] reported that MgNb<sub>2</sub>O<sub>6</sub> and Mg<sub>4</sub>Nb<sub>2</sub>O<sub>9</sub> are the only stable phases that exist at room temperature. It is known that synthesis of Mg<sub>4</sub>Nb<sub>2</sub>O<sub>9</sub> phase by the conventional method, by react-

\* Tel.: +66-53-943376; fax: +66-53-357512. *E-mail address:* supon@chiangmai.ac.th (S. Ananta). ing individual oxides, generally results in varying amounts of the columbite-like MgNb<sub>2</sub>O<sub>6</sub> phase alongside the corundum phase [10-12]. Thus, a number of chemical routes using expensive precursors, for example solgel [13] and co-precipitation [14], have been developed as alternatives to the conventional solid state reaction of mixed oxides. All of these techniques are aimed at reducing the temperature of preparation of the compound even though they are more involved and complicated than the mixed oxide route. Generally, the mixed oxide method involves the heating of a mixture of magnesium oxide and niobium oxide above 1300 °C for long times, i.e. 24 h [15], 48 h [11] or 72 h [16], and has been employed intensively in the last decade [10-12,15,16]. The optimisation of calcination conditions used in the mixed oxide process, however, have not received detailed attention, and the effects of applied dwell time and heating/cooling rates have not yet been studied extensively. The purpose of this work was to explore a simple mixed oxide synthetic route for the production of Mg<sub>4</sub>Nb<sub>2</sub>O<sub>9</sub> (MN) powders and perform a systematic study of the reaction between the starting magnesium oxide and niobium oxide precursors. The phase formation, and morphology of the powder calcined at various conditions will be studied and discussed.

### 2. Experimental procedure

The starting materials were commercially available magnesium oxide, MgO (periclase: JCPDS file number 71-1176) (Fluka, 98% purity) and niobium oxide, Nb<sub>2</sub>O<sub>5</sub> (JCPDS file number 80-2493) (Aldrich, 99.9% purity). The two oxide powders exhibited an average particle size in the range of 3.0 to 5.0 µm. Mg<sub>4</sub>Nb<sub>2</sub>O<sub>9</sub> powder was synthesised by the solid state reaction of thoroughly ground mixtures of MgO and Nb2O5 powders that were milled in the required stoichiometric ratio. The milling operation was carried out for 24 h in isopropanal. High purity corundum balls with diameter of 10 mm were used as the milling media. After drying at 120 °C, various calcination conditions, i.e. temperatures ranging from 550 to 1100 °C, dwell times ranging from 0.5 to 48 h and heating/cooling rates ranging from 5 to 25 °C/min, were applied, in order to investigate the formation of Mg<sub>4</sub>Nb<sub>2</sub>O<sub>9</sub>. The reactions of the uncalcined MN powders taking place during heat treatment were investigated by thermogravimetric and differential thermal analysis (TG-DTA, Shimadzu) using a heating rate of 10 °C/min in air from room temperature up to 1100 °C. Calcined powders were subsequently examined by room temperature X-ray diffraction (XRD; Philips PW 1729 diffractometer) using Ni filtered  $CuK_{\alpha}$  radiation, to identify the phases formed and optimum calcination conditions for the manufacture of MN powder. The powder morphology was examined using scanning electron microscopy (SEM; JEOL JSM-840A). The chemical compositions of the phases formed were elucidated by an energy-dispersive X-ray (EDX) analyser with an ultra-thin window. EDX spectra were quantified with the virtual standard peaks supplied with the Oxford Instruments eXL software.

#### 3. Results and discussion

The TG-DTA simultaneous analysis for a powder mixed in the stoichiometric proportions of Mg<sub>4</sub>Nb<sub>2</sub>O<sub>9</sub> is shown in Fig. 1. The TG curve shows two distinct weight losses. In the temperature range from room temperature to  $\sim 150$  °C, both small exothermic and endothermic peaks are observed in the DTA curve in consistent with the first weight loss. These observations can be attribute to the decomposition of the organic species from the milling process. Increasing the temperature up to ~ 800 °C, the solid-state reaction occurs between MgO and Nb<sub>2</sub>O<sub>5</sub> [12,17]. The broad exothermic peak in the DTA curve represents that reaction, which has a maximum at  $\sim 600$  °C. This is supported by a second fall in sample weight over the same temperature range. No further significant weight loss was observed for the temperatures above 600 °C in the TG-curve, indicating the minimum firing temperature to get MgO-Nb<sub>2</sub>O<sub>5</sub> compounds in good agreement with XRD result (Fig. 2) and other workers [18,19]. However, the DTA curve shows that there are another small peaks at ~ 1070 °C. It is to be noted that there is no obvious interpretation of these peaks, although it is likely to correspond to a phase transition reported earlier [20]. These data were used to define the range of temperatures for XRD investigation to between 500 and 1100 °C.

Powder XRD patterns of the calcined powders are given in Figs. 2–5, with the corresponding JCPDS patterns also shown. From Fig. 2, it is seen that the powder fired at 550  $^{\circ}\text{C}$  consisted of the mixed phases of MgO and Nb<sub>2</sub>O<sub>5</sub> precursors, which could be matched with JCPDS file numbers 71-1176 and 80-2493, respectively [21,22]. Little crystalline phase of MgNb<sub>2</sub>O<sub>6</sub> ( $\triangledown$ ) with orthorhombic symmetry (JCPDS file no. 33-875 [23]) was developed

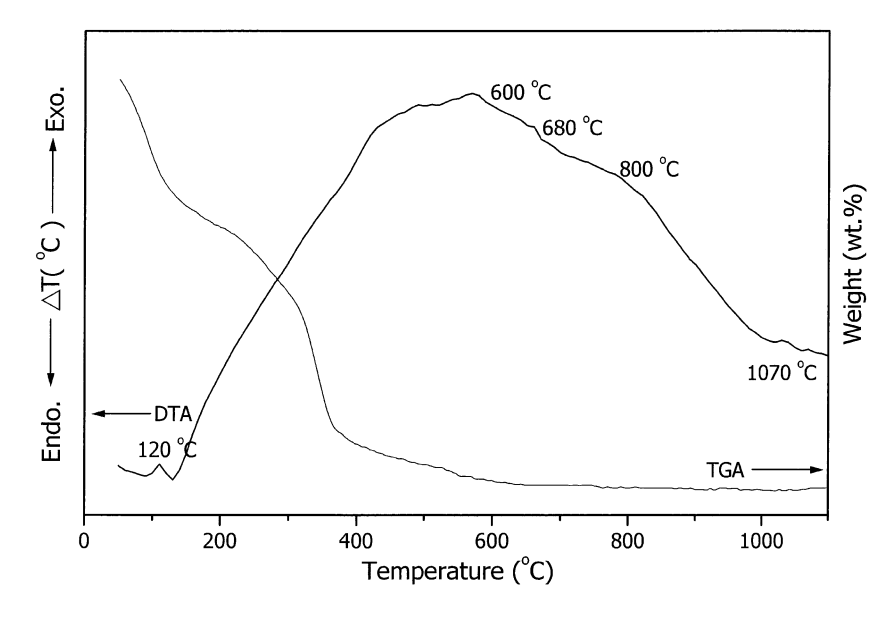


Fig. 1. TG-DTA curves for the mixture of MgO-Nb<sub>2</sub>O<sub>5</sub> powder.

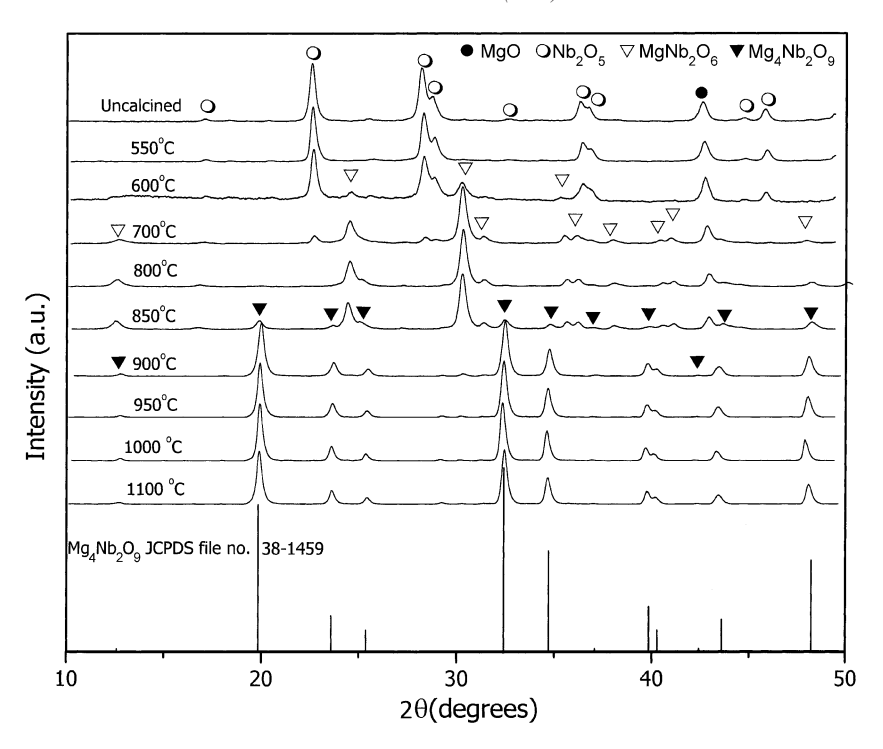


Fig. 2. XRD patterns of MN powder calcined at various temperatures for 2 h with heating/cooling rates of 10 °C/min.

accompanying MgO and Nb<sub>2</sub>O<sub>5</sub> as separated phases, when it was calcined at 600 °C. This observation agrees well with those derived from the TG–DTA results and other workers [24–26]. As the temperature increased to 800 °C, the intensity of the columbite-like MgNb<sub>2</sub>O<sub>6</sub> peaks was further enhanced. Moreover, the precursor phase of Nb<sub>2</sub>O<sub>5</sub> has been found to completely disappear, and crystalline MgNb<sub>2</sub>O<sub>6</sub> with small amount of MgO are the only detectable phases in

the powder. Calcinations at 850 °C resulted in some new peaks ( $\blacktriangledown$ ) of the corundum Mg<sub>4</sub>Nb<sub>2</sub>O<sub>9</sub> phase (JCPDS file no. 38-1459 [27]) mixing with the columbite MgNb<sub>2</sub>O<sub>6</sub> phase and some residual MgO. Upon calcination at 900 °C, the corundum Mg<sub>4</sub>Nb<sub>2</sub>O<sub>9</sub> phase becomes the predominant phase and the residual MgO has been found to completely disappear. However, the traces of minor phase MgNb<sub>2</sub>O<sub>6</sub> at  $2\theta \sim 30.16^\circ$  and  $31.30^\circ$  could not be completely eliminated.

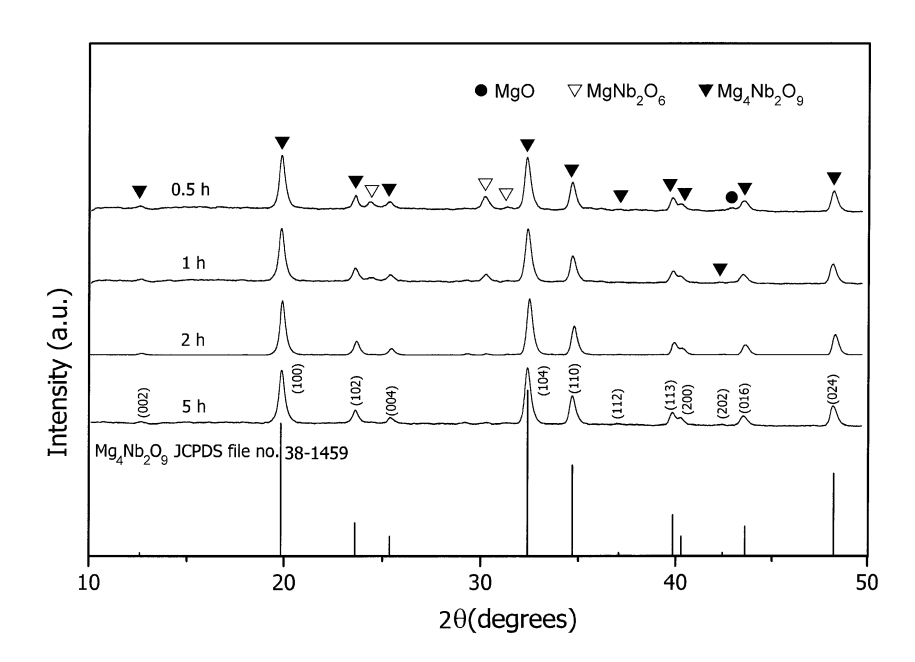


Fig. 3. XRD patterns of MN powder calcined at 950 °C for various dwell times with heating/cooling rates of 10 °C/min.

Table 1 Calculated Mg<sub>4</sub>Nb<sub>2</sub>O<sub>9</sub> phase as a function of calcination conditions

Calcination conditions		Qualitative concentrations of Mg <sub>4</sub> Nb <sub>2</sub> O <sub>9</sub> phase		
Temperature (°C)	Time (h)	Rate (°C/min)	Mg <sub>4</sub> Nb <sub>2</sub> O <sub>9</sub> (wt.%)	MgNb <sub>2</sub> O <sub>6</sub> (wt.%)
900	0.5	10	75	25
900	1	10	81	19
900	2	10	96	4
900	5	10	100	0
900	24	10	100	0
900	48	10	100	0
900	5	25	100	0
950	0.5	10	76	24
950	1	10	83	17
950	2	10	100	0
950	5	10	100	0
950	2	5	100	0
950	2	15	100	0
950	2	20	100	0
950	2	25	100	0
1000	2	10	100	0
1100	2	10	100	0

The estimated precision of the concentrations for the two phases is  $\pm 0.1\%$ .

The percentage of corundum phase ( $\sim$  96 wt.%) formed at 900 °C is comparable to that obtained by Ananta et al. [20]. The amount of corundum phase present in each of the powder was estimated using the following equation:

wt.% corundum phase = 
$$\left(\frac{I_{\rm Cor}}{I_{\rm Cor} + I_{\rm Col}}\right) \times 100.$$
 (1)

This equation is analogous to the well known equation [6,15,20] widely employed in connection with the fabrication of complex perovskite materials. It should be seen as a

first approximation since its applicability requires comparable maximum intensities of the peaks of corundum and columbite phases. Here  $I_{\text{Cor}}$  refers to the intensity of the corundum (104) peak and  $I_{\text{Col}}$  the intensity of the columbite (131) peak [20]. For the purpose of estimating the concentrations of the phases present, Eq. (1) has been applied to the powder XRD patterns obtained as given in Table 1.

After calcination at 950 °C, a single phase of the corundum  $Mg_4Nb_2O_9$  is formed. The XRD pattern of the  $Mg_4Nb_2O_9$  calcined at 950 °C for 2 h was indexable according to a corundum-type structure with the space group  $p\bar{3}c1$  (no. 165) and the hexagonal unit cell with lattice parameters a=516 and c=1402 pm, in consistent with literature [12,28]. In conventional mixed oxide route reported earlier [5,15,16], major phase of  $Mg_4Nb_2O_9$  was obtained for a calcination temperature above 1200 °C. However, for the present work, there are no significant different between the powders calcined at temperature ranging from 950 to 1100 °C (see also Fig. 2 and Table 1).

Apart from the calcination temperature, the effect of dwell time was also found to be quite significant. It is seen that the single phase of Mg<sub>4</sub>Nb<sub>2</sub>O<sub>9</sub> (yield of 100% within the limitations of the XRD technique, as given in Table 1) was found to be possible in powders calcined at either 950 °C with dwell time of at least 2 h (Fig. 3) or 900 °C for 5 h or more (Fig. 4). In earlier work [11,15] long heat treatments at ~ 1200–1300 °C for 24 h and 48 h were proposed for the formation of Mg<sub>4</sub>Nb<sub>2</sub>O<sub>9</sub> by a conventional mixed oxide synthetic route, although no details on phase formation were provided. In the present study (Fig. 3), it was found that there are no significant different between the powders calcined at 900 °C with dwell time ranging from 5 to 48 h, as shown in Fig. 4.

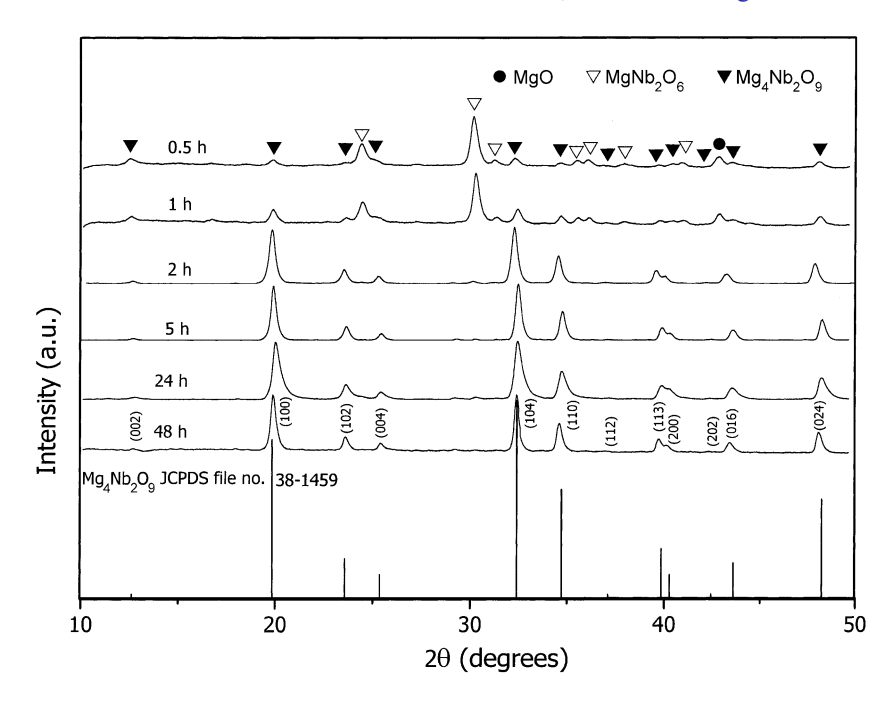


Fig. 4. XRD patterns of MN powder calcined at 900 °C for various dwell times with heating/cooling rates of 10 °C/min.

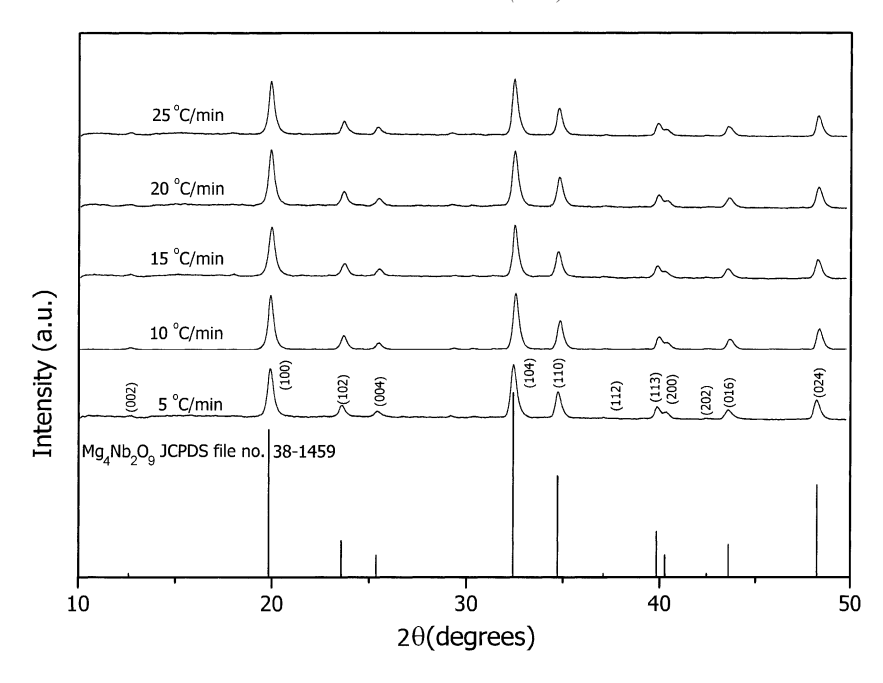


Fig. 5. XRD patterns of MN powder calcined at 950 °C for 2 h with various heating/cooling rates.

In the present study, an attempt was also made to calcine MN powders under various heating/cooling rates (Fig. 5). In this connection, it is shown that the yield of  $Mg_4Nb_2O_9$ 

phase did not vary significantly with different heating/cooling rates ranging from 5 to 25 °C/min. Based on the TG-DTA and XRD data, it may be concluded that, over a wide

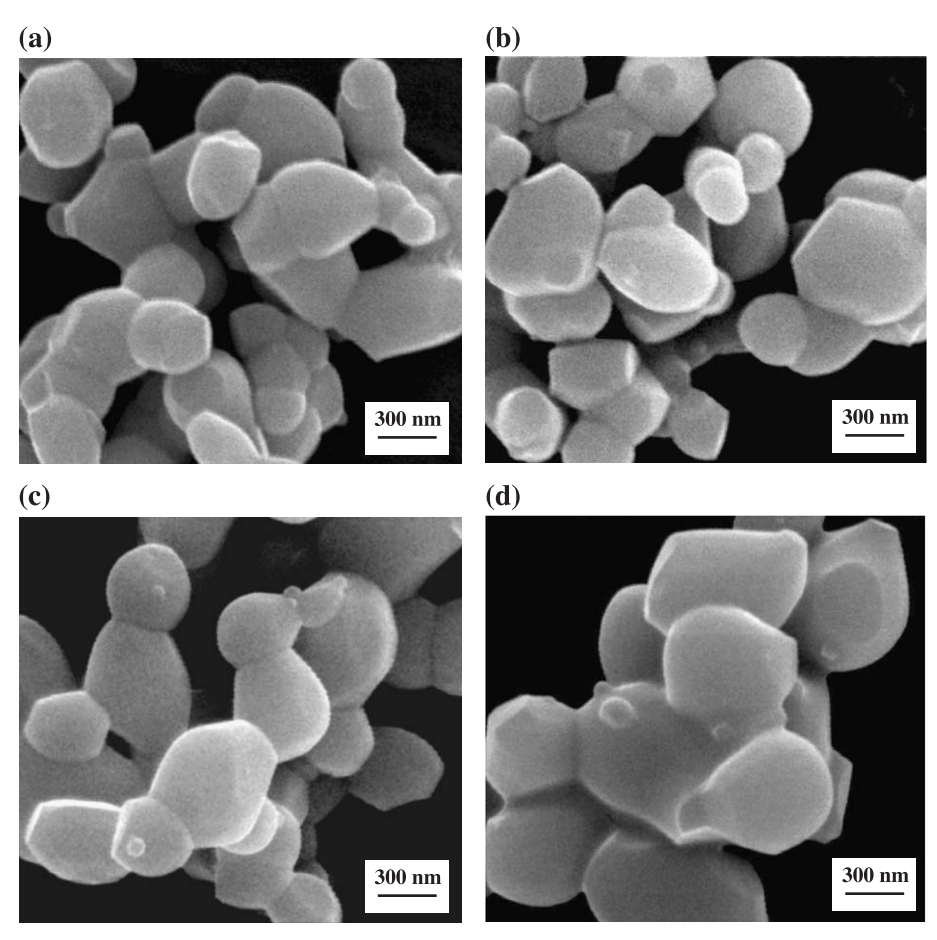


Fig. 6. SEM micrographs of the MN powders calcined at (a) 900  $^{\circ}$ C, (b) 950  $^{\circ}$ C, (c) 1000  $^{\circ}$ C and (d) 1100  $^{\circ}$ C for 2 h with heating/cooling rates of 10  $^{\circ}$ C/min.

range of calcination conditions, single phase  $Mg_4Nb_2O_9$  cannot be straightforwardly formed via a solid-state mixed oxide synthetic route. It is well documented that powders prepared by a conventional mixed oxide method have spatial fluctuations in their compositions. The extent of the fluctuation depends on the characteristics of the starting powders as well as the processing schedules [6,11,20].

The experimental work carried out here suggests that the optimal calcination conditions for single phase  $Mg_4Nb_2O_9$  (with impurities undetected by XRD technique) are 950 °C for 2 h or 900 °C for 5 h, with heating/cooling rates as fast as 25 °C/min. Moreover, the formation temperature and dwell time for  $Mg_4Nb_2O_9$  observed in this work are also much lower than those reported earlier [11,15,16].

The morphological changes in the Mg<sub>4</sub>Nb<sub>2</sub>O<sub>9</sub> powders formed by a mixed oxide are illustrated in Figs. 6 and 7 as a function of formation temperature. After calcinations at 900 to 1100 °C, the powders have similar morphology. In general, the particles are agglomerated and basically irregular in shape, with a substantial variation in particle size, particularly in samples calcined at high temperatures. This structure is similar to that of ZrTiO<sub>4</sub> powders synthesised by previous researchers [29]. The range of

particle size was found to be about 0.23-0.65, 0.30-0.73, 0.33-0.83 and 0.35-1.02 µm for the samples calcined at 900, 950, 1000 and 1100 °C for 2 h, respectively (Fig. 6(a-d)). The results indicate that averaged particle size and degree of agglomeration tend to increase with calcination temperature.

The effects of heating/cooling rates and dwell time on the morphology of the calcined powders were also found to be quite significant. As shown in Fig 7 (a-d), the range of particle size was found to be about 0.10-0.37, 0.10-0.30, 0.30-0.73 and 0.50-0.93 µm for the samples calcined at 950 °C for 2 h with heating/cooling rates of 15 and 20 °C/ min and at 900 °C for 24 and 48 h, respectively. It is seen that by increasing the heating/cooling rates, averaged particle size tends to decrease whilst the degree of agglomeration tends to increase (Figs. 6(b) and 7(a,b)). This observation could be attributed to the mechanism of surface energy reduction of the ultrafine powders, i.e. the smaller the powder the higher the specific surface area [30]. As expected, it is seen that longer heat treatment leads to larger particle sizes and hard agglomeration (Figs. 6(a) and 7(c,d)). In general, EDX analysis using a 20 nm probe from a large number of particles of the calcined powders confirmed the

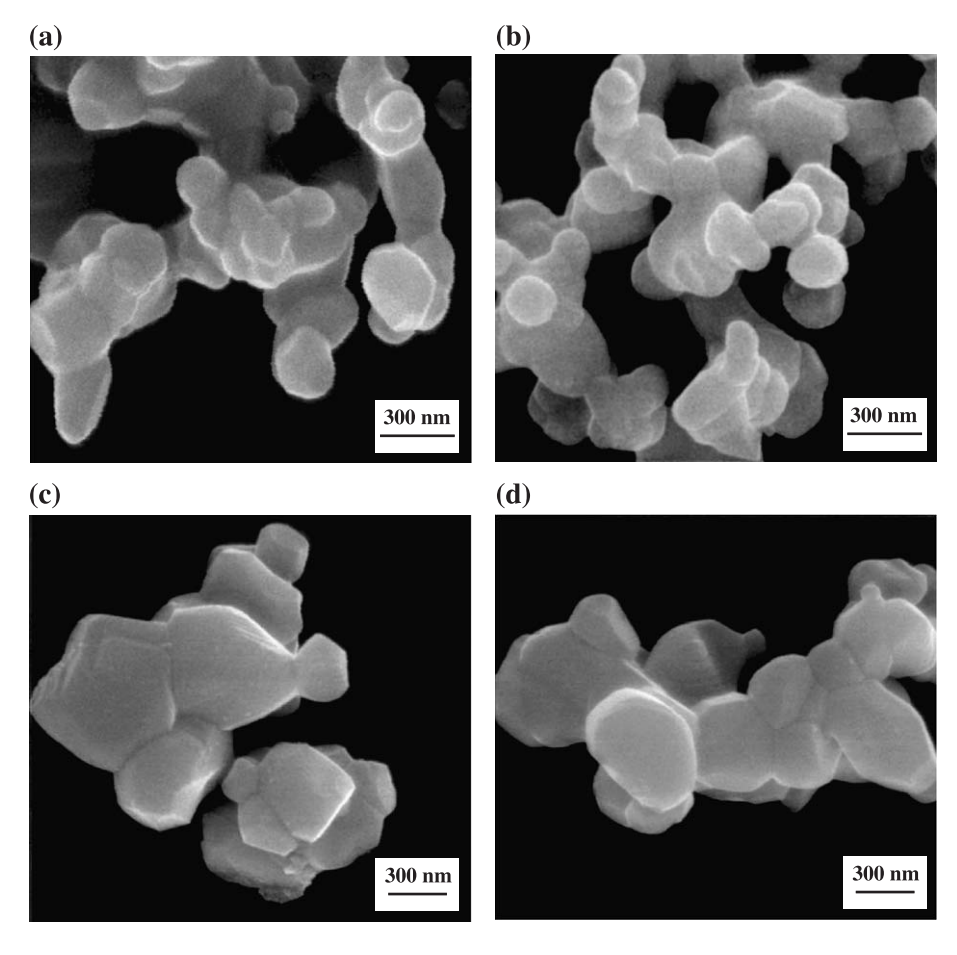


Fig. 7. SEM micrographs of the MN powders calcined at 950  $^{\circ}$ C for 2 h with heating/cooling rates of (a) 15 and (b) 25  $^{\circ}$ C/min, and at 900  $^{\circ}$ C with heating/cooling rates of 10  $^{\circ}$ C/min for (c) 24 and (d) 48 h.

parent composition to be  $Mg_4Nb_2O_9$  in agreement with XRD results. A combination of SEM and EDX techniques has demonstrated that an MgO-rich phase (spherical particles with diameter  $\sim 50-100$  nm) exists neighbouring the  $Mg_4Nb_2O_9$  parent phase, as shown in Figs. 6(c,d). Moreover, a variation in the Mg/Nb ratio was also found in good agreement with other work [12,31,32]. The existence of a discrete nano-sized MgO phase points to the poor reactivity of MgO, although the concentration is too low for detection by XRD.

#### 4. Conclusions

The corundum-type compound  $Mg_4Nb_2O_9$  has been prepared by a solid-state mixed oxide synthetic route. The preparative method involved the use of inexpensive and widely available oxide precursors, moderately low calcination temperatures and dwell times, together with fast heating/cooling rates. Evidence has been gained from XRD that single phase of corundum  $Mg_4Nb_2O_9$  powder has been obtained in this study by using a calcination temperature of either 950 °C for 2 h or 900 °C for 5 h, with heating/cooling rates of 25 °C/min.

### Acknowledgements

This work was supported by the Thailand Research Fund (TRF).

#### References

- H. Ogawa, A. Kan, S. Ishihara, Y. Higashida, J. Eur. Ceram. Soc. 23 (2003) 2485.
- [2] V.M. Ferreia, J.L. Baptista, Mater. Res. Bull. 29 (1994) 1017.
- [3] A. Wachtel, J. Electrochem. Soc. 111 (1964) 534.
- [4] C.W. Hwang, S.K. Lee, Japanese Patent No. JP 97-293619.

- [5] C.H. Lu, H.S. Yang, Mater. Sci. Eng., B, Solid-State Mater. Adv. Technol. 84 (2001) 159.
- [6] S.L. Swartz, T.R. Shrout, Mater. Res. Bull. 17 (1982) 1245.
- [7] A.J. Moulson, J.M. Herbert, Electroceramics, 2nd ed., Wiley-Interscience, New York, 2003.
- [8] G. Haertling, J. Am. Ceram. Soc. 82 (1999) 797.
- [9] P. Norim, C.G. Arbin, B. Nalander, Acta Chem. Scand. 26 (1972) 3389.
- [10] Y.C. You, H.L. Park, Y.G. Song, H.S. Moon, G.C. Kim, J. Mater. Sci. Lett. 13 (1994) 1487.
- [11] K. Sreedhar, N.R. Pavaskar, Mater. Lett. 53 (2002) 452.
- [12] S. Pagola, R.E. Carbonio, J.A. Alonso, M.T. Fernández-Díaz, J. Solid State Chem. 134 (1997) 76.
- [13] H. Cheng, B. Xu, J. Ma, J. Mater. Sci. Lett. 16 (1997) 1570.
- [14] P.A. Joy, Mater. Lett. 32 (1997) 347-349.
- [15] P.A. Joy, K. Sreedhar, J. Am. Ceram. Soc. 80 (1997) 770.
- [16] W. Wong-Ng, H.F. McMurdie, B. Paretzkin, C.R. Hubbard, A.L. Dragoo, J.M. Stewart, Powder Diffr. 2 (1987) 111.
- [17] E. Brűck, R.K. Route, R.J. Raymakers, R.S. Feigelson, J. Cryst. Growth 128 (1993) 842.
- [18] Y.S. Hong, H.B. Park, S.J. Kim, J. Eur. Ceram. Soc. 18 (1998) 613.
- [19] E.R. Carmargo, E. Longo, D.R. Leite, J. Sol-Gel Sci. Technol. 17 (2000) 111.
- [20] S. Ananta, R. Brydson, N.W. Thomas, J. Eur. Ceram. Soc. 19 (1999) 355.
- [21] Powder Diffraction File No. 71-1176. International Centre for Diffraction Data, Newton Square, PA, 2000.
- [22] Powder Diffraction File No. 80-2493. International Centre for Diffraction Data, Newton Square, PA, 2000.
- [23] Powder Diffraction File No. 33-875. International Centre for Diffraction Data, Newton Square, PA, 2000.
- [24] N.K. Kim, Mater. Lett. 32 (1997) 127.
- [25] L.B. Kong, J. Ma, H. Huang, R.F. Zhang, J. Alloys Compd. 340 (2002) L1.
- [26] Y. Yu, C. Feng, C. Li, Y. Yang, W. Yao, H. Yan, Mater. Lett. 51 (2001) 490.
- [27] Powder Diffraction File No. 38-1459. International Centre for Diffraction Data, Newton Square, PA, 2000.
- [28] N. Kumada, K. Taki, N. Kinomura, Mater. Res. Bull. 35 (2000) 1017.
- [29] S. Ananta, R. Tipakontitikul, T. Tunkasiri, Mater. Lett. 57 (2003) 2637.
- [30] J.S. Reed, Principles of Ceramics Processing, 2nd ed., Wiley-Interscience, New York, 1995.
- [31] S. Ananta, R. Brydson, N.W. Thomas, J. Eur. Ceram. Soc. 20 (2000) 2315
- [32] A. Mergen, W.E. Lee, J. Eur. Ceram. Soc. 17 (1997) 1033.







materials letters

Materials Letters 58 (2004) 2781-2786

www.elsevier.com/locate/matlet

# Phase and morphology evolution of magnesium niobate powders synthesized by solid-state reaction

S. Ananta\*

Department of Physics, Faculty of Science, Chiang Mai University, Chiang Mai 50200, Thailand Received 3 November 2003; received in revised form 25 March 2004; accepted 5 April 2004 Available online 9 June 2004

#### **Abstract**

Magnesium niobate (MgNb<sub>2</sub>O<sub>6</sub>; MN) powders have been prepared and characterized by TG-DTA, XRD, SEM and EDX techniques. The effect of calcination temperature, dwell time and heating/cooling rates on phase formation, morphology and chemical composition of the powders are examined. The calcination temperature and dwell time have been found to have a pronounced effect on the phase formation of the calcined magnesium niobate powders. It has been found that the minor phases of unreacted MgO and Nb<sub>2</sub>O<sub>5</sub> phases tend to form together with the columbite-type MgNb<sub>2</sub>O<sub>6</sub> phase, depending on calcination conditions. It is seen that optimisation of calcination conditions can lead to a single-phase MgNb<sub>2</sub>O<sub>6</sub> in an orthorhombic phase. Higher calcination times and heating/cooling rates clearly favoured particle growth and the formation of large and hard agglomerates. © 2004 Published by Elsevier B.V.

Keywords: Magnesium niobate; MgNb<sub>2</sub>O<sub>6</sub>; Columbite; Calcination; Phase formation; Powders—solid-state reaction

#### 1. Introduction

Magnesium niobate (MgNb<sub>2</sub>O<sub>6</sub>; MN) is one of the binary niobate compounds which exhibits excellent dielectric properties at microwave frequencies [1-3]. It has very low loss and high dielectric constant and is a promising candidate for application in microwave devices. This compound with a columbite crystal structure is also a suitable reference material for investigating the defect induced in LiNbO<sub>3</sub> substrates for waveguide fabrication [4-6]. Moreover, recently, it is well known as the key precursor for the successful preparation of single-phase relaxor perovskite Pb(Mg<sub>1/3</sub>Nb<sub>2/3</sub>)O<sub>3</sub> (PMN), which is becoming increasingly important for transducer, electrostrictor and actuator applications [7-10].

It is known that various compositions are possible in the Mg-Nb-O system [11]. To date, four possible magnesiumniobium oxides have been identified: MgNb<sub>2</sub>O<sub>6</sub>, Mg<sub>4</sub>Nb<sub>2</sub>O<sub>9</sub>,  $Mg_5Nb_4O_{15}$  and  $Mg_{2/3}Nb_{11(1/3)}O_{29}$  [11,12]. You et al. [13] reported that MgNb<sub>2</sub>O<sub>6</sub> and Mg<sub>4</sub>Nb<sub>2</sub>O<sub>9</sub> are the only stable phases that exist at room temperature. It is known that

E-mail address: supon@chiangmai.ac.th (S. Ananta).

\* Tel.: +66-53-943376; fax: +66-53-357512.

synthesis of MgNb<sub>2</sub>O<sub>6</sub> phase by the conventional method, by reacting individual oxides, generally results in varying amounts of the corundum Mg<sub>4</sub>Nb<sub>2</sub>O<sub>9</sub> phase alongside the columbite phase [7,8,14]. Thus, a number of chemical routes using expensive precursors, for example, citrate gel [15], coprecipitation [16], and polymerised complex [17], have been developed as alternatives to the conventional solid-state reaction of mixed oxides. All of these techniques are aimed at reducing the temperature of preparation of the compound even though they are more involved and complicated than the mixed oxide route.

The mixed oxide synthetic route is probably one of the most fundamental, practical routine methods which has been used, and it has been developed and modified in both scientific research and industrial mass production for many years [17–20]. Generally, the mixed oxide method involves the heating of a mixture of magnesium oxide and niobium oxide above 1100 °C for long times, i.e., 6 h [17], 20 h [7], 24 h [12] and 48 h [8], and has been employed intensively in the last decade [17-20]. The optimisation of calcination conditions used in the mixed oxide process, however, have not received detailed attention, and the effects of applied dwell time and heating/cooling rates have not yet been studied extensively. The purpose of this work was to explore a simple mixed oxide synthetic route for the production of  $MgNb_2O_6$  (MN) powders via a rapid vibro-milling technique and perform a systematic study of the reaction between the starting magnesium oxide and niobium oxide precursors. The phase formation and morphology of the powder calcined at various conditions will be studied and discussed.

### 2. Experimental procedure

The starting materials were commercially available magnesium oxide, MgO (periclase: JCPDS file number 71-1176) and niobium oxide, Nb<sub>2</sub>O<sub>5</sub> (JCPDS file number 80-2493) (Aldrich, 99.9% purity). The two oxide powders exhibited an average particle size in the range of 3.0–5.0 μm. MgNb<sub>2</sub>O<sub>6</sub> powder was synthesised by the solid-state reaction of thoroughly ground mixtures of MgO and Nb2O5 powders that were milled in the required stoichiometric ratio. Instead of employing a ball-milling procedure (ZrO<sub>2</sub> media under acetone for 24 h [8]), use was made of a McCrone vibromilling. In order to improve the reactivity of the constituents, the milling process was carried for 2 h (instead of 30 min [19]) with corundum media in isopropyl alcohol (IPA). Although the use of IPA in place of acetone was dictated by the use of the McCrone mill, an associated benefit is the avoidance of unpleasant vapours associated with the use of acetone. Drying was carried out at 120 °C for 2h, prior to sieving through a 100-µm mesh. After sieving, various calcination conditions, i.e., temperatures ranging from 500 to 1200 °C, dwell times ranging from 2 to 12 h and heating/ cooling rates ranging from 10 to 30 °C/min were applied in order to investigate the formation of MgNb<sub>2</sub>O<sub>6</sub>. The reactions of the uncalcined MN powders taking place during heat treatment were investigated by thermogravimetric and differential thermal analysis (TG-DTA, Shimadzu), using a heating rate of 10 °C/min in air from room temperature up to 1100 °C. Calcined powders were subsequently examined by room temperature X-ray diffraction (XRD; Philips PW 1729 diffractometer), using Ni-filtered CuK<sub>α</sub> radiation to identify the phases formed and optimum calcination con-

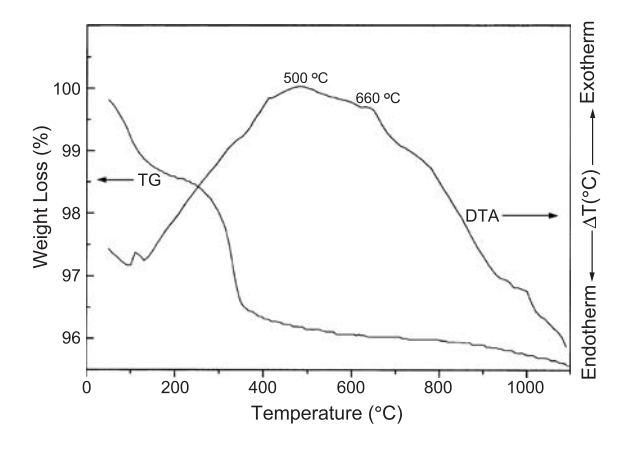


Fig. 1. TG-DTA curves for the mixture of MgO-Nb<sub>2</sub>O<sub>5</sub> powder.

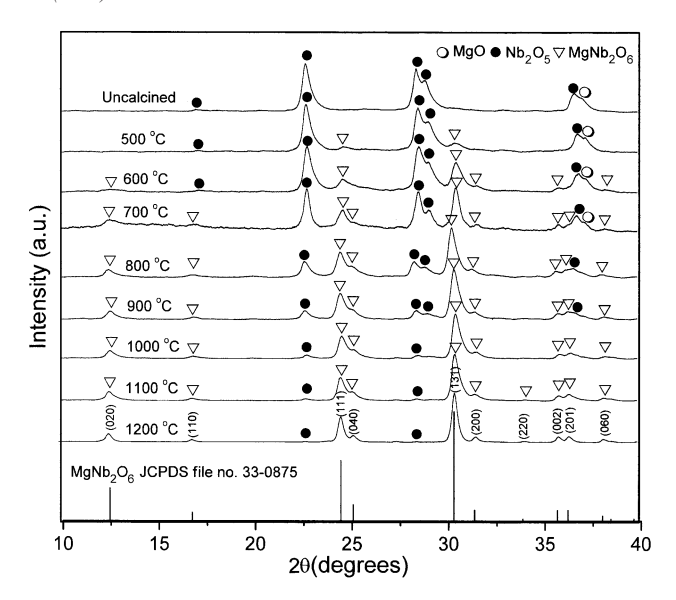


Fig. 2. XRD patterns of MN powder calcined at various temperatures for 3 h with heating/cooling rates of 10  $^{\circ}$ C/min.

ditions for the manufacture of MN powder. Powder morphologies and particle sizes were directly imaged, using scanning electron microscopy (SEM; JEOL JSM-840A). The chemical compositions of the phases formed were elucidated by an energy-dispersive X-ray (EDX) analyser with an ultra-thin window. EDX spectra were quantified with the virtual standard peaks supplied with the Oxford Instruments eXL software.

#### 3. Results and discussion

The TG-DTA simultaneous analysis of a powder mixed in the stoichiometric proportions of MgNb<sub>2</sub>O<sub>6</sub> is shown in Fig. 1. The TG curve shows two distinct weight losses. In the temperature range from room temperature to  $\sim 150~^{\circ}\text{C},$  both small exothermic and endothermic peaks are observed in the DTA curve in consistent with the first weight loss

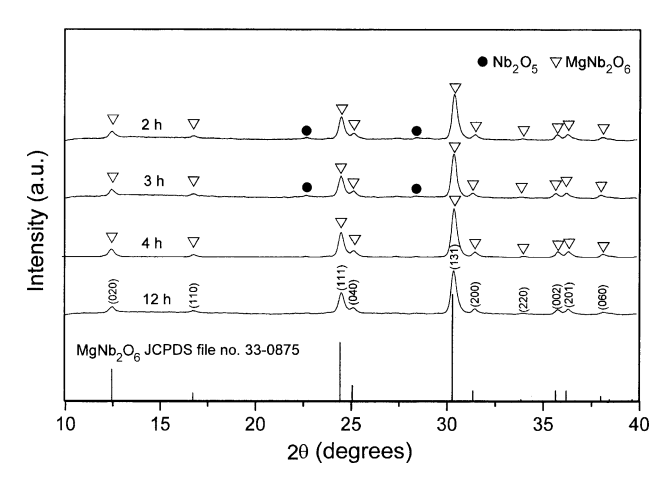


Fig. 3. XRD patterns of MN powder calcined at 1000  $^{\circ}\text{C}$  for various dwell times with heating/cooling rates of 10  $^{\circ}\text{C/min}.$ 

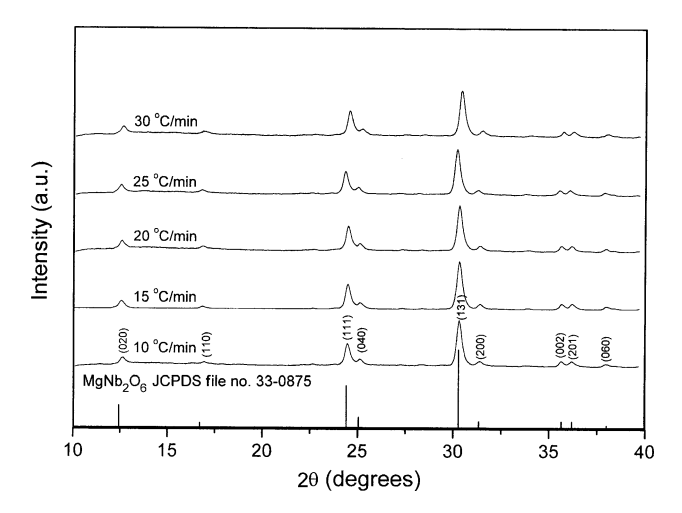


Fig. 4. XRD patterns of MN powder calcined at 1000 °C for 4 h with various heating/cooling rates.

( $\sim 1.2\%$ ). These observations can be attributed to the decomposition of the organic species from the milling process. Increasing the temperature up to  $\sim 1000$  °C, the solid-state reaction occurred between MgO and Nb<sub>2</sub>O<sub>5</sub> [7,21]. The broad exotherm in the DTA curve represents that reaction, which has a maximum at  $\sim 500$  °C. This is supported by a second fall in sample weight ( $\sim 2.3\%$ ) over the same temperature range. No further significant weight loss was observed for the temperatures above 500 °C in the

TG-curve, indicating that the minimum firing temperature to get MgO–Nb<sub>2</sub>O<sub>5</sub> compounds is in good agreement with XRD result (Fig. 2) and those of other workers [11,14]. However, the DTA curve shows that there are other small peaks at  $\sim 660$  and 1000 °C. It is to be noted that there is no obvious interpretation of these peaks, although it is likely to correspond to a phase transition reported earlier [8,13,14]. These data were used to define the range of temperatures for XRD investigation to between 500 and 1200 °C.

To further study the phase development with increasing calcination temperature in the powders, they were calcined for 3 h in air at various temperatures, up to 1200 °C, followed by phase analysis using XRD. As shown in Fig. 2, for the uncalcined powder, only X-ray peaks of precursors MgO and Nb<sub>2</sub>O<sub>5</sub>, which could be matched with JCPDS file numbers 71-1176 [22] and 80-2493 [23], respectively, are present, indicating that no reaction had yet been triggered during the milling process. After calcination at 500 °C, little crystalline phase of MgNb<sub>2</sub>O<sub>6</sub> ( ♥ ) was developed accompanying with MgO and Nb<sub>2</sub>O<sub>5</sub> as separated phases. This observation agrees well with those derived from the TG-DTA results and those of other workers [14]. As the temperature increased to 600 °C, the intensity of the columbite-like MgNb<sub>2</sub>O<sub>6</sub> peaks was further enhanced. Upon calcination at temperatures ranging from 700 to 1200 °C, the MgNb<sub>2</sub>O<sub>6</sub> phase became the predominant phase. It should be noted that after calcination at 800 °C, the peak

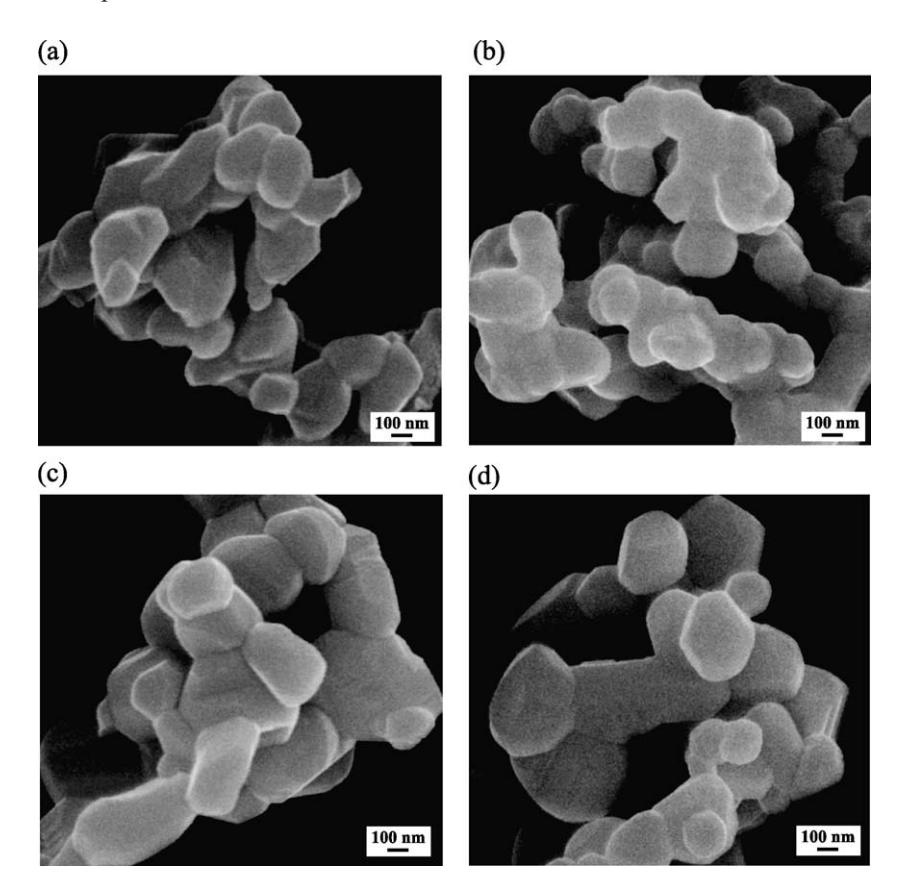


Fig. 5. SEM micrographs of the MN powders calcined at 1000 °C with heating/cooling rates of 10 °C/min for (a) 2 h, (b) 3 h, (c) 4 h and (d) 12 h.

corresponding to MgO (O) disappeared (not detectable), whereas the traces of minor phases of unreacted  $Nb_2O_5$  ( $\bullet$ ) could not be completely eliminated.

The XRD pattern of this MgNb<sub>2</sub>O<sub>6</sub> phase was indexable according to an orthorhombic columbite-type structure with lattice parameters a=570 pm, b=1419 pm and c=503 pm, space group *Pscan* (no. 60), consistent with JCPDS file numbers 33-875 [24] and literature [8,12,19]. In conventional mixed oxide route reported earlier [7,8,18,19], the major phase of MgNb<sub>2</sub>O<sub>6</sub> was obtained for a calcination temperature above 1100 °C. However, for the present work, there are no significant different between the powders calcined at temperature ranging from 1000 to 1200 °C (Fig. 2). Further increase of the calcination temperature to 1200 °C does not result in very much increase in the amount of MgNb<sub>2</sub>O<sub>6</sub>, whereas unreacted Nb<sub>2</sub>O<sub>5</sub> could not be completely eliminated. This could be attributed to the poor reactivity of magnesium and niobium species [18,19].

Apart from the calcination temperature, the effect of dwell time was also found to be quite significant. From Fig. 3, it can be seen that the single phase of MgNb<sub>2</sub>O<sub>6</sub> (yield of 100% within the limitations of the XRD technique) was found to be possible in powders calcined at 1000 °C with dwell time of 4 h or more. This was apparently a consequence of the enhancement in crystallinity of the MgNb<sub>2</sub>O<sub>6</sub> phase with increasing dwell time. In earlier work [7,8,20], long heat treatments at  $\sim 1100-1300$  °C for 6, 20

and 48 h were proposed for the formation of MgNb<sub>2</sub>O<sub>6</sub> by a conventional mixed oxide synthetic route, although no details on phase formation were provided. Furthermore, Saha et al. [7] have also reported their attempts to prepare solid-state-derived MgNb<sub>2</sub>O<sub>6</sub> powder via the introduction of re-grinding and re-calcination processes were successful. However, in the present study, it was found that there are no significant differences between the powders calcined at 1000 °C with dwell time ranging from 4 to 12 h, as shown in Fig. 3. Moreover, it is clear that an essentially monophasic MgNb<sub>2</sub>O<sub>6</sub> of columbite structure was already obtained when the calcination time was extended to 4 h without any introduction of pre-firing and remixing processes. This could be attributed to the better mixing of magnesium and niobium oxides since in this study the milling time was extended to 2 h instead of 30 min [19]. The observation that the milling time effect may also play an important role on the phase formation is also consistent with other work [21]. To further study the phase development with increasing heating/cooling rates in the powders, an attempt was also made to calcine MN powders under various heating/cooling rates (Fig. 4). In this connection, it is shown that the yield of MgNb<sub>2</sub>O<sub>6</sub> phase did not vary significantly with different heating/cooling rates ranging from 10 to 30 °C/min, in good agreement with the early results reported by Ananta et al. [25] for the mixture of the two kinds of refractory oxides.

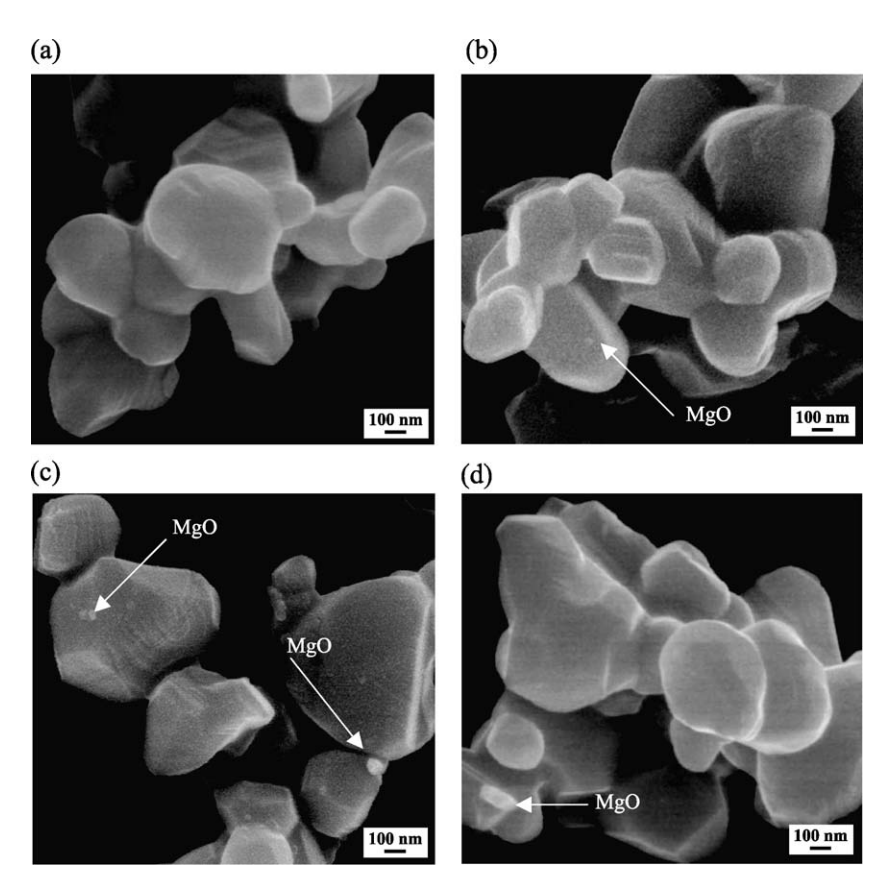


Fig. 6. SEM micrographs of the MN powders calcined at 1000 °C for 4 h with heating/cooling rates of (a) 15, (b) 20, (c) 25 and (d) 30 °C/min.

Table 1 Particle size range of  $MgNb_2O_6$  powders calcined at 1000 °C for various dwell times and heating/cooling rates

Dwell time (h)	Heating/cooling rates (°C/min)	Particle size range (±5 nm)
2	10	125-500
3	10	175-575
4	10	200-625
12	10	250-855
4	15	200-650
4	20	250 - 700
4	25	250 - 745
4	30	250 - 780

Based on the TG-DTA and XRD data, it may be concluded that, over a wide range of calcination conditions, single-phase MgNb<sub>2</sub>O<sub>6</sub> cannot be straightforwardly formed via a solid-state mixed oxide synthetic route. It is well documented that powder prepared by a conventional mixed oxide method have spatial fluctuations in their compositions. The extent of the fluctuation depends on the characteristics of the starting precursors as well as the processing schedules [7,14,18]. It is rather surprising that no evidence of the corundum Mg<sub>4</sub>Nb<sub>2</sub>O<sub>9</sub> [14,19] was found in this study, nor was there any indication of the Mg<sub>5</sub>Nb<sub>4</sub>O<sub>15</sub> [12] being present. The experimental work carried out here suggests that the optimal calcination condition for single-phase MgNb<sub>2</sub>O<sub>6</sub> (with impurities undetected by XRD technique) is 1000 °C for 4 h, with heating/cooling rates as fast as 30 °C/min. Moreover, the formation temperature and dwell time for MgNb<sub>2</sub>O<sub>6</sub> observed in this work are also lower than those reported earlier [8,14,20].

The morphological changes in the MgNb<sub>2</sub>O<sub>6</sub> powders formed by a mixed oxide method are illustrated in Figs. 5 and 6 as a function of dwell times and heating/cooling rates. The influence of heat treatment conditions on particle size is given in Table 1. After calcination at 1000 °C for various dwell times (Fig. 5) and heating/cooling rates (Fig. 6), the powders seem to have similar morphology. In general, the particles are agglomerated and basically irregular in shape, with a substantial variation in particle size, particularly in samples calcined for longer dwell time or with fast heating/ cooling rates. This structure is also similar to that of FeNbO<sub>4</sub> powders synthesised by previous researchers [26]. The effects of dwell time and heating/cooling rates on the particle size and degree of agglomeration of the calcined MgNb<sub>2</sub>O<sub>6</sub> powders were found to be quite significant. As shown in Table 1, it is seen that particle size range and degree of agglomeration tend to increase with dwell time and heating/ cooling rates. To the author's knowledge, the present data are the first results for the morphology-calcination relationship of MgNb<sub>2</sub>O<sub>6</sub> powders prepared by the solid-state reaction. It is also of interest to point out that the particle size range of single-phase MgNb<sub>2</sub>O<sub>6</sub> powders found here is significantly lower than that reported by Ananta et al. [19] (>3 µm) where the milling time of 30 min was used. The results obtained in

this study suggest that a systematic study of the effect of milling parameters such as milling times and milling speed on the phase and morphology evolutions of the magnesium niobate powders are required for better understanding and verifying the attractiveness of the vibro-milling technique. Further investigation of this relationship is under way and will be reported in the future.

In general, EDX analysis using a 20-nm probe from a large number of particles of the calcined powders confirmed the parent composition to be  $MgNb_2O_6$  in agreement with XRD results. A combination of SEM and EDX techniques has demonstrated that an MgO-rich phase (spherical particles with diameter  $\sim 25-100$  nm) exists neighbouring the  $MgNb_2O_6$  parent phase, as shown in Fig. 6b-d. Moreover, a variation in the Mg/Nb ratio was also found in good agreement with other work [18,19]. The existence of a discrete nanosized MgO phase points to the poor reactivity of MgO, although the concentration is too low for detection by XRD.

#### 4. Conclusions

The columbite-type compound  $MgNb_2O_6$  has been prepared by a solid-state mixed oxide synthetic route. The preparative method involved the use of inexpensive and widely available oxide precursors, moderately low calcination temperatures and dwell times, together with fast heating/cooling rates. Evidence gained from XRD revealed that single phase of columbite  $MgNb_2O_6$  powder with particle size ranging from 250 to 780 nm has been obtained in this study by using a calcination temperature of 1000 °C for 4 h, with heating/cooling rates of 30 °C/min.

### Acknowledgements

This work was supported by the Thailand Research Fund (TRF).

### References

- [1] Y.C. Zhang, Z.X. Yue, Z. Gui, L.T. Li, Mater. Lett. 57 (2003) 4531.
- [2] H. Ogawa, A. Kan, S. Ishihara, Y. Higashida, J. Eur. Ceram. Soc. 23 (2003) 2485.
- [3] V.M. Ferreia, J.L. Baptista, Mater. Res. Bull. 29 (1994) 1017.
- [4] A.Z. Simoes, A.H.M. Gonzalez, A.A. Cavalheiro, M.A. Zaghete, B.D. Stojanovic, J.A. Varela, Ceram. Int. 28 (2002) 265.
- [5] C. Zaldo, M.J. Martin, C. Coya, K. Polgar, A. Peter, J. Paitz, J. Phys.: Condens. Matter. 7 (1995) 2249.
- [6] L.J. Hu, Y.H. Chang, I.N. Lin, S.J. Yang, J. Cryst. Growth 114 (1991) 191
- [7] D. Saha, A. Sen, H.S. Maiti, J. Mater. Sci. Lett. 13 (1994) 723.
- [8] K. Sreedhar, A. Mitra, Mater. Res. Bull. 32 (1997) 1643.
- [9] G. Haertling, J. Am. Ceram. Soc. 82 (1999) 797.
- [10] A.J. Moulson, J.M. Herbert, Electroceramics, 2nd ed., Wiley-Interscience, New York, 2003.

- [11] P. Norin, C.G. Arbin, B. Nalander, Acta Chim. Scand. 26 (1972) 3389.
- [12] S. Pagola, R.E. Carbonio, J.A. Alonso, M.T. Fernández-Díaz, J. Solid State Chem. 134 (1997) 76.
- [13] Y.C. You, H.L. Park, Y.G. Song, H.S. Moon, G.C. Kim, J. Mater. Sci. Lett. 13 (1994) 1487.
- [14] Y. Yu, C. Feng, C. Li, Y. Yang, W. Yao, H. Yan, Mater. Lett. 51 (2001)
- [15] Y.S. Hong, H.B. Park, S.J. Kim, J. Eur. Ceram. Soc. 18 (1998) 613.
- [16] N.K. Kim, Mater. Lett. 32 (1997) 127.
- [17] E.R. Camargo, M. Kakihana, E. Longo, E.R. Leite. J. Alloy. Compd. 314 (2001) 140.
- [18] S.L. Swartz, T.R. Shrout, Mater. Res. Bull. 17 (1982) 1245.
- [19] S. Ananta, R. Brydson, N.W. Thomas, J. Eur. Ceram. Soc. 19 (1999) 355.

- [20] A.L. Costa, C. Galassi, E. Roncari, J. Eur. Ceram. Soc. 22 (2002) 2093.
- [21] L.B. Kong, J. Ma, H. Huang, R.F. Zhang, J. Alloys Compd. 340 (2002) L1.
- [22] Powder Diffraction File No. 71-1176. International Centre for Diffraction Data, Newton Square, PA, 2000.
- [23] Powder Diffraction File No. 80-2493. International Centre for Diffraction Data, Newton Square, PA, 2000.
- [24] Powder Diffraction File No. 33-875. International Centre for Diffraction Data, Newton Square, PA, 2000.
- [25] S. Ananta, R. Tipakontitikul, T. Tunkasiri, Mater. Lett. 57 (2003) 2637
- [26] S. Ananta, R. Brydson, N.W. Thomas, J. Eur. Ceram. Soc. 19 (1999) 489







materials letters

Materials Letters 58 (2004) 2834-2841

www.elsevier.com/locate/matlet

# Effects of starting precursor and calcination condition on phase formation characteristics of Mg<sub>4</sub>Nb<sub>2</sub>O<sub>9</sub> powders

### Supon Ananta\*

Department of Physics, Faculty of Science, Chiang Mai University, Chiang Mai 50200, Thailand

Received 23 October 2003; received in revised form 19 April 2004; accepted 29 April 2004

Available online 19 June 2004

#### Abstract

A corundum-like phase of magnesium niobate,  $Mg_4Nb_2O_9$  (MN), has been synthesised by a rapid vibro-milling technique. Both magnesium carbonate and magnesium carbonate hydroxide pentahydrate have been investigated as magnesium precursors, with the formation of the  $Mg_4Nb_2O_9$  phase investigated as a function of calcination temperature, dwell time and heating rate by DTA and XRD. Moreover, morphology and phase composition have been determined via SEM and EDX techniques. The starting precursor and calcination temperature have been found to have a pronounced effect on the phase formation of the calcined  $Mg_4Nb_2O_9$  powders. It is seen that optimisation of calcination conditions can lead to a single-phase  $Mg_4Nb_2O_9$  in a hexagonal form. Among the two magnesium precursors, it is seen that the formation temperature of single-phase  $Mg_4Nb_2O_9$  powder was lower for the synthetic method employing magnesium carbonate hydroxide pentahydrate.

© 2004 Published by Elsevier B.V.

Keywords: Magnesium niobate; Mg<sub>4</sub>Nb<sub>2</sub>O<sub>9</sub>; Powder synthesis; Oxides; Calcination; X-ray diffraction

### 1. Introduction

The quest for optimal powder characteristics (controlled chemical composition, homogeneity, reactivity, particle size and shape) in the fabrication of materials has directed attention particularly towards powder production techniques. Magnesium niobate, Mg<sub>4</sub>Nb<sub>2</sub>O<sub>9</sub>, is one of the ordered corundum-type hexagonal structures which has been investigated as potential candidates for the synthesis of microwave dielectric materials [1]. It is also an important material which shows self-activated photoluminescence at room temperature [2]. You et al. [3] reported that cerium-doped Mg<sub>4</sub>Nb<sub>2</sub>O<sub>9</sub> exhibits improved luminescence properties. Recent work on the preparation of lead magnesium niobate,  $Pb(Mg_{1/3}Nb_{2/3})O_3$  or PMN [4,5], has also shown that Mg<sub>4</sub>Nb<sub>2</sub>O<sub>9</sub> is a better precursor than the columbite MgNb<sub>2</sub>O<sub>6</sub> [6] for the successful preparation of single-phase perovskite PMN which is becoming increasingly important for multilayer ceramic capacitor, electrostrictor and actuator applications [7,8].

\* Tel: +66-53-943376; fax: +66-53-357512. *E-mail address:* supon@chiangmai.ac.th (S. Ananta).

The evolution of a method to produce a particular powder of precise stoichiometry and desired properties is complex, depending on a number of variables such as raw materials, their purities, processing history, temperature, time, etc. For example, the synthesis of stoichiometric lead magnesium niobate (PMN) using Mg<sub>4</sub>Nb<sub>2</sub>O<sub>9</sub> (MN) as a key precursor by the conventional solid-state reaction [5] requires an additional amount of PbO to convert the pyrochlore phase to PMN. However, the effect of excess PbO on PMN preparation is still a matter of debate and appears to depend critically on the amount of PbO added [9-11]. Determination of the appropriate excess of PbO is currently a matter of trial and error. Furthermore, it has been reported that residual MgO present in the sample after the reaction has to be removed by treating with dilute nitric acid. Interestingly, a two-stage mixed oxide route has also been employed with minor modifications in the synthesis of Mg<sub>4</sub>Nb<sub>2</sub>O<sub>9</sub> itself [12,13]. In general, production of single-phase Mg<sub>4</sub>Nb<sub>2</sub>O<sub>9</sub> is not straightforward, as minor concentrations of the MgNb<sub>2</sub>O<sub>6</sub> phases and/or MgO inclusion are sometimes formed alongside the major phase of Mg<sub>4</sub>Nb<sub>2</sub>O<sub>9</sub> [13,14].

The development of  $Mg_4Nb_2O_9$  powders, to date, has not been as extensive as that of  $MgNb_2O_6$ . Much of the work concerning the compound  $Mg_4Nb_2O_9$  has been directed towards fabrication of PMN powder [4,5]. Only limited attempts have been made to improve the yield of  $Mg_4Nb_2O_9$  by optimising starting materials and processing steps. Whereas purity and reactivity are crucial, attention should also be given to the phase formation characteristics and processing–property relationships of this material, with a view to enhancing overall understanding. The purpose of this work was to compare the two simple mixed oxide synthetic routes of  $Mg_4Nb_2O_9$  formation and the characteristics of the resulting powders. The phase formation and morphology of the powder calcined at various conditions will be studied and discussed.

### 2. Experimental procedure

Mg<sub>4</sub>Nb<sub>2</sub>O<sub>9</sub> was synthesised by the solid-state reaction of appropriate amounts of magnesium carbonate, MgCO<sub>3</sub> (Aldrich, 99% purity) and niobium oxide, Nb<sub>2</sub>O<sub>5</sub> (Aldrich, 99% purity). In order to improve the reactivity of the magnesium starting precursor, an alternative route employing magnesium carbonate hydroxide pentahydrate, (MgCO<sub>3</sub>)<sub>4</sub>·Mg(OH)<sub>2</sub>·5H<sub>2</sub>O (Aldrich, 99% purity), was also investigated. These three oxide powders exhibited an average particle size in the range of 3.0–10.0 μm. The following reaction sequences are proposed for the formation of Mg<sub>4</sub>Nb<sub>2</sub>O<sub>9</sub>:

(a) The mixed oxide route I

$$4MgCO_3 + Nb_2O_5 \Rightarrow Mg_4Nb_2O_9 + 4CO_2 \tag{1}$$

(b) The mixed oxide route II

$$4[(MgCO_3)_4 \cdot Mg(OH)_2 \cdot 5H_2O] + 5Nb_2O_5$$
  

$$\Rightarrow 5Mg_4Nb_2O_9 + 16CO_2 + 24H_2O.$$
 (2)

A McCrone vibro-milling technique was employed in order to combine mixing capability with a significant time saving (only 30 min instead of 24 h, as required in conventional ball-milling [5,13,14]). The milling operation was carried out in isopropanal. High-purity corundum cylindrical media were used as the milling media. After drying at 120 °C, various calcination conditions, i.e. temperatures ranging from 500 to 950 °C, dwell times ranging from 0.5 to 6 h and heating/cooling rates ranging from 5 to 30 °C/min, were applied in order to investigate the formation of Mg<sub>4</sub>Nb<sub>2</sub>O<sub>9</sub>. The reactions of the uncalcined powders taking place during heat treatment were investigated by thermal gravimetric and differential thermal analysis (TG-DTA, Shimadzu) using a heating rate of 10 °C/min in air from room temperature up to 1100 °C. Calcined powders were subsequently examined by room

temperature X-ray diffraction (XRD; Philips PW 1729 diffractometer) using Ni-filtered  $\text{CuK}_{\alpha}$  radiation to identify the phases formed and optimum calcination conditions for the manufacture of  $\text{Mg}_4\text{Nb}_2\text{O}_9$  powder. The powder morphology was analyzed using scanning electron microscopy (SEM; JEOL JSM-840A). The chemical compositions of the phases formed were elucidated by an energy-dispersive X-ray (EDX) analyser with an ultrathin window. EDX spectra were quantified with the virtual standard peaks supplied with the Oxford Instruments eXL software.

#### 3. Results and discussion

TGA and DTA results for both MN precursors are shown in Figs. 1 and 2, respectively. In general, similar thermal characteristics are observed in both precursors. As shown in Fig. 1, the precursor prepared via both synthetic routes demonstrates two distinct weight losses below 600 °C. The first weight loss occurs below 200 °C and the second one above 250 °C. In the temperature range from room temperature to ~ 150 °C, both samples show small exothermic peaks in the DTA curves at ~ 120 °C (Fig. 2), which are related to the first weight loss. These DTA peaks can be attributed to the decomposition of the organic species from the milling process [15]. In comparison between the two synthetic routes, after the first weight loss, the precursor derived from route II (b-curve) shows a more steady weight loss over the temperature range of ~ 150-250 °C, followed by a much more sharp fall in specimen weight with increasing temperature from 250 to 350 °C. This precursor also exhibits a slightly smaller overall weight loss ( $\sim 3.75\%$ ) than that of the route I ( $\sim 4.00\%$ ). This may be accounted for by the fact that the magnesium carbonate hydroxide pentahydrate starting precursor is highly hygroscopic and is able to adsorb moisture quickly from the atmosphere [16].

Corresponding to the second fall in specimen weight, by increasing the temperature up to ~ 800 °C, the solid-state reaction occurs between magnesium source and niobium oxide. The broad exothermic characteristic in both DTA curves represents that reaction, which has a maximum at ~ 580 and 500 °C for routes I and II, respectively. Moreover, another exothermic peaks with maximum at ~ 690 and 660 °C for routes I and II, respectively, were also observed in these profiles. These temperatures have been obtained from the calibration of the sample thermocouple. It is to be noted that there is no obvious interpretation of the peaks, although it is likely to correspond to a phase transition reported by a number of workers [14.17]. The different temperature, intensities and shapes of the thermal peaks for the two precursors here probably are related to the different natures of the starting precursors and, consequently, caused by the removal of organic species and rearrangement of species differently bounded in the

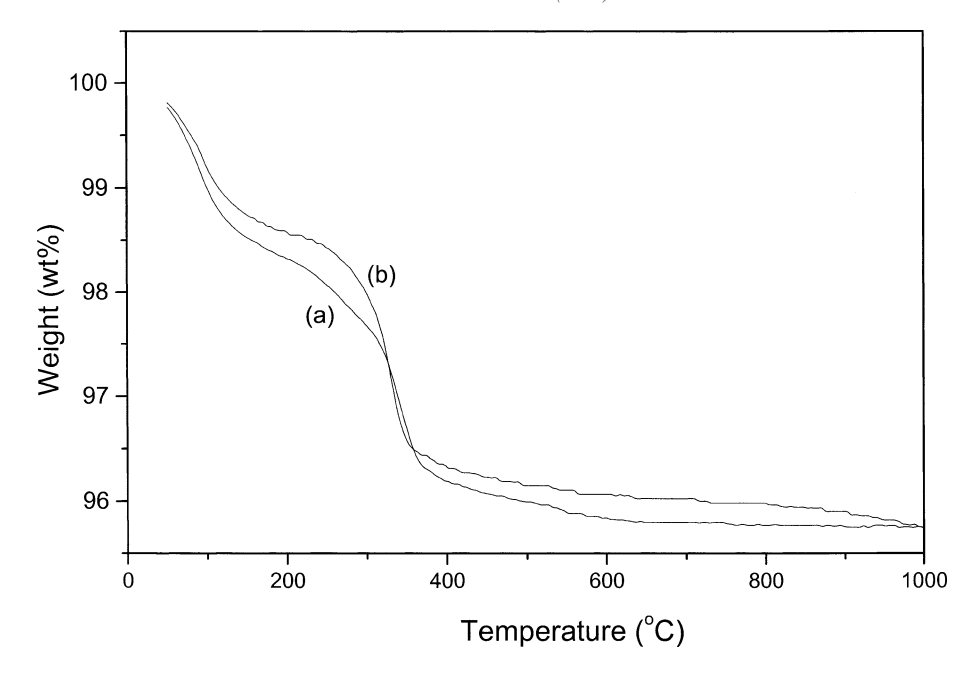


Fig. 1. TGA curves of the two MN precursors; (a) route I and (b) route II.

network. These data were used to define the range of temperatures for XRD investigation to between 500 and 950  $^{\circ}\mathrm{C}.$ 

To further study the phase development with increasing calcination temperature in each of the two precursors, they were calcined for 2 h in air at various temperatures, up to 950 °C, followed by phase analysis using XRD. As shown in Figs. 3 and 4, for the powders calcined at 500 °C, only X-ray peaks of MgO and Nb<sub>2</sub>O<sub>5</sub> are present, indicating that the decomposition processes of both magnesium sources and the elimination of their organic species occur below 500 °C, which agrees with the result of TG-DTA determined previously. The strongest reflections of the mixed

phases of MgO and  $Nb_2O_5$  can be correlated with JCPDS file no. 71-1176 [18] and 28-0317 [19], respectively.

From Fig. 3, it is seen that little crystalline phase of MgNb<sub>2</sub>O<sub>6</sub> ( $\nabla$ ), earlier reported by many researchers [6,14,17], was found at 600 °C as separated phases in the powder synthesised by route I. In a remarkable contrast, the columbite-type MgNb<sub>2</sub>O<sub>6</sub> becomes the predominant phase in the powder synthesised by route II at 600 °C, as shown in Fig. 4. This could be attributed to the different reactivity of the employed starting magnesium precursors. This MgNb<sub>2</sub>O<sub>6</sub> phase (JCPDS file no. 33-875 [20]) has a columbite-type structure with an orthorhombic unit cell (a=3.78 Å and c=9.51 Å), space group  $I4_1/amd$  (no.

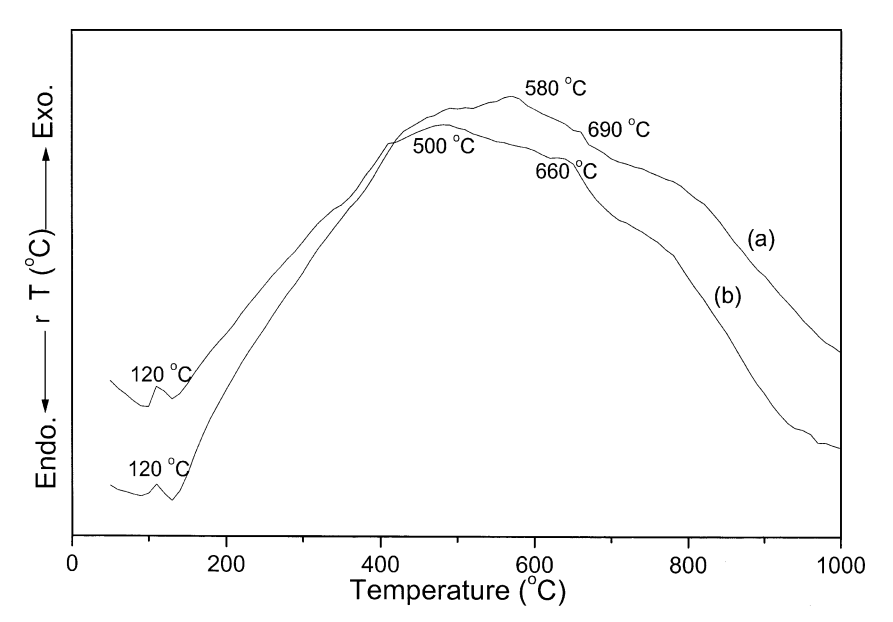


Fig. 2. DTA curves of the two MN precursors; (a) route I and (b) route II.

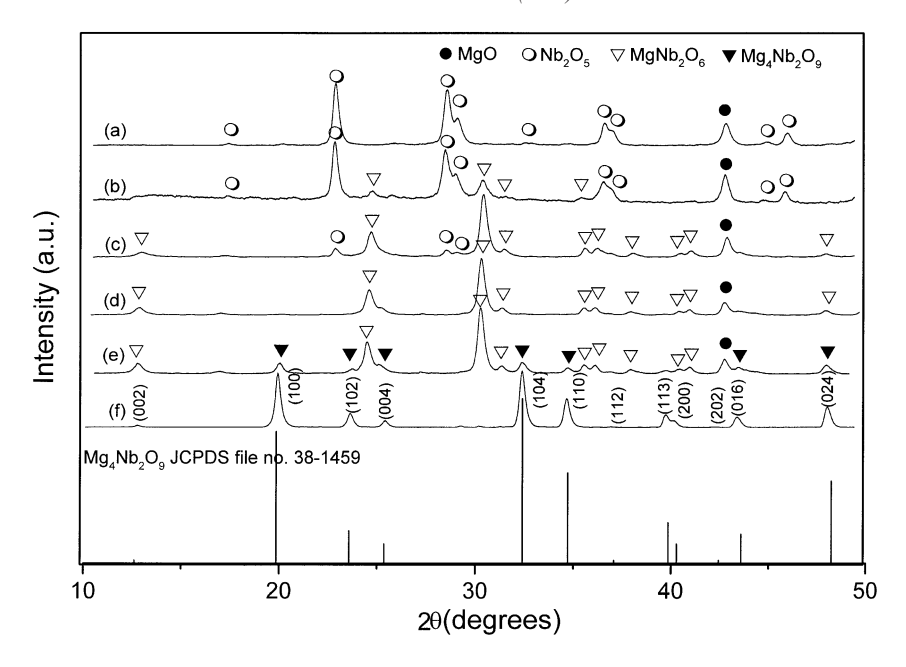


Fig. 3. Powder XRD patterns of the calcined MN powder (route I) at (a) 500  $^{\circ}$ C, (b) 600  $^{\circ}$ C, (c) 700  $^{\circ}$ C, (d) 800  $^{\circ}$ C, (e) 900  $^{\circ}$ C and (f) 950  $^{\circ}$ C, for 2 h with heating/cooling rates of 10  $^{\circ}$ C/min.

141), in agreement with literature [14,17,21]. As the temperature increased to 700 °C, the intensity of the MgNb<sub>2</sub>O<sub>6</sub> peaks in the powder synthesised by route I was further enhanced (Fig. 3), whereas some new peaks ( $\blacktriangledown$ ) of the desired Mg<sub>4</sub>Nb<sub>2</sub>O<sub>9</sub> started to appear, mixing with MgNb<sub>2</sub>O<sub>6</sub> and MgO phases in the powder synthesised by route II (Fig. 4). To a first approximation, this Mg<sub>4</sub>Nb<sub>2</sub>O<sub>9</sub> phase (JCPDS file no. 38-1459 [22]) has a corundum-type structure with a hexagonal unit cell (a=516 pm and c=1402 pm), space

group  $P\bar{3}c1$  (no. 165), consistent with other researchers [5,23]. From Figs. 3 and 4, it is seen that the peaks corresponding to Nb<sub>2</sub>O<sub>5</sub> phase were completely eliminated after calcination at 800 and 700 °C in the powders synthesised by routes I and II, respectively. These observations are associated to the DTA peaks found at the same temperature range within the broad exothermic effects in Fig. 2.

Upon calcination at 800  $^{\circ}$ C, the major phase of  $Mg_4Nb_2O_9$  has been clearly identified in the powders

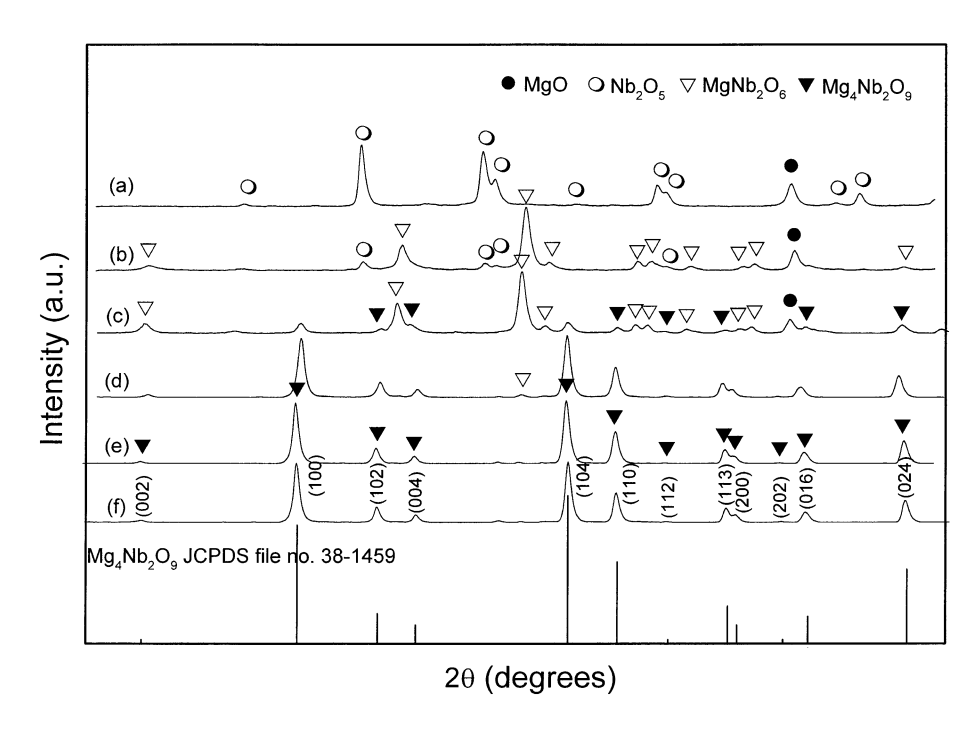


Fig. 4. Powder XRD patterns of the calcined MN powder (route II) at (a) 500  $^{\circ}$ C, (b) 600  $^{\circ}$ C, (c) 700  $^{\circ}$ C, (d) 800  $^{\circ}$ C, (e) 900  $^{\circ}$ C and (f) 950  $^{\circ}$ C, for 2 h with heating/cooling rates of 10  $^{\circ}$ C/min.

synthesised by route II and most of second phases were eliminated. In particular, the peaks corresponding to MgO disappeared (not detectable by XRD). After calcination at 900 °C, little crystalline phase of Mg<sub>4</sub>Nb<sub>2</sub>O<sub>9</sub> was found to coexist along with the MgNb<sub>2</sub>O<sub>6</sub> and MgO phases in precursor route I. However, in comparison, a single phase of Mg<sub>4</sub>Nb<sub>2</sub>O<sub>9</sub> is already formed when the precursor synthesised by route II was calcined at 900 °C. An essentially monophasic Mg<sub>4</sub>Nb<sub>2</sub>O<sub>9</sub> of corundum structure is also obtainable in powder synthesised by route I when the calcination temperature was extended to 950 °C, which is 50 °C higher than that observed in precursor route II. According to the TG-DTA results previously discussed, a slight drop in weight is also observed above 900 °C for the route II sample (Fig. 1) associated with little DTA peaks at the same temperature range (Fig. 2) and may be attributed to the crystallization of this Mg<sub>4</sub>Nb<sub>2</sub>O<sub>9</sub> phase.

It is well established that the columbite-type  $MgNb_2O_6$  tends to form together with the corundum-type  $Mg_4Nb_2O_9$ , depending on calcination conditions [14,17]. In the work reported here, evidence for the formation of  $MgNb_2O_6$  phase, which coexists with the  $Mg_4Nb_2O_9$  phase, is found after calcination at low temperature (  $\sim 700-900~^{\circ}C$ ). No evidence of  $Mg_5Nb_4O_{15}$  was found, nor was there any indication of the orthorhombic phase of  $Mg_{2/3}Nb_{11(1/3)}O_{29}$  [24,25] being present. Apart from the calcination temperature, the effect of dwell time was also found to be quite significant (Figs. 5 and 6). It is seen that the single phase of  $Mg_4Nb_2O_9$  (yield of 100% within the limitations of the XRD technique) was found to be possible only in powders, calcined at 950  $^{\circ}C$  (route I) and 900  $^{\circ}C$  (route II), with dwell time of 2 h or more. The formation temperature and

dwell times for high-purity  $Mg_4Nb_2O_9$  observed in the powders derived from a combination of a mixed oxide synthetic route and a rapid vibro-milling technique (especially with magnesium carbonate hydroxide pentahydrate as the precursor) are much lower than those reported for the powders prepared via many other conventional mixed oxide methods [3–5,13]. In the present study, an attempt was also made to calcine both precursors under various heating/cooling rates (Fig. 7). In this connection, it is shown that the yield of  $Mg_4Nb_2O_9$  phase did not vary significantly with different heating/cooling rates ranging from 5 to 30 °C/min, in good agreement with the early results reported by Ananta et al. [15] for the mixture of the two kinds of refractory oxides.

Based on the DTA and XRD data, it may be concluded that, over a wide range of calcination conditions, singlephase Mg<sub>4</sub>Nb<sub>2</sub>O<sub>9</sub> cannot be straightforwardly formed via a solid-state mixed oxide synthetic route. The experimental work carried out here suggests that the optimal calcination conditions for single-phase Mg<sub>4</sub>Nb<sub>2</sub>O<sub>9</sub> are 950 °C (route I) and 900 °C (route II), for 2 h with heating/cooling rates as fast as 30 °C/min. The optimised formation temperature of single-phase Mg<sub>4</sub>Nb<sub>2</sub>O<sub>9</sub> was lower for the route II method probably due to the higher reactivity of the magnesium carbonate hydroxide pentahydrate precursor. Therefore, in general, the methodology presented in this work provides a simple method for preparing corundum Mg<sub>4</sub>Nb<sub>2</sub>O<sub>9</sub> powders via a solid-state mixed oxide synthetic route. It is interesting to note that, by using either magnesium carbonate or magnesium carbonate hydroxide pentahydrate as a magnesium source, with optimal calcination conditions, the reproducible, lower cost and faster process involving vibromilling can produce high-purity corundum Mg<sub>4</sub>Nb<sub>2</sub>O<sub>9</sub> (with

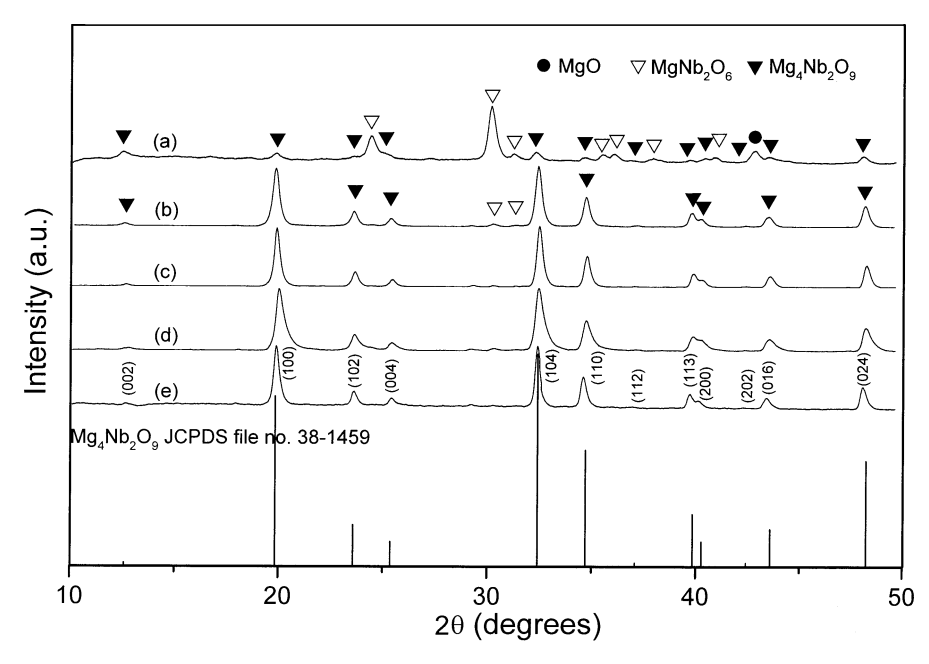


Fig. 5. Powder XRD patterns of the calcined MN powder (route I) at 950 °C, for (a) 0.5 h, (b) 1 h, (c) 2 h, (d) 4 h and (e) 6 h, with heating/cooling rates of 10 °C/min.

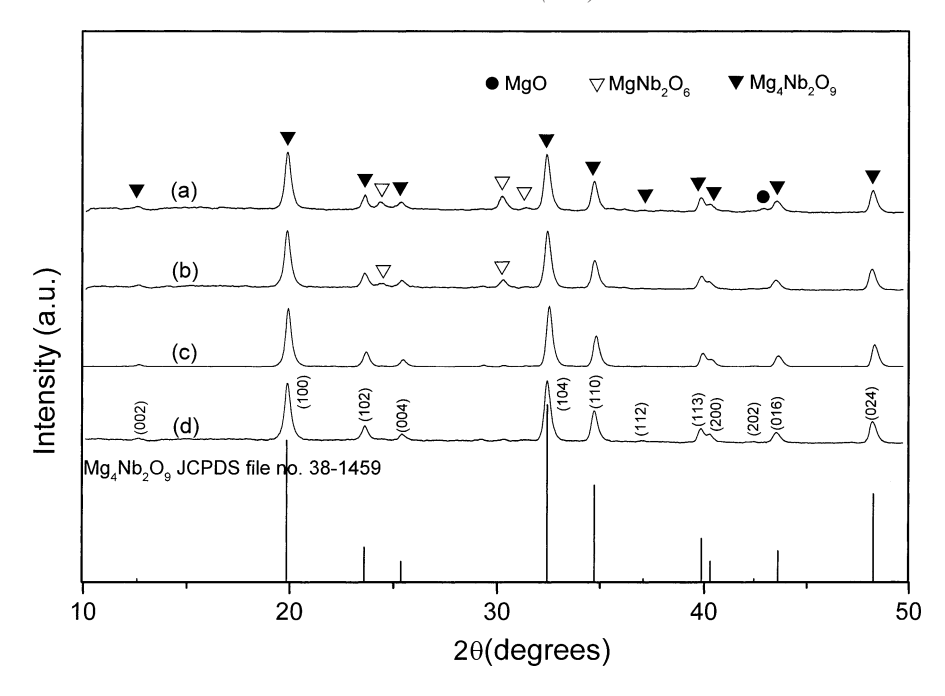


Fig. 6. Powder XRD patterns of the calcined MN powder (route II) at 900 °C, for (a) 0.5 h, (b) 1 h, (c) 2 h and (d) 6 h, with heating/cooling rates of 10 °C/min.

impurities undetected by XRD technique) from inexpensive commercially available raw materials.

The morphological evolution during calcination was investigated by scanning electron microscopy (SEM). Fig. 8 shows the morphologies of Mg<sub>4</sub>Nb<sub>2</sub>O<sub>9</sub> powders synthesised by route I (a and b) and II (c and d). In general, the particles are agglomerated and basically irregular in shape, with a substantial variation in particle size, particularly in

samples synthesised by route I. It is seen that large particle agglomerates occur in powders route I, although the primary particles in these powders could be identified at high magnification (Fig. 8b), ranging in diameter from about 0.35 to 1.00  $\mu$ m. In comparison, the route II-derived Mg<sub>4</sub>Nb<sub>2</sub>O<sub>9</sub> powders, which are of dimension in the range of  $\sim 0.25-1.00~\mu$ m (Fig. 8d), are much finer in particle size and lower in particle agglomeration than the route I-

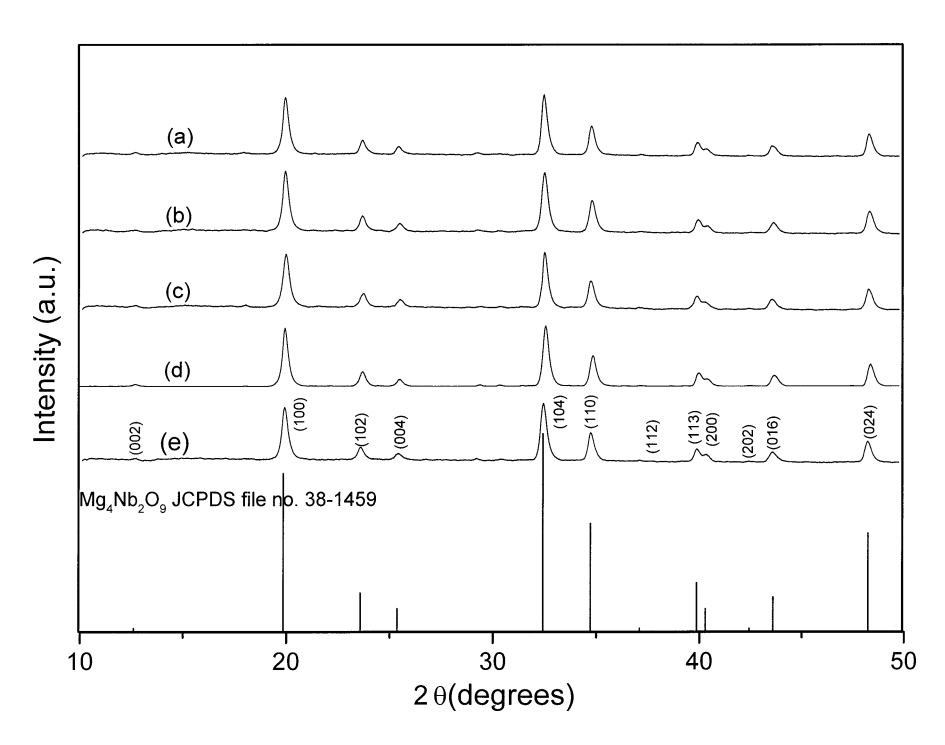


Fig. 7. Powder XRD patterns of the calcined MN powders; route I at 950 °C for 2 h, with heating/cooling rates of (a) 5 °C/min, (b) 10 °C/min and (c) 30 °C/min, and route II at 900 °C for 2 h, with heating/cooling rates of (d) 5 °C/min and (e) 30 °C/min.

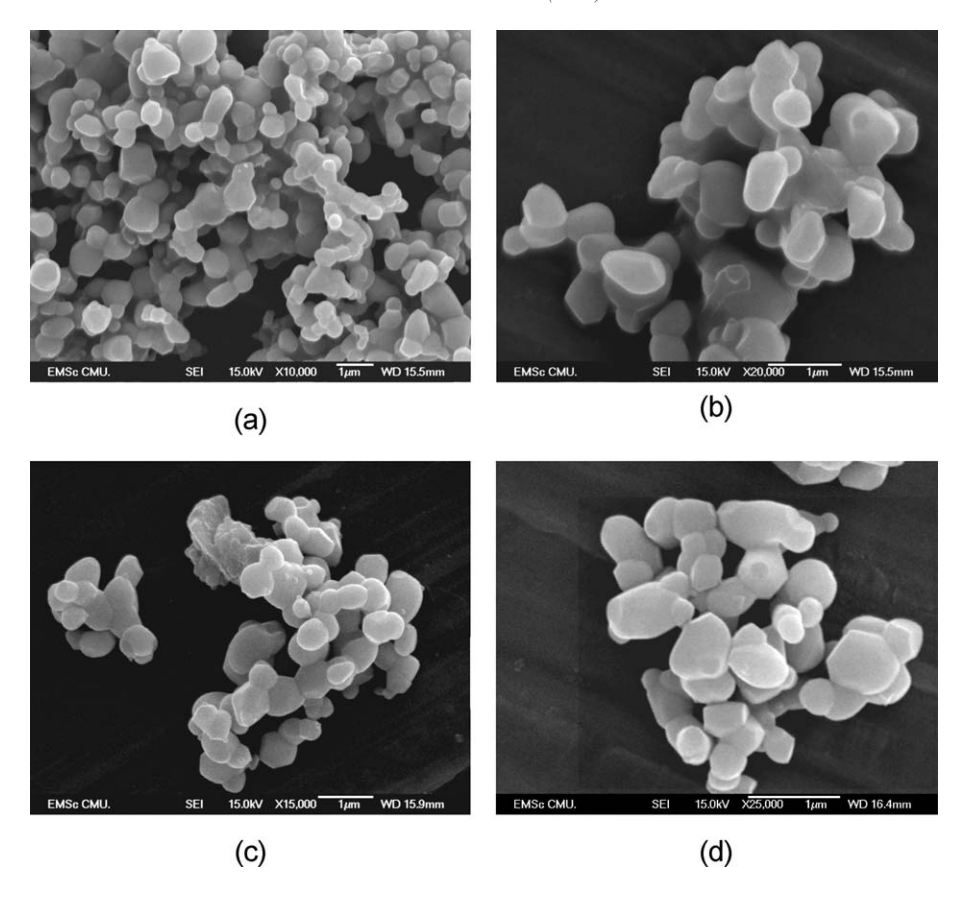


Fig. 8. SEM micrographs of the MN powders calcined at their optimised conditions for (a and b) route I and (c and d) route II.

derived powders. The particle size of Mg<sub>4</sub>Nb<sub>2</sub>O<sub>9</sub> powder with finer particle size is regarded to have advantage for better reactivity. Energy dispersive X-ray (EDX) analysis showed the calcined compositions of the powder calcined at their optimised conditions to be Mg<sub>4</sub>Nb<sub>2</sub>O<sub>9</sub>, in agreement with XRD results.

#### 4. Conclusions

It has been shown that pure corundum Mg<sub>4</sub>Nb<sub>2</sub>O<sub>9</sub> powders can be formed by the reaction of niobium oxide with either magnesium carbonate or magnesium carbonate hydroxide pentahydrate at about 800-900 °C. A combination of a rapid vibro-milling technique, together with a careful calcination treatment, represents significant time savings compared to synthetic procedures currently advocated and requires only relatively impure and inexpensive raw materials. Evidence for the formation of a columbite MgNb<sub>2</sub>O<sub>6</sub> phase, which coexists with the corundum Mg<sub>4</sub>Nb<sub>2</sub>O<sub>9</sub> phase, is found at calcination temperature ranging from 700 to 900 °C. Among the two methods, it is seen that lower optimised calcination temperature for the production of pure Mg<sub>4</sub>Nb<sub>2</sub>O<sub>9</sub> powder may be obtained by using magnesium carbonate hydroxide pentahydrate precursor.

#### Acknowledgements

The author gratefully acknowledges the Thailand Research Fund (TRF) for financial support.

- H. Ogawa, A. Kan, S. Ishihara, Y. Higashida, J. Eur. Ceram. Soc. 23 (2003) 2485.
- [2] A. Wachtel, J. Electrochem. Soc. 111 (1964) 534.
- [3] Y.C. You, N. Park, K.H. Jung, H.L. Park, K.C. Kim, S.I. Mho, T.W. Kim, J. Mater. Sci. Lett. 13 (1994) 1682.
- [4] P.A. Joy, K. Sreedhar, J. Am. Ceram. Soc. 80 (1997) 770.
- [5] C.H. Lu, H.S. Yang, Mater. Sci. Eng. B84 (2001) 159.
- [6] S.L. Swartz, T.R. Shrout, Mater. Res. Bull. 17 (1982) 1245.
- [7] G. Haertling, J. Am. Ceram. Soc. 82 (1999) 797.
- [8] K. Uchino, Piezoelectrics and Ultrasonic Applications, Kluwer, Deventer, 1998.
- [9] E. Goo, T. Yamamoto, K. Okazaki, J. Am. Ceram. Soc. 69 (1986) C-188.
- [10] D.H. Kang, K.H. Yoon, Ferroelectrics 87 (1988) 255.
- [11] P.A. Joy, Mater. Lett. 32 (1997) 347.
- [12] Y.C. You, H.L. Park, Y.G. Song, H.S. Moon, G.C. Kim, J. Mater. Sci. Lett. 13 (1994) 1487.
- [13] K. Sreedhar, N.R. Pavaskar, Mater. Lett. 53 (2002) 452.
- [14] N.K. Kim, Mater. Lett. 32 (1997) 127.
- [15] S. Ananta, R. Tipakontitikul, T. Tunkasiri, Mater. Lett. 57 (2003) 2637.

- [16] S. Ananta, R. Brydson, N.W. Thomas, J. Eur. Ceram. Soc. 20 (2000) 2315
- [17] S. Ananta, R. Brydson, N.W. Thomas, J. Eur. Ceram. Soc. 19 (1999) 355.
- [18] Powder Diffraction File no. 71-1176, International Centre for Diffraction Data, Newton Square, PA, 2000.
- [19] Powder Diffraction File no. 28-317, International Centre for Diffraction Data, Newton Square, PA, 2000.
- [20] Powder Diffraction File no. 33-875, International Centre for Diffraction Data, Newton Square, PA, 2000.
- [21] Y.S. Hong, H.B. Park, S.J. Kim, J. Eur. Ceram. Soc. 18 (1998) 613.
- [22] Powder Diffraction File no. 38-1459, International Centre for Diffraction Data, Newton Square, PA, 2000.
- [23] N. Kumada, K. Taki, N. Kinomura, Mater. Res. Bull. 35 (2000) 1017.
- [24] S. Pagola, R.E. Carbonio, J.A. Alonso, M.T. Fernández-Díaz, J. Solid State Chem. 134 (1997) 76.
- [25] E. Brück, R.K. Route, R.J. Raymakers, R.S. Feigelson, J. Cryst. Growth 128 (1993) 842.





Materials Letters 58 (2004) 853-858



### Chemical synthesis of magnesium niobate powders

L. Srisombat<sup>a</sup>, Supon Ananta<sup>b,\*</sup>, S. Phanichphant<sup>a</sup>

<sup>a</sup>Department of Chemistry, Faculty of Science, Chiang Mai University, Chiang Mai 50200, Thailand <sup>b</sup>Department of Physics, Faculty of Science, Chiang Mai University, Chiang Mai 50200, Thailand

Received 6 January 2003; received in revised form 8 July 2003; accepted 9 July 2003

#### Abstract

Magnesium niobate  $(MgNb_2O_6)$  powders in orthorhombic form have been successfully prepared via an oxalate synthetic route. Solutions of magnesium chloride hexahydrate and niobium pentachloride were used as the starting materials in the synthesis of  $MgNb_2O_6$  powders. The formation mechanism of  $MgNb_2O_6$  was clarified by TG-DTA, FT-IR and X-ray diffraction (XRD). The morphology of the formed powders was examined by scanning electron microscopy (SEM). It was found that the second phases of MgO,  $Nb_2O_5$  and  $Mg_{0.66}Nb_{1.33}O_{29}$  tend to form together with  $MgNb_2O_6$ , depending on calcination conditions. However, single-phase  $MgNb_2O_6$  powders consisting of nanoparticles 100-300 nm were successfully obtained for a calcination temperature of 750 °C for 13 h with the introduction of pre-firing (750 °C/2 h) and remixing processes.

© 2003 Elsevier B.V. All rights reserved.

Keywords: MgNb<sub>2</sub>O<sub>6</sub>; Magnesium niobate; Columbite; Powder synthesis; Calcination; Phase development

#### 1. Introduction

Lead magnesium niobate, Pb(Mg<sub>1/3</sub>Nb<sub>2/3</sub>)O<sub>3</sub> or PMN, is one of the perovskite-type relaxor ferroelectric materials which has been investigated extensively as potential candidates for electroceramic components such as multilayer ceramic capacitors and electrostrictive actuators [1–3]. It is of interest owing to its high dielectric constant with flat temperature dependence and low firing temperature [2,3]. However, a practical limitation to the utilisation of this compound in device applications has been the lack of a simple, reproducible preparation technique for a pure perovskite phase with consistent properties. The formation of PMN perovskite is often accompanied by the occurrence of one or more undesirable pyrochlore phases, which significantly degrades the dielectric properties of PMN [4–6].

A breakthrough was made in 1982 by Swartz and Shrout [7], who introduced a two-stage process to PMN synthesis bypassing the formation of pyrochlore phases, called the Columbite method. In this process, the constituents MgO and  $\mathrm{Nb_2O_5}$  are first mixed and reacted together to form

magnesium niobate (MgNb<sub>2</sub>O<sub>6</sub>), prior to mixing and reacting with PbO in the second step of calcinations at elevated temperature. Interestingly, a two-stage mixed oxide route has been employed with minor modifications in the synthesis of MgNb<sub>2</sub>O<sub>6</sub> itself [8,9]. In general, production of single-phase MgNb<sub>2</sub>O<sub>6</sub> is not straightforward, as minor concentrations of the phase Mg<sub>4</sub>Nb<sub>2</sub>O<sub>9</sub> and/or MgO are sometimes formed alongside the major phase of MgNb<sub>2</sub>O<sub>6</sub> [10]. The solid-state reaction among constituent oxides of MgO and Nb<sub>2</sub>O<sub>5</sub> at an elevated temperature always results in inhomogeneous composition, irregular grain shape, and larger grain size with broad distribution [9]. Moreover, the formation of magnesium niobate phase required long heat treatment, e.g., 20, 22, and 24 h [8-10]. Hence, the quest for other potential powder production techniques is needed. Although a number of investigations on powder preparation using chemical processing routes have been made and their excellent capability have been widely demonstrated, only limited attention has been made to improve the yield of magnesium niobate by employing the chemical processes [11,12]. Thus, in the present study, the primary attention was aimed towards the preparation of homogeneous and stoichiometric MgNb<sub>2</sub>O<sub>6</sub> powders by oxalate co-precipitation. The powder characteristics of the oxalate-derived MgNb<sub>2</sub>O<sub>6</sub> has also been thoroughly investigated.

<sup>\*</sup> Corresponding author. Tel.: +66-5394-3376; fax: +66-5335-7512. *E-mail address:* supon@chiangmai.ac.th (S. Ananta).

#### 2. Method

#### 2.1. Sample preparation

MgNb<sub>2</sub>O<sub>6</sub> was synthesised by an oxalate synthetic route as shown schematically in Fig. 1. In this method, the complexation of metallic ions was brought about by using diethyl oxalate and ammonium hydroxide aqueous solution. Magnesium chloride hexahydrate, MgCl<sub>2</sub>.6H<sub>2</sub>O (98.0%, Fluka), niobium pentachloride, NbCl<sub>5</sub> (99%, Aldrich) and hydrogen peroxide, H<sub>2</sub>O<sub>2</sub> (30%, Carbo Erba) were used as reagents. After dissolving magnesium chloride in deionized water, niobium chloride, dissolved in 30% H<sub>2</sub>O<sub>2</sub> aqueous solution was mixed in a molar ratio of 1:2. An excess amount of diethyl oxalate was added in a small amount at a time into the solution, which was heated at 80 °C with constant stirring for 20 min. After adjusting the pH of the

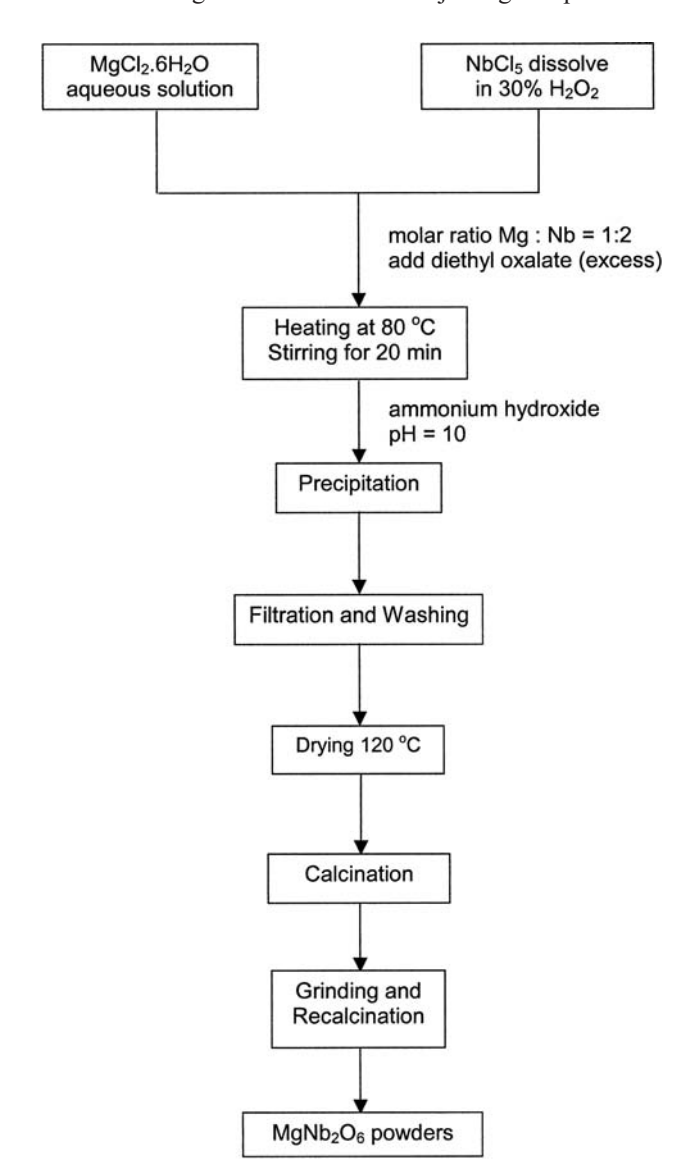


Fig. 1. Oxalate processing flow diagram for the preparation of  $MgNb_2O_6$  powders.

final solution to 10 with dilute ammonium hydroxide, fine pale-brown powders were obtained. Further heating for 10 min was continued to ensure complete precipitation. The sample was filtered and washed with deionized water for several times and then with ethanol. The resulting solid was dried at 120 °C for 2 h in an oven before high temperature processing.

#### 2.2. Sample characterization

The reactions taking place during heat treatment were investigated by thermal gravimetric and differential thermal analysis (TG-DTA, Shimadzu) using a heating rate of 10 °C min<sup>-1</sup> in the temperature range from 25 to 1100 °C. Dried powders (35 mg) were placed into a platinum holder and measured in air, with alumina powder as a reference. The infrared absorption spectra of the oxalate precursors were performed on a Nicolet FT-IR spectrometer (Model 510). Samples were in the form of mixed KBr/ metal-oxalate complex disks. Having established the optimum firing temperature range via TG-DTA and FT-IR results, various calcination conditions, i.e. temperature ranging from 600 to 1300 °C with constant soaking time of 2 h and heating/cooling rate of 10 °C min<sup>-1</sup>, were selected, in order to investigate the formation of magnesium niobate. Calcined powders were examined by X-ray diffraction (XRD; Philips PW 1700 diffractometer) using CuK<sub>α</sub> radiation to identify the phases formed and optimum calcination conditions for the formation of magnesium niobate powders. Powder morphologies and grain sizes were directly imaged using scanning electron microscopy (SEM; JEOL JSM-840A).

#### 3. Results and discussion

The results of TG-DTA measurements for the dried precipitate are shown in Fig. 2. The endotherm below 100 °C is probably originated from the removal of the residual of solvent and the second peak, near ~ 300 °C, may be attributed to the decompositon of oxalate group corresponding to subsequent condensations. The largest mass lost and a large exotherm were observed between  $\sim 250$  and  $\sim 400$  °C (8.8%), corresponding to the combustion of the remaining oxalate groups. The decomposition went on further to give exothermic response at  $\sim 600$  °C, which might be due to the crystallisation of columbite phase. No significant weight loss was observed for temperatures higher than 600 °C in the TG-curve, indicating the minimum firing temperature to get organic-free MgNb<sub>2</sub>O<sub>6</sub> powder was in good agreement with those reported earlier [11,12].

In order to monitor the formation mechanism of metal—oxalate complex, FT-IR spectra were taken at room temperature for powders thermally treated at various temperatures. From Fig. 3, it is seen that the carboxylate group

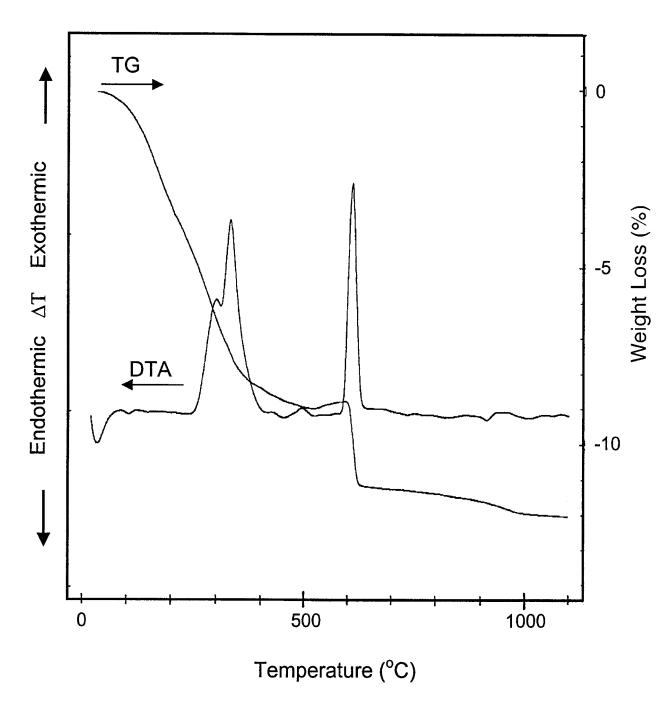


Fig. 2. TG-DTA curves of the dried precipitate measured at a heating rate of 10  $^{\circ}$ C min  $^{-1}$ .

coordinated to metal gave rise to symmetric and asymmetric strethching bands at 1406 and 1600 cm<sup>-1</sup>, respectively, whereas the free carboxylic acid showed a typical absorption band at 1375–1705 cm<sup>-1</sup>. The large metal oxide

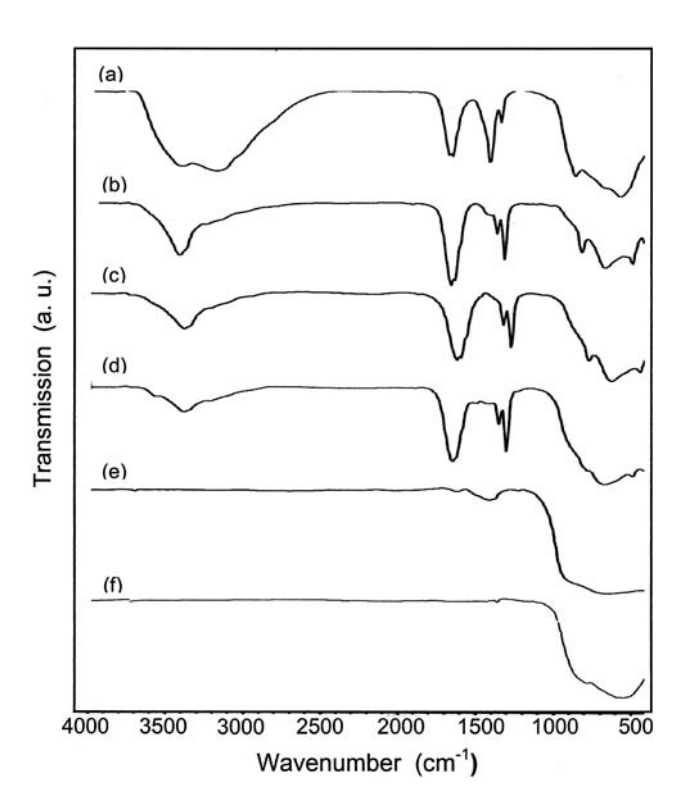


Fig. 3. FT-IR spectra of the dried precipitate fired at various temperatures: (a) uncalcined, (b) 200  $^{\circ}$ C, (c) 300  $^{\circ}$ C, (d) 400  $^{\circ}$ C, (e) 500  $^{\circ}$ C and (f) 600  $^{\circ}$ C.

band was detected at 400–900 cm<sup>-1</sup>. By increasing the firing temperature, both carboxylate and carbonate bands decreased significantly and disappears at 600 °C, which was also consistent with earlier work of Hong et al. [11]. The FT-IR spectra results indicate that MgNb<sub>2</sub>O<sub>6</sub> already has been formed in the powder calcined at 600 °C, in good agreement with the TG-DTA determined previously (Fig. 2).

To further study the phase development with increasing calcination temperature in the precipitated powders, they were calcined for 2 h in air at various temperatures, up to 1300 °C, followed by phase analysis using XRD. From Fig. 4, it is seen that the powder fired at 600 °C consisted of the mixed phases of MgO and Nb<sub>2</sub>O<sub>5</sub> which could be matched with JCPDS file no. 71-1176 and 28-0317, respectively. Moreover, very little crystalline phase of MgNb<sub>2</sub>O<sub>6</sub> with orthorhombic symmetry (JCPDS file no. 33-0875) was also

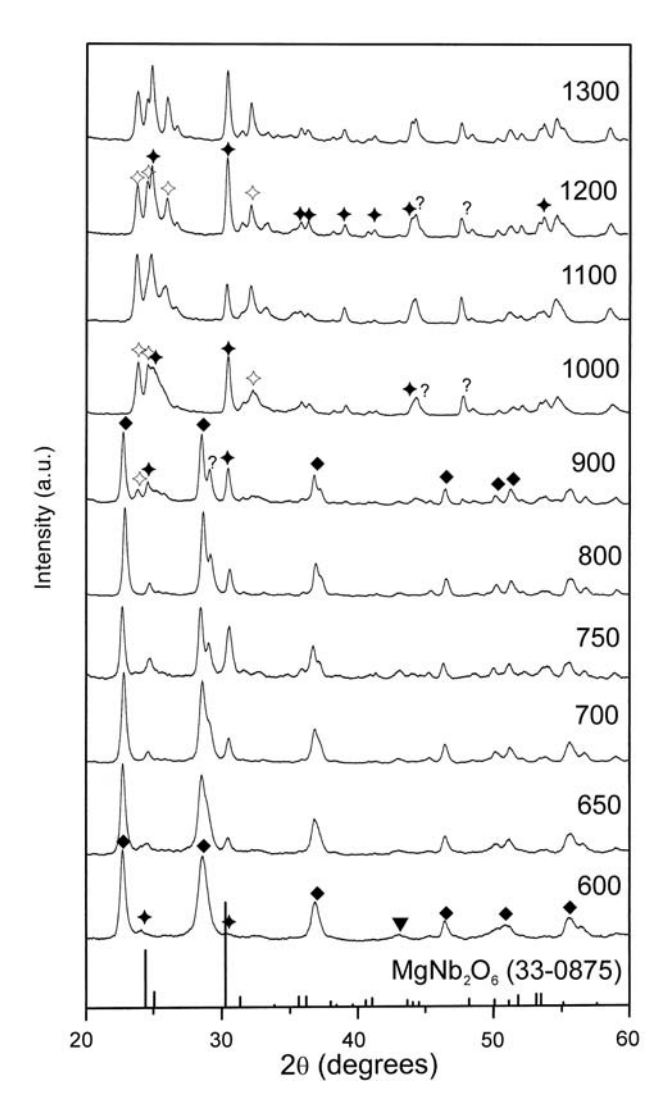


Fig. 4. Powder XRD patterns of the samples calcined at various temperatures for 2 h ( $\nabla = MgO$ ;  $\Phi = Nb_2O_5$ ;  $\Phi = MgNb_2O_6$ ;  $\diamondsuit = Mg_{0.66}Nb_{11.33}O_{29}$ ; ?= unknown phase).

found as separated phases. This observation agrees well with those derived from our TG-DTA, FT-IR and other researchers [13-15]. As the temperature increased to 800 °C, the intensity of the columbite MgNb<sub>2</sub>O<sub>6</sub> peaks was further enhanced. After calcination at 900 °C, some new peak (◊) of  $Mg_{0.66}Nb_{11.33}O_{29}$  (JCPDS file no. 26-1219) and unknown phase (?) started to appear, mixing with MgNb<sub>2</sub>O<sub>6</sub>, Nb<sub>2</sub>O<sub>5</sub> and MgO phases. Calcination at 1000 °C resulted in a further development of  $Mg_{0.66}Nb_{11.33}O_{29}$  phase and most of second phases were eliminated. In particular, the peaks corresponding to Nb<sub>2</sub>O<sub>5</sub> disappeared (not detectable), revealing that Nb<sub>2</sub>O<sub>5</sub> has completely reacted with MgO phase. In conventional mixed oxide route, major phase of MgNb<sub>2</sub>O<sub>6</sub> was obtained for a calcination temperature above 1100 °C [9,13]. However, for the present work, there are no significant differences between the powders calcined at temperatures ranging from 1100 to 1300 °C. Further increase of the calcination temperature to 1300 °C does not result in very much increase in the amount of Mg<sub>0.66</sub>Nb<sub>11.33</sub>O<sub>29</sub>, whereas MgNb<sub>2</sub>O<sub>6</sub> remains unchanged.

As expected, there is evidence that, even for a wide range of calcination conditions, single-phase  $MgNb_2O_6$  cannot easily be produced, in agreement with the literature [8–12].

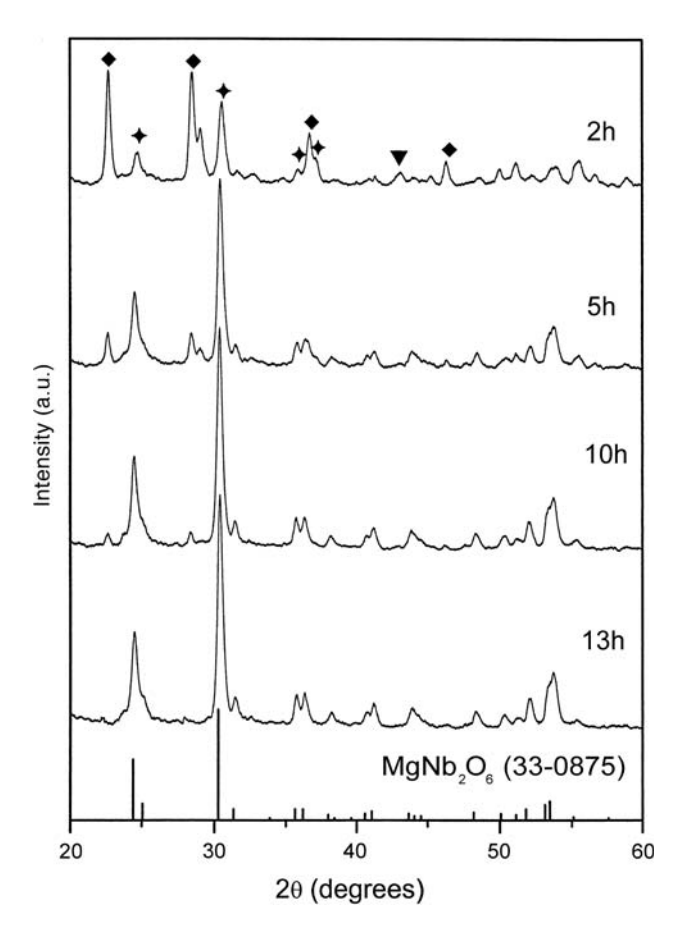
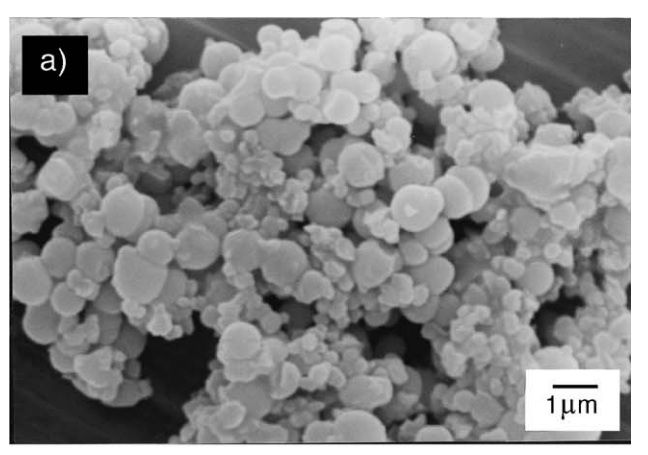
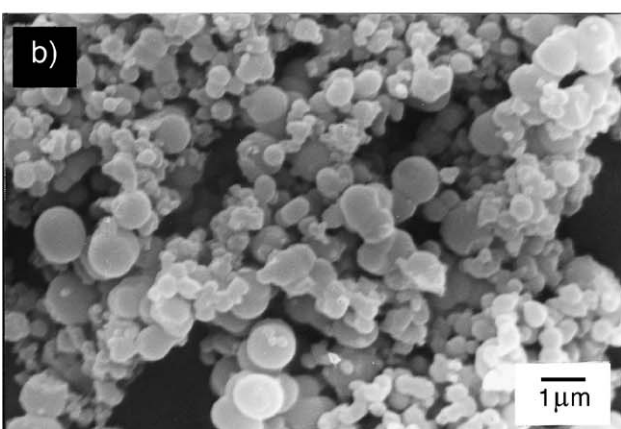


Fig. 5. Powder XRD patterns of the samples calcined at 750 °C for different soaking times, after pre-fired at 750 °C for 2 h ( $\blacktriangledown=MgO$ ;  $\spadesuit=Nb_2O_5$ ;  $\spadesuit=MgNb_2O_6$ ).





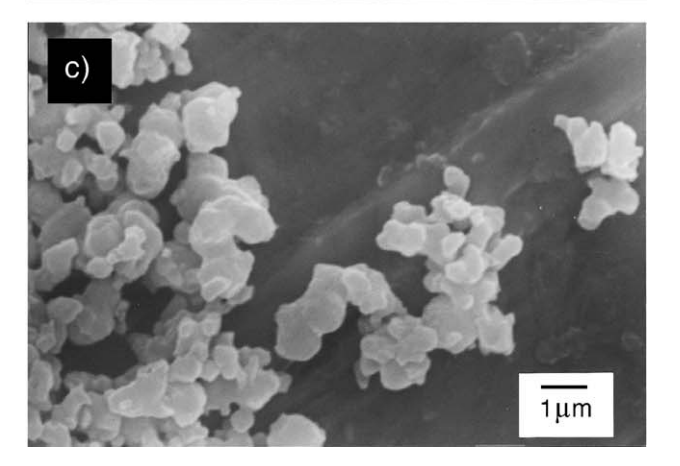
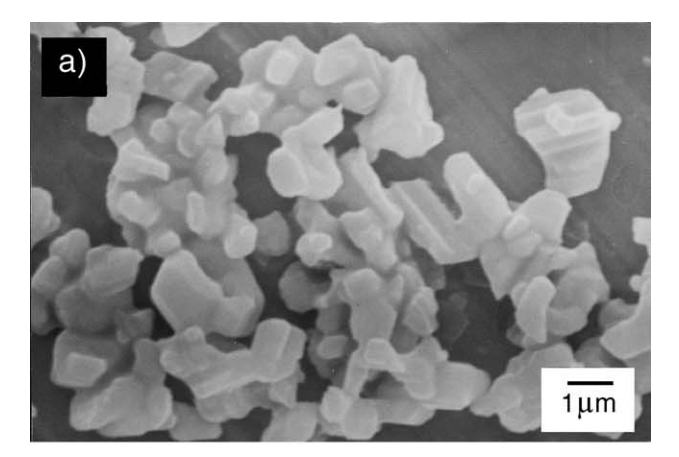
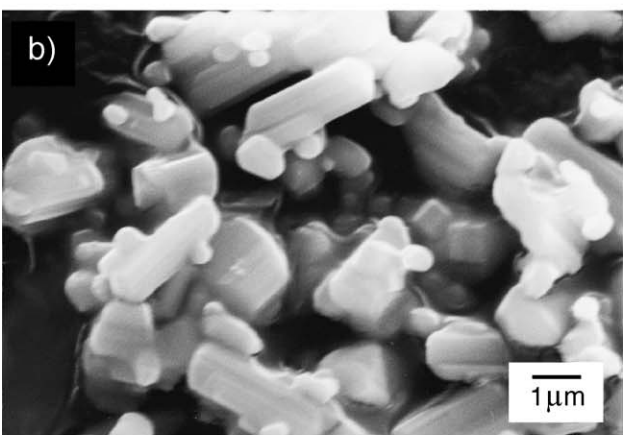


Fig. 6. SEM micrographs of the powders calcined at: (a) 750  $^{\circ}$ C, (b) 900  $^{\circ}$ C, and (c) 1000  $^{\circ}$ C, for 2 h.

At the temperature range of 600-800 °C (before Mg<sub>0.66</sub> Nb<sub>11.33</sub>O<sub>29</sub> was formed), the yield of MgNb<sub>2</sub>O<sub>6</sub> phase was maximum at 750 °C but the second phases of MgO and Nb<sub>2</sub>O<sub>5</sub> could not be completely eliminated. This could be attributed to the poor reactivity of magnesium and niobium species [9]. In order to improve the reactivity of both constituents, the pre-fired powders (750 °C 2 h) were subsequently ground in an agate mortar and recalcined at 750 °C for different soaking times (Fig. 5). Saha et al. [8] have also reported that their attempts to prepare solid-state





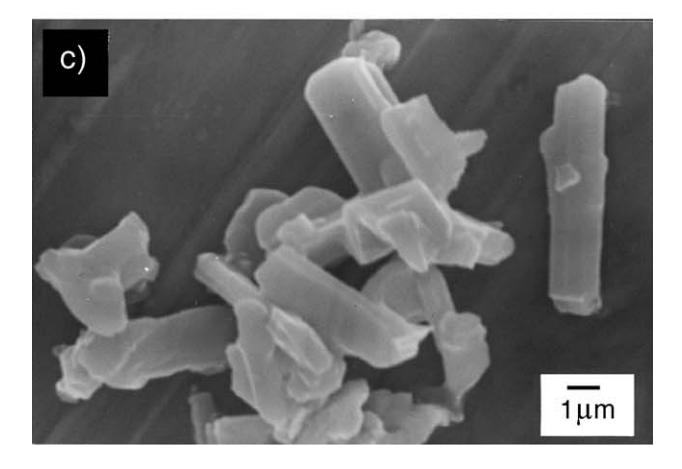


Fig. 7. SEM micrographs of the powders calcined at: (a) 1100  $^{\circ}$ C, (b) 1200  $^{\circ}$ C, and (c) 1300  $^{\circ}$ C, for 2 h.

derived MgNb<sub>2</sub>O<sub>6</sub> via this approach were successful. From Fig. 5, it is clear that the intensity of the columbite peaks ( $\blacklozenge$ ) was further enhanced when the soaking times of the recalcination process was extended to 5 h and then to 10 h at the expense of MgO and Nb<sub>2</sub>O<sub>5</sub> phases. An essentially monophasic MgNb<sub>2</sub>O<sub>6</sub> of columbite structure was obtained when the calcination time was extended to 13 h. This was apparently a consequence of the enhancement in crystallinity of the columbite phase with increasing degree of mixing and soaking time.

The powder morphology, as a function of calcination temperature, is given by the SEM micrographs (Figs. 6 and 7). The particles calcined at lower temperatures (750 to 1000 °C) had almost the same morphology (Fig. 6). In general, the particles are highly agglomerated (lumpy) and irregular in shape, with a substantial variation in particle size  $(0.1-1.2 \mu m)$ . However, at higher calcination temperatures (1100 to 1300 °C), powders obtained by the oxalate route have shown very interesting morphologies (Fig. 7). For the calcination temperature of 1100 °C (Fig. 7(a)), powders showed two distinctly different morphologies, acicular and lumpy. It should be noted that the morphology of the lumpy particles is very similar to that of MgNb<sub>2</sub>O<sub>6</sub> powder (Fig. 6(a)). There is no obvious interpretation of the difference between the SEM image of 1000 °C and that of 1100 °C, although it is likely to correspond to a phase transition observed in the XRD pattern at  $2\theta \sim 25-26^{\circ}$ ,  $32^{\circ}$  and  $34^{\circ}$ . Comparing the powder morphologies obtained at 1100 °C to those at 1200 °C (Fig. 7(b)) and 1300 °C (Fig. 7(c)), one can conclude that the length and concentration of acicular particles increased with increasing calcination temperature. Because Mg<sub>0.66</sub>Nb<sub>11.33</sub>O<sub>29</sub> phase was observed in XRD for powders calcined above 900 °C (Fig. 4), depending on calcination temperature, it is likely that these lumpy and acicular morphologies may be corresponded to the MgNb<sub>2</sub>O<sub>6</sub> and Mg<sub>0.66</sub>Nb<sub>11.33</sub>O<sub>29</sub> phases, respectively.

#### 4. Conclusions

An oxalate synthetic route for magnesium niobate (MgNb<sub>2</sub>O<sub>6</sub>) nanopowders with size ranging from 100 to 300 nm has been developed. Single-phase of MgNb<sub>2</sub>O<sub>6</sub> fine powders was obtained at 750 °C with grinding and recalcination for 13 h. A considerable decrease in the processing temperature has been obtained in comparison to processes, which involve powder mixing and solid-state reactive firing at higher temperatures.

#### Acknowledgements

The authors would like to acknowledge the Thailand Research Fund (TRF) for the financial support. Thanks are also due to Mr. S. Chaisupun for the XRD assistance and the Graduate School, Chiang Mai University, Thailand for the support.

- [1] G.H. Haertling, J. Am. Ceram. Soc. 82 (1999) 797.
- [2] L.E. Cross, Mater. Chem. Phys. 43 (1996) 108.
- [3] T.R. Shrout, A. Halliyal, Am. Ceram. Soc. Bull. 66 (1987) 704.
- [4] M. Lejeune, J.P. Boilot, Ceram. Int. 8 (1982) 99.
- [5] M. Dambekalne, I. Brante, A. Sternberg, Ferroelectrics 90 (1989) 1.
- [6] K. Singh, S.A. Band, Ferroelectrics 175 (1996) 193.

- [7] S.L. Swartz, T.R. Shrout, Mater. Res. Bull. 17 (1982) 1245.
- [8] D. Saha, A. Sen, H.S. Maiti, J. Mater. Sci. Lett. 13 (1994) 723.
- [9] S. Ananta, R. Brydson, N.W. Thomas, J. Eur. Ceram. Soc. 19 (1999) 355.
- [10] K. Sreedhar, A. Mitra, Mater. Res. Bull. 32 (1997) 1643.
- [11] Y.S. Hong, H.B. Park, S.J. Kim, J. Eur. Ceram. Soc. 18 (1998) 613.
- [12] E.R. Carmargo, E. Longo, D.R. Leite, J. Sol-Gel Sci. Technol. 17 (2000) 111.
- [13] N.K. Kim, Mater. Lett. 32 (1997) 127.
- [14] L.B. Kong, J. Ma, H. Huang, R.F. Zhang, J. Alloys Compd. 340 (2002) L1.
- [15] Y. Yu, C. Feng, C. Li, Y. Yang, W. Yao, H. Yan, Mater. Lett. 51 (2001) 490.



### Available online at www.sciencedirect.com

SCIENCE ODIRECT®

Current Applied Physics 4 (2004) 186-188

Current
Applied
Physics
Physics, Chemistry and Materials Science

www.elsevier.com/locate/cap

## The phase formation of lead titanate powders prepared by solid-state reaction

A. Udomporn, S. Ananta \*

Department of Physics, Faculty of Science, Chiang Mai University, Chiang Mai 50200, Thailand

#### **Abstract**

The phase formation of ultrafine lead titanate powders prepared via a rapid vibro-milling technique has been investigated by thermal analysis and X-ray diffraction. The results showed that single-phase PbTiO<sub>3</sub> (PT) nanopowders were successfully obtained for a calcination condition of 550 °C for 4 h with heating/cooling rates of 20 °C/min. The increased firing temperature was found to play a significant role in the formation of the perovskite phase. SEM results showed that the platelet morphology PT particles have a size of around 75–385 nm.

© 2003 Published by Elsevier B.V.

PACS: 77.84.Dy; 81.07.Wx

Keywords: Lead titanate; Perovskite; Nanopowders; Phase development

#### 1. Introduction

Lead titanate (PbTiO<sub>3</sub>; PT) has a tetragonal structure at room temperature and transforms to cubic at around 490 °C. It is an important end member of the lead zirconate titanate (PZT) series and has been extensively investigated because of its useful ferroelectric, pyroelectric and piezoelectric properties [1-3]. Because of these important properties, there has been a great deal of interest in the preparation of pure PT powders as well as in the sintering and electrical properties of PT-based ceramics [4-6]. In order to improve the sintering behaviour of this material, a crucial focus of powder synthesis in recent years has been the formation of uniformly sized, single morphology particulates ranging from nanometer to micron sized. The main hindrance to the commercial exploitation of conventional solid-state derived PT powders arises from processing difficulties, concerned with the high volatility of lead oxide and the formation of pyrochlore phases [7,8]. Therefore, in the present work, the potential of a vibro-milling technique as a significant time-saving method to obtain single-

#### 2. Experimental

PbTiO<sub>3</sub> was synthesised by the solid-state reaction of appropriate amounts of reagent grade lead oxide, PbO and titanium oxide, TiO<sub>2</sub> (Fluka, >99% purity). The two oxide powders exhibited an average particle size in the range of 3.0–5.0 μm. The methods of mixing, drying, grinding, firing and sieving of the products were similar to those employed in the preparation of the other perovskite materials, as described previously [9,10]. A McCrone vibro-milling technique was employed in order to combine mixing capability with a significant time-saving (only 30 min instead of 24 h, as required in conventional ball-milling [11]). The reactions of the uncalcined PT powders taking place during heat treatment were investigated by differential thermal analysis (DTA; NETZSCH-Gerätebau GmbH Thermal Analysis STA 409) using a heating rate of 10 °C/min in air from room temperature up to 1000 °C. Calcined powders were subsequently examined by room temperature Xray diffraction (XRD; Philips PW 1729 diffractometer) using  $Cu K_{\alpha}$  radiation to identify the phases formed and optimum calcination conditions for the formation of PT powder. Powder morphologies and grain sizes were

phase lead titanate powders, at low temperature and with small particles was examined.

<sup>\*</sup> Corresponding author. Tel.: +66-53-943376; fax: +66-53-357512. E-mail address: supon@chiangmai.ac.th (S. Ananta).

directly imaged using scanning electron microscopy (SEM; JEOL JSM-840A). EDX spectra were quantified with the virtual standards peaks supplied with the Oxford Instruments eXL software.

#### 3. Results and discussion

The DTA curve recorded at a heating rate of 10 °C/ min in air for an equimolar mixture of lead oxide and titanium oxide is shown in Fig. 1. Three exothermic peaks are observed in the approximate range from 280 to 340 °C, 360 to 450 °C and 480 to 680 °C. The first exothermic peak is believed to relate to the elimination of organic residuals from the rubber lining contamination during milling. However, it is to be noted that there is no obvious interpretation of the peaks after 340 °C, although it is likely to correspond to a phase transition reported by a number of workers [12–14]. To study the effect of heat treatment temperature on the perovskite phase formation, the precursor powders were calcined between 400 and 600 °C for 4 h. Room temperature Xray diffraction revealed that the uncalcined powder and the powder calcined at 400 °C contained only the precursors PbO and TiO<sub>2</sub> (Fig. 2), indicating that no reaction was triggered during the vibro-milling or low firing processes. The peaks of the nanosized lead deficient phase, PbTi<sub>3</sub>O<sub>7</sub> (**a**) earlier reported by many researchers [13,14] have been found at 450 °C, which is associated with the second DTA exothermic effect in Fig. 1. The identification of this pyrochlore phase suggests phase segregation or stoichiometric deviation during synthesis. However, at higher calcination temperature, this pyrochlore phase is converted to the perovskite phase. It is seen that fine PT crystallites were developed in the powder at a calcination temperature as low as 500 °C. The results of the X-ray diffraction measurement support the DTA observation (Fig. 1) that PbTiO<sub>3</sub> is formed at approximately 480–680 °C. In

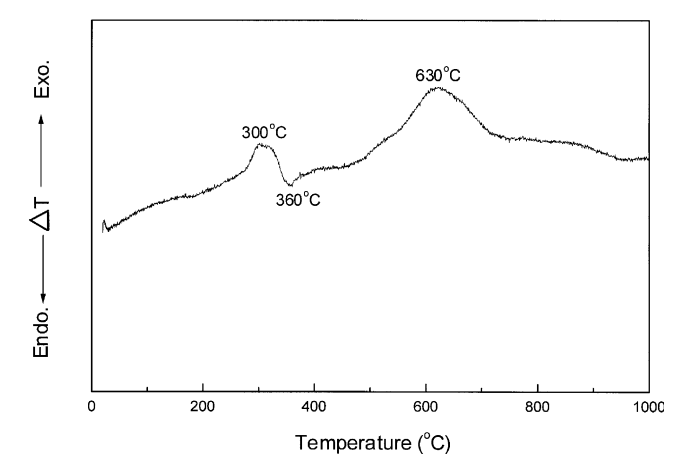


Fig. 1. A DTA curve for the mixture of PbO-TiO<sub>2</sub> powder.

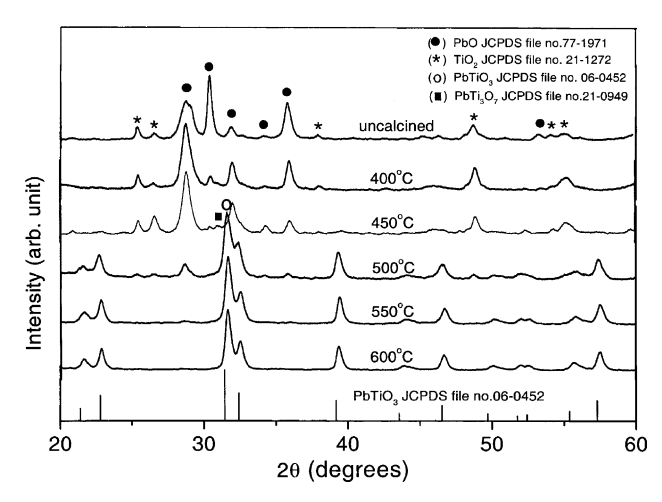


Fig. 2. XRD patterns of PT powder calcined at various temperatures for 4 h with heating/cooling rates of 20 °C/min.

general, the strongest reflections apparent in the majority of this XRD pattern indicate the formation of the lead titanate PbTiO<sub>3</sub> (O). These can be matched with JCPDS file number 06-0452 for the tetragonal phase, in space group P4/mmm with cell parameters a = 389.93pm and c = 415.32 pm. The well-known crystallographic-ferroelectric transition temperature of lead titanate at 490 °C [1] is within the temperature range of this DTA peak. Depending on the calcination conditions, at least three minor phases were identified, i.e. PbO (●), anatase-TiO<sub>2</sub> (\*), and PbTi<sub>3</sub>O<sub>7</sub> (■), which can be correlated with JCPDS files numbers 77-1971, 21-1272 and 21-0949, respectively. Unreacted PbO and TiO<sub>2</sub> phases from the original mixture were detected up to 500 °C, whereas a minor amount of PbTi<sub>3</sub>O<sub>7</sub> observed at 450 °C totally disappeared at higher temperatures. By increasing the calcination temperature from 450 to 600 °C, the yield of the tetragonal PT phase increases significantly until at 550 °C, a single-phase of PbTiO<sub>3</sub> is formed. It is to be noted that the large temperature decrease observed at a temperature greater than 850 °C in the DTA curve may be attributed to lead vaporization. In earlier works [7,8], synthesis of PT powder via conventional mixed-oxide methods is usually only possible at temperatures at which loss of volatile lead (~886 °C) becomes a problem. However, in the work reported here, it is to be noted that single-phase of PT powder was successfully obtained at a calcination temperature of 550 °C with a soaking time of 4 h. This is probably due to the effectiveness of vibro-milling and a carefully optimised reaction. An SEM micrograph of the calcined PbTiO<sub>3</sub> powder (550 °C for 4 h) is shown in Fig. 3. The platelet-morphology particles are agglomerated with a substantial variation in size ( $\sim$ 75–385 nm). EDX analysis using a 20 nm probe of a large number of particles of the calcined powder confirmed the parent composition to be PbTiO<sub>3</sub> (Fig. 4).

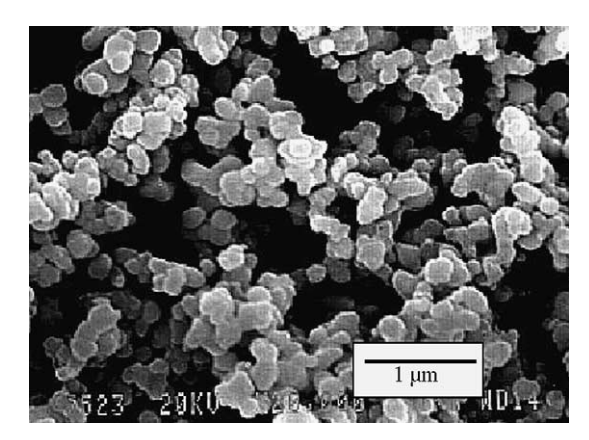


Fig. 3. SEM micrograph of the PT powders calcined at 550  $^{\circ}$ C for 4 h with heating/cooling rates of 20  $^{\circ}$ C/min.

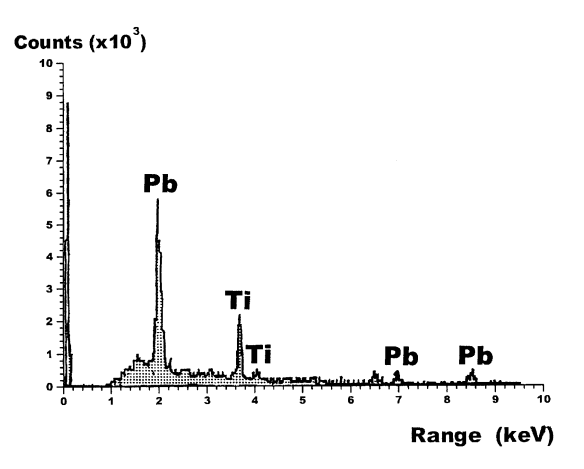


Fig. 4. EDX analysis of the PT powders calcined at 550  $^{\circ}\text{C}$  for 4 h with heating/cooling rates of 20  $^{\circ}\text{C/min}.$ 

#### 4. Summary and conclusion

Single-phase of lead titanate nanosized powders may be produced by the solid-state reaction via a rapid vibromilling technique. The optimum calcination condition for the formation of high purity PT phase was found to be 550 °C for 4 h with heating/cooling rates of 20 °C/min. The resulting PT powders consist of agglomerated nano-sized particles, which are plate-like in morphology. The preparative method involves the use of laboratory-grade precursors, low milling times, together with moderately low calcination temperatures and times. They represent significant time savings compared to synthetic procedures currently advocated, and required only relative impure laboratory-grade precursors.

#### Acknowledgement

This work was supported by the Thailand Research Fund (TRF).

- [1] B. Jaffe, W.R. Cook Jr., H. Jaffe, Piezoelectric Ceramics, Academic Press, New York, 1971.
- [2] K. Uchino, Piezoelectrics and Ultrasonic Applications, Kluwer Academic Publishers, Dordrecht, 1998.
- [3] G.H. Haertling, J. Am. Ceram. Soc. 82 (1999) 797.
- [4] L.B. Kong, W. Zhu, O.K. Tan, J. Mater. Sci. Lett. 19 (2002) 1963.
- [5] M.C. Gelabert, B.L. Gersten, R.E. Riman, J. Cryst. Growth 211 (2000) 497.
- [6] K.P. Chen, C. Li, X. Zhang, Y. Huang, Mater. Lett. 57 (2002) 20.
- [7] J. Tartaj, J.F. Fernandez, M.E. Villafuerte-Castrejon, Mater. Res. Bull. 36 (2001) 479.
- [8] J. Fang, J. Wang, L.M. Gan, S.C. Ng, Mater. Lett. 52 (2002) 304.
- [9] S. Ananta, N.W. Thomas, J. Eur. Ceram. Soc. 19 (1999) 155.
- [10] S. Ananta, R. Brydson, N.W. Thomas, J. Eur. Ceram. Soc. 20 (2000) 2315.
- [11] T.Y. Tien, W.G. Carlson, J. Am. Ceram. Soc. 45 (1962) 567.
- [12] C.G. Pillai, P.V. Ravindran, Thermochim. Acta 66 (1996) 109.
- [13] J. Tartaj, C. Moure, L. Lascano, P. Duran, Mater. Res. Bull. 36 (2001) 2301.
- [14] M. Calzada, M. Alguero, L. Pardo, J. Sol-Gel Sci. Tech. 13 (1998) 837.



Available online at www.sciencedirect.com

SCIENCE DIRECT

ORDINATION

OF THE COMMON C

Materials Letters 58 (2004) 1154-1159



# Effect of calcination condition on phase formation and particle size of lead titanate powders synthesized by the solid-state reaction

A. Udomporn, S. Ananta\*

Department of Physics, Faculty of Science, Chiang Mai University, Chiang Mai 50200, Thailand Received 13 March 2003; received in revised form 15 August 2003; accepted 20 August 2003

#### Abstract

A perovskite-like phase of lead titanate, PbTiO<sub>3</sub>, has been synthesized by a solid-state reaction via a rapid vibro-milling technique. Phase formation of the calcined powders has been investigated as a function of calcination temperature, soaking time and heating/cooling rates by DTA and X-ray diffraction (XRD) techniques. Moreover, morphology and particle size evolution have been determined via SEM technique, respectively. It has been found that single-phase PbTiO<sub>3</sub> powders were successfully obtained for calcination conditions of 550 °C for 4 h or 600 °C for 1 h with heating/cooling rates of 20 °C/min. Higher temperatures clearly favoured particle growth and the formation of large and hard agglomerates.

© 2003 Elsevier B.V. All rights reserved.

Keywords: Lead titanate; PT powder; Perovskite; Calcination; Phase formation; Powders, solid-state reaction

#### 1. Introduction

Lead titanate (PbTiO<sub>3</sub>; PT), which exhibits a perovskite structure and a high Curie temperature (~490 °C), is a common ferroelectric material with a high dielectric constant, large mechanical-quality factor (>1000) and large pyroelectric coefficient [1,2]. These characteristics make PT a promising candidate for high frequency and high temperature applications [2,3]. Lead titanate when combined with other oxides can form a series of solid solutions such as  $Pb(Zr_{1-x}, Ti_x)O_3$  (PZT),  $Pb(Mg_{1/3}Nb_{2/3})O_3$ -PbTiO<sub>3</sub> (PMNT) and Pb(Zn<sub>1/3</sub>Nb<sub>2/3</sub>)O<sub>3</sub>-PbTiO<sub>3</sub> (PZN-PT) [3-5]. These ferroelectrics are widely used in ultrasonic transducers, nonvolatile memories, microactuators, multilayer capacitors and electro-optic devices. Because of these important technological applications, there has been a great deal of interest in the preparation of pure PT powders as well as in the sintering and electrical properties of PT-based ceramics [2,6].

The stoichiometry of lead titanate is known to be an important factor for ensuring good electrical characteristics [3]. To obtain stoichiometric PT, different prepara-

tive methods have been introduced, such as sol-gel [7], co-precipitation [8], emulsion [9] or hydrothermal treatment [10], besides the conventional solid-state reaction of mixed oxides [11]. All these techniques are aimed at reducing the temperature of preparation of the compound even though they are more involved and complicated in approach than the solid-state reaction method. Moreover, high-purity PT powders are still not available in mass quantity and also very expensive. Therefore, in the present work, a modified mixed oxide method has been developed to resolve these problems. The overall aim of the work describe here is to refine the mixed oxide method further. The effect of calcination conditions (i.e. firing temperature, soaking time and heating/cooling rates) on the development of phase and particle size of lead titanate powders are investigated in this connection. The potentiality of a vibro-milling technique as a significant time-saving method to obtain single-phase lead titanate powders at low temperature and with small particles was also examined.

#### 2. Experimental procedure

Laboratory-grade purity oxides of lead oxide, PbO (JCPDS file number 77-1971) and titanium oxide, TiO<sub>2</sub>

<sup>\*</sup> Corresponding author. Tel.: +66-53-943376; fax: +66-53-357512. E-mail address: supon@chiangmai.ac.th (S. Ananta).

(anatase: JCPDS file number 21-1272) (Fluka, >99% purity) were used in this study. The two oxide powders exhibited an average particle size in the range of 3.0-5.0 μm. PbTiO<sub>3</sub> powder was synthesised by the solid-state reaction of these raw materials. The methods of mixing, drying, grinding, firing and sieving of the products were similar to those employed in the preparation of the perovskite-like Pb(Mg<sub>1/3</sub>Nb<sub>2/3</sub>)O<sub>3</sub>, Pb(Fe<sub>1/2</sub>Nb<sub>1/2</sub>)O<sub>3</sub> and La(Mg<sub>2/3</sub>Nb<sub>1/3</sub>)O<sub>3</sub>, as described previously [12,13]. Instead of employing a ball-milling procedure (ZrO2 media under acetone for 24 h Ref. [14]), use was made of a McCrone vibro-mill, milling for 30 min with corundum media in isopropyl alcohol (IPA). Although the use of IPA in place of acetone was dictated by the use of the McCrone mill, an associated benefit is the avoidance of unpleasant vapours associated with the use of acetone. Drying was carried out for 2 h, prior to sieving through a 100-µm mesh. Various calcination conditions, i.e. temperatures ranging from 400 to 800 °C, soaking times ranging from 0.5 to 4 h and heating/cooling rates ranging from 3 to 20 °C/min, were selected, in order to investigate the formation of lead titanate. The reactions of the uncalcined PT powders taking place during heat treatment were investigated by differential thermal analysis (DTA) (NETZSCH-Gerätebau Thermal Analysis STA 409) using a heating rate of 10 °C/min in air from room temperature up to 1000 °C. Calcined powders were subsequently examined by room temperature X-ray diffraction (XRD; Philips PW 1729 diffractometer) using CuK<sub>\alpha</sub> radiation to identify the phases formed and optimum calcination conditions for the formation of PT powder. Powder morphologies and grain sizes were directly imaged using scanning electron microscopy (SEM; JEOL JSM-840A).

#### 3. Results and discussion

DTA curve recorded at a heating rate of 10 °C/min in air for an equimolar mixture of lead oxide and titanium oxide is shown in Fig. 1. Three exothermic peaks are observed in the approximate range from 280 to 340, 360 to 450, and 480 to 680 °C. These temperatures have been obtained from the calibration of the sample thermocouple. The first exothermic peak is believed to relate to the elimination of organic residuals from the rubber lining contamination during milling. However, it is to be noted that there is no obvious interpretation of the peaks after 340 °C, although it is likely to correspond to a phase transition reported by a number of workers [15–17]. These data were used to define the ranges of temperatures (400–800 °C) for XRD investigation.

All calcined powders together with that of the starting powder mixtures were examined by XRD in order to investigate the phase development (Figs. 2-6). As shown in Fig. 2, for the uncalcined powder and the powder calcined at 400 °C, only X-ray peaks of precursors PbO and TiO2 are present, indicating that no reaction was yet triggered during the vibro-milling or low firing processes. The formation of lead deficient phase, PbTi<sub>3</sub>O<sub>7</sub> (■) earlier reported by many researchers [16,17] has been found at 450 °C, which is associated to the second DTA exothermic effect in Fig. 1. This pyrochlore (or a metastable intermediate) phase has a monoclinic structure with cell parameter a = 107.32 pm, b = 381.2 pm, c = 657.8 pm and  $\beta = 98.08^{\circ}$  (JCPDS file number 21-949) [18]. It is seen that fine PT crystallites were developed in the powder at a calcination temperature as low as 500 °C. The results of X-ray diffraction measurement supported the DTA observation (Fig. 1) that PbTiO<sub>3</sub> is formed at

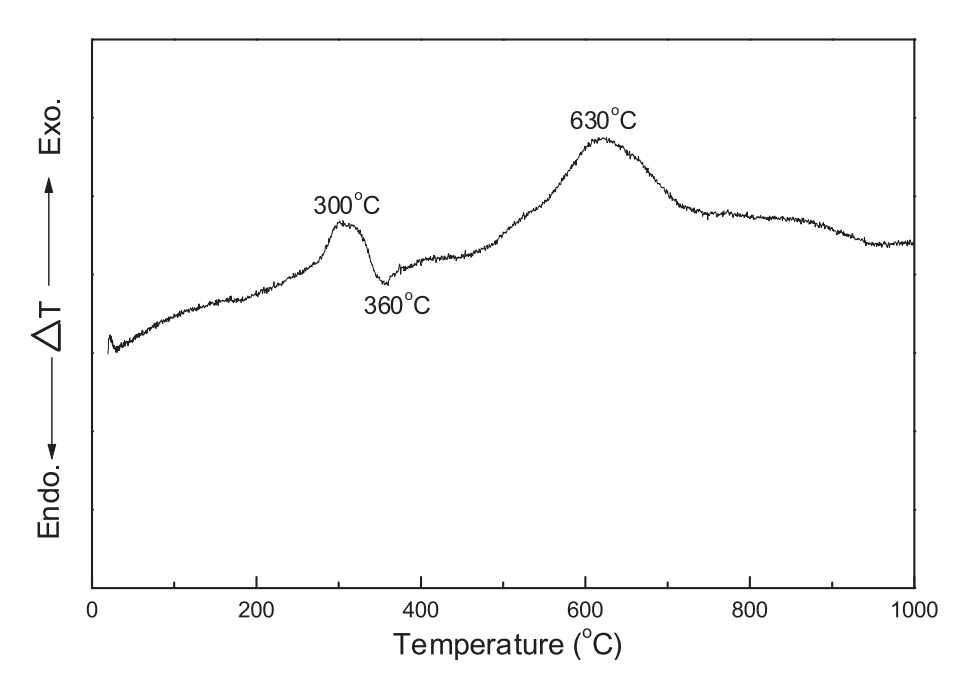


Fig. 1. A DTA curve for the mixture of PbO-TiO2 powder.

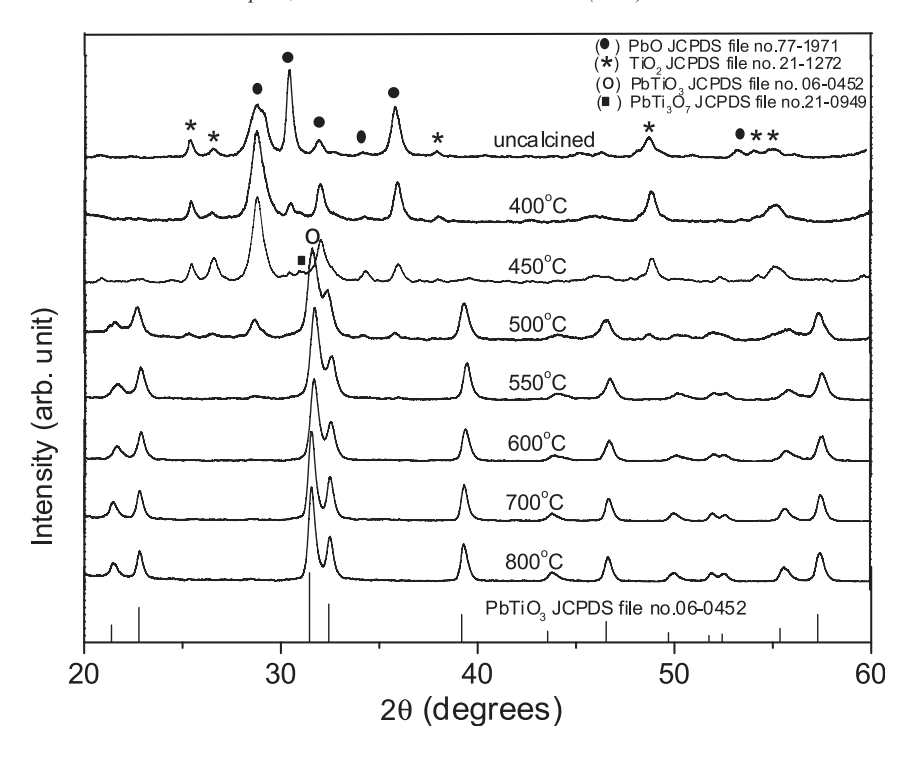


Fig. 2. XRD patterns of PT powder calcined at various temperatures for 1 h with heating/cooling rates of 10 °C/min.

approximately 480-680 °C. In general, the strongest reflections apparent in the majority of this XRD pattern indicate the formation of the lead titanate, PbTiO<sub>3</sub> (O). These can be matched with JCPDS file number 6-452 for the tetragonal phase, in space group P4/mmm with cell parameters a=389.93 pm and c=415.32 pm [19]. Depending on the calcination conditions, at least three minor phases were identified, i.e. PbO ( ), anatase-TiO<sub>2</sub> (\*) and PbTi<sub>3</sub>O<sub>7</sub> ( ), which can be correlated with

JCPDS files numbers 77-1971, 21-1272 and 21-949, respectively. Unreacted PbO and TiO<sub>2</sub> phases are detected from the original mixture up to 550 °C, whereas minor amount of PbTi<sub>3</sub>O<sub>7</sub> is observed at 450 °C and totally disappeared at higher temperature. By increasing the calcination temperature from 450 to 800 °C, the yield of the tetragonal PT phase increases significantly until at 600 °C, a single phase of PbTiO<sub>3</sub> is formed. This study also shows that crystalline tetragonal PT is the only

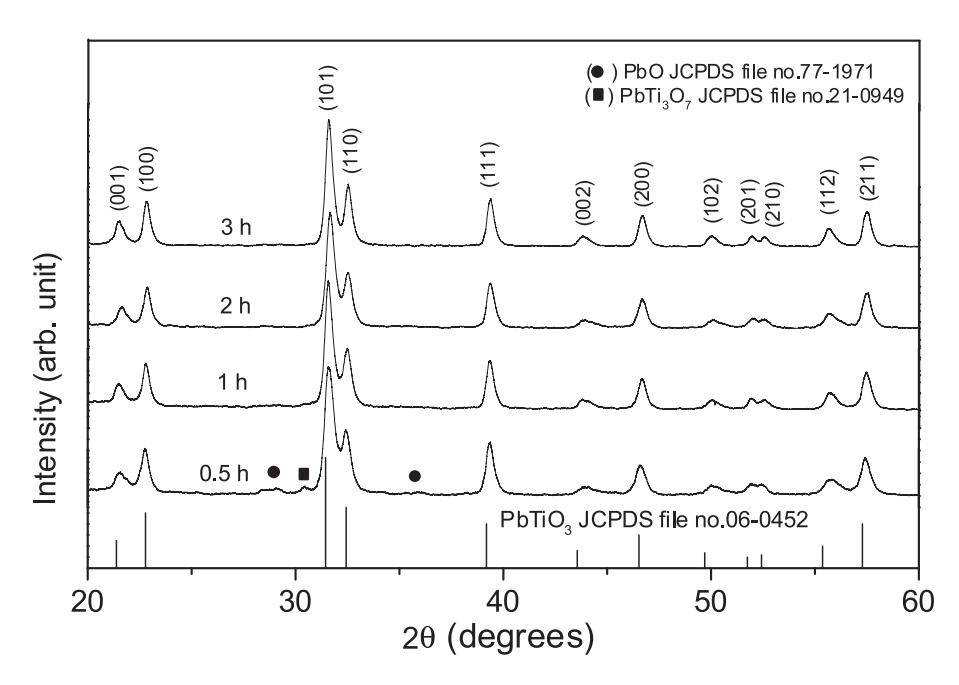


Fig. 3. XRD patterns of PT powder calcined at 600 °C with heating/cooling rates of 10 °C/min for various soaking times.

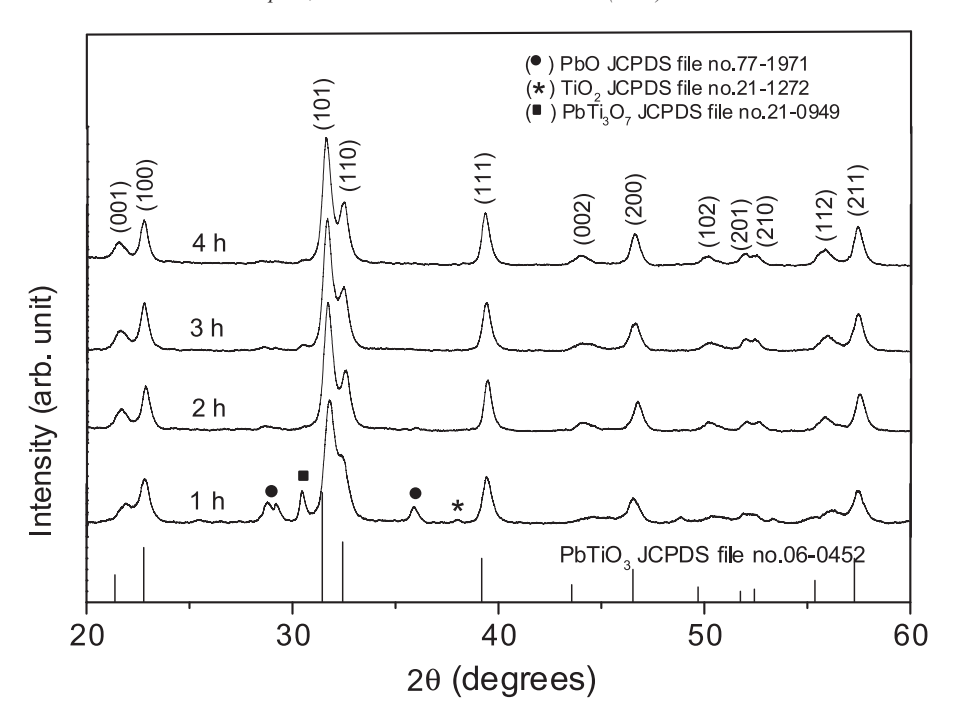


Fig. 4. XRD patterns of PT powder calcined at 550 °C with heating/cooling rates of 10 °C/min for various soaking times.

detectable phase in the powder, after calcination in the range 600-800 °C. It is to be noted that a large temperature decrease observed at temperature greater than 850 °C in the DTA curve may be attribute to the PbO volatilisation, in consistent with other works [12,15].

Having established the optimum calcination temperature, alternative soaking times of 0.5, 1, 3 and 4 h with constant heating/cooling rates of 10 °C/min were applied at 600 and 550 °C, as shown in Figs. 3 and 4, respec-

tively. In Fig. 3, the single phase of perovskite PT (yield of 100% within the limitations of the XRD technique) was found to be possible only in powders, calcined at 600 °C with soaking time of 1 h or more. The appearance of PbO and PbTi<sub>3</sub>O<sub>7</sub> phases indicated that full crystallization have not occurred at relatively shorter calcination times. However, in the work reported here, it is to be noted that single phase of PT powder was also successfully obtained for a calcination temperature of 550 °C with soaking time

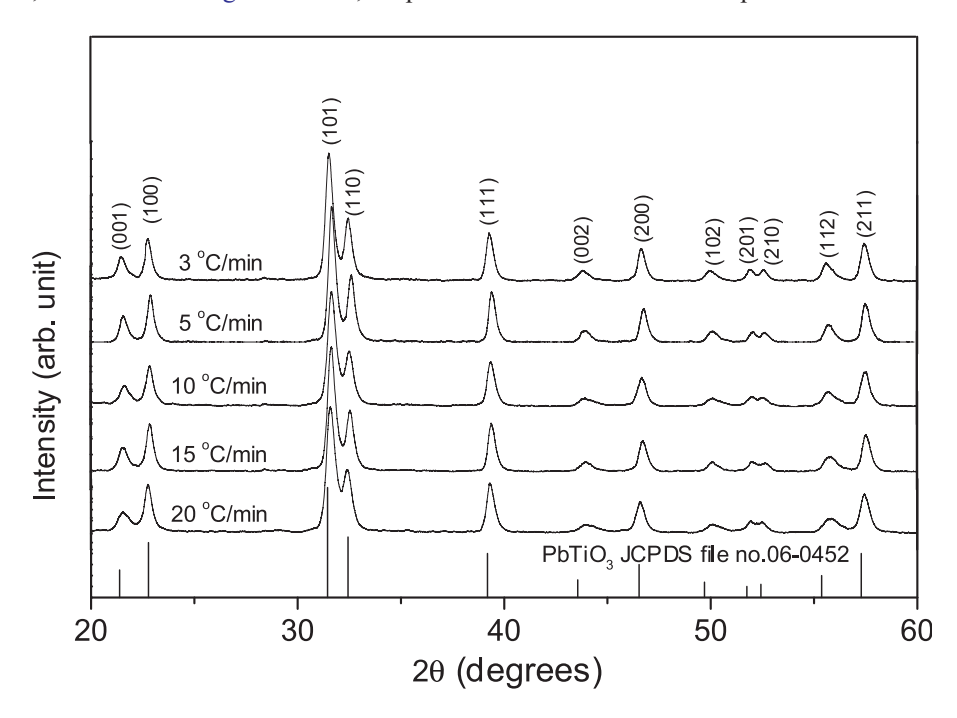


Fig. 5. XRD patterns of PT powder calcined at 600 °C for 1 h with various heating/cooling rates.

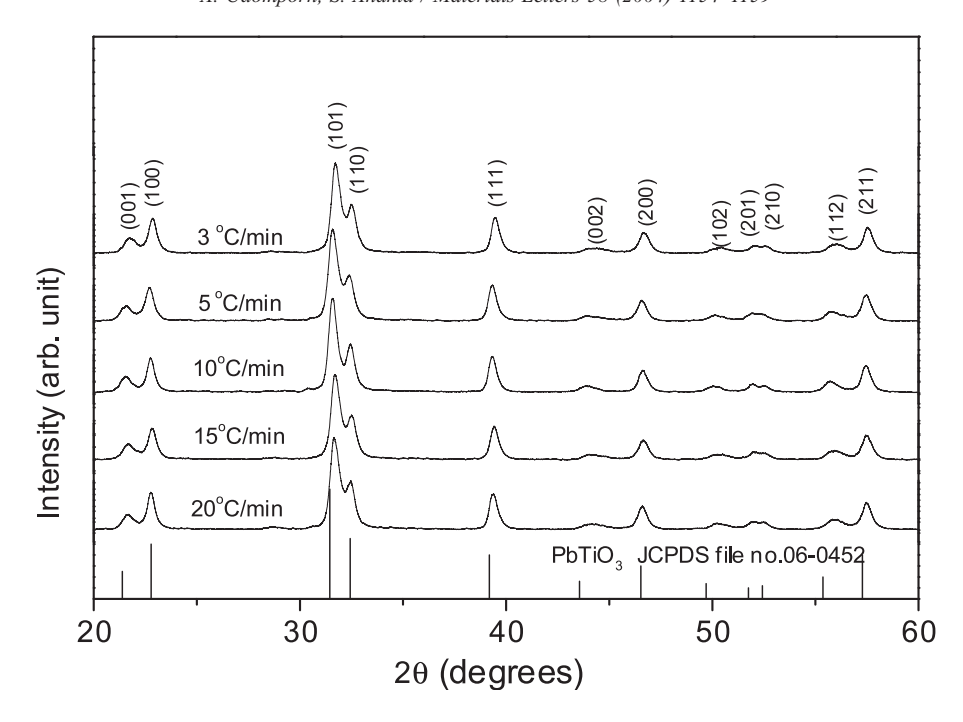


Fig. 6. XRD patterns of PT powder calcined at 550 °C for 4 h with various heating/cooling rates.

of 4 h applied (Fig. 4). This is probably due to the effectiveness of vibro-milling and a carefully optimised reaction. The observation that the soaking time effect may

also play an important role in obtaining a single-phase perovskite product is also consistent with other similar systems [12,13].

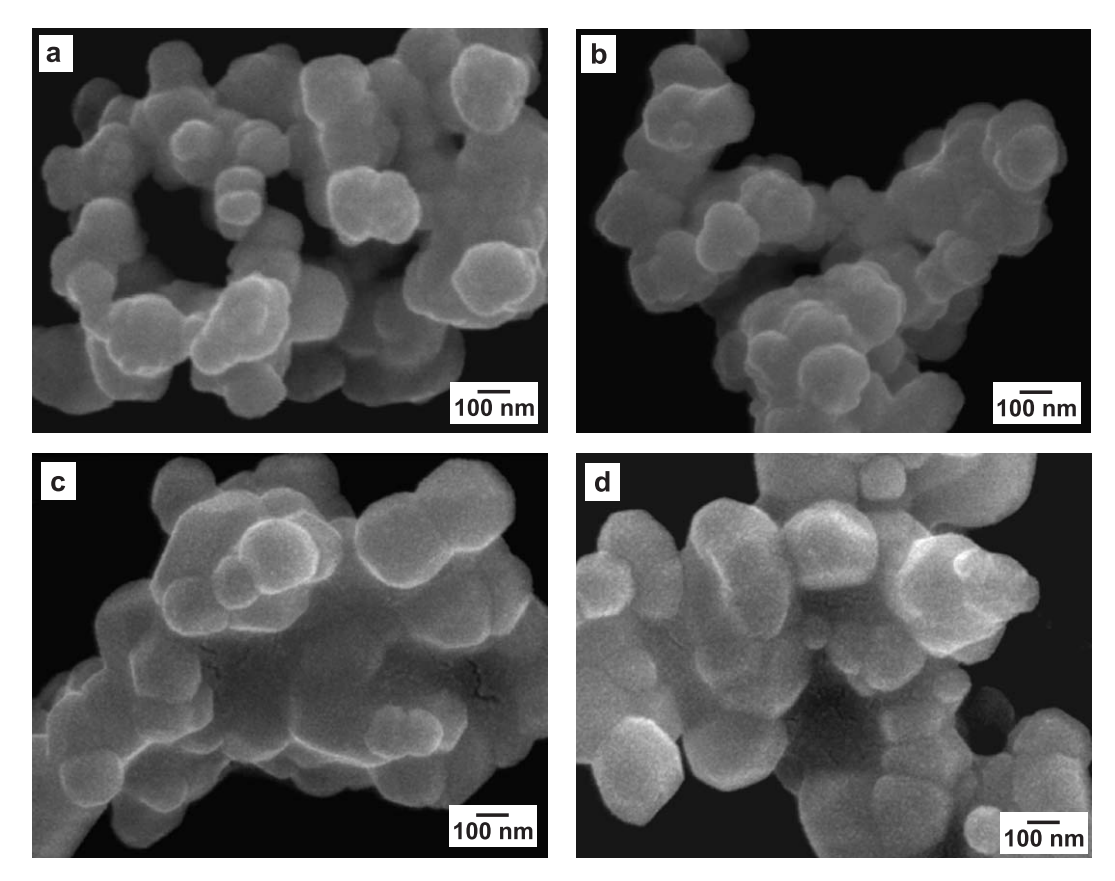


Fig. 7. SEM micrographs of the PT powders calcined at (a)  $600~^{\circ}$ C/1 h, (b)  $600~^{\circ}$ C/4 h, (c)  $700~^{\circ}$ C/1 h and (d)  $800~^{\circ}$ C/1 h, with heating/cooling rates of  $20~^{\circ}$ C/min.

Apart from the calcination temperature and soaking time, the effect of heating/cooling rates on the formation behaviour of PT was also investigated. Five heating/cooling rates (3, 5, 10, 15 and 20 °C/min) were selected for calcination conditions of 550 °C/4 h (Fig. 5 and 600 °C/1 h (Fig. 6). In this connection, it is shown that the yield of PT phase did not vary significantly with heating/cooling rates, indicating that fast heating/cooling rates can lead to full crystallization of PT phase without time for the formation of pyrochlore phase or lead vaporization. The observation that faster heating/cooling rates are required for lead-based ferroelectrics is also consistent with other investigators [20,21].

Based on the DTA and XRD data, it may be concluded that, over a wide range of calcination conditions, single-phase PbTiO<sub>3</sub> cannot be straightforwardly formed via a solid-state mixed oxide synthetic route. The experimental work carried out here suggests that the optimal calcination conditions for single-phase PbTiO<sub>3</sub> is 600 °C for 1 h or 550 °C for 4 h with heating/cooling rates as fast as 20 °C/min, which is closed to that of Pillai and Ravindran [15] (  $\sim$  600 °C for 2 h). However, the optimal firing temperatures found here are significantly lower than that reported by Jaffe et al. [11] and Shirane et al. [22] (>1000 °C).

Fig. 7 shows the morphological evolution of all samples as a function of the calcination conditions. In general, the particles are agglomerated and basically irregular in shape, with a substantial variation in particle sizes. The result indicates that degree of agglomeration tends to increase with calcination temperature and soaking time. However, the smallest particle size (estimated from SEM micrographs to be  $\sim 160$  nm) and the morphology of the calcined powders are almost the same. It is also of interest to point out that no evidence has been obtained for the existence of the plate-like morphology as that of the hydrothermally derived PT powders [23].

#### 4. Conclusions

The effect of calcination conditions on phase formation and particle size of perovskite lead titanate synthesized by the solid-state reaction via a rapid vibro-milling technique was investigated. This work demonstrated that single phase of lead titanate powders may be produced via this technique by employing a calcination temperature of 550 °C for 4 h or 600 °C for 1 h, with heating/cooling rates

of 20 °C/min. The resulting PT powders consist of a variety of agglomerated particle sizes, depending on calcination conditions.

#### Acknowledgements

This work was supported by the Thailand Research Fund (TRF). One of the authors (A.U.) wishes to thank the Mahasarakarm University and the Graduated School, Chiang Mai University, Thailand, for the support.

- B. Jaffe, W.R. Cook Jr., H. Jaffe, Piezoelectric Ceramics, Academic Press, New York, 1971.
- [2] K. Uchino, Piezoelectrics and Ultrasonic Applications, Kluwer, Deventer, 1998.
- [3] G.H. Haertling, J. Am. Ceram. Soc. 82 (1999) 797.
- [4] A.B. Panda, P. Pramanik, Mater. Lett. 56 (2002) 435.
- [5] M.L. Mulvihill, L.E. Cross, K. Uchino, J. Am. Ceram. Soc. 78 (1995) 3345.
- [6] K.P. Chen, C. Li, X. Zhang, Y. Huang, Mater. Lett. 57 (2002) 20.
- [7] J. Tartaj, J.F. Fernandez, E. Villafuerte-Castrejon, Mater. Res. Bull. 36 (2001) 479.
- [8] J. Fang, J. Wang, L.M. Gan, S.C. Ng, Mater. Lett. 52 (2002) 304.
- [9] J. Fang, J. Wang, S.C. Ng, C.H. Chew, L.M. Gan, J. Mater. Sci. 34 (1999) 1943.
- [10] M.C. Gelabert, B.L. Gersten, R.E. Riman, J. Cryst. Growth 211 (2000) 497.
- [11] X. Zeng, Y. Liu, X. Wang, W. Yin, L. Wang, H. Guo, Mater. Chem. Phys. 77 (2002) 209.
- [12] S. Ananta, N.W. Thomas, J. Eur. Ceram. Soc. 19 (1999) 155.
- [13] S. Ananta, R. Brydson, N.W. Thomas, J. Eur. Ceram. Soc. 20 (2000) 2315
- [14] T.Y. Tien, W.G. Carlson, J. Am. Ceram. Soc. 45 (1962) 567.
- [15] C.G. Pillai, P.V. Ravindran, Thermochim. Acta 66 (1996) 109.
- [16] J. Tartaj, C. Moure, L. Lascano, P. Duran, Mater. Res. Bull. 36 (2001) 2301.
- [17] M.L. Calzada, M. Alguero, L. Pardo, J. Sol-Gel Sci. Technol. 13 (1998) 837.
- [18] JCPDS-ICDD Card No. 21-949. International Centre for Diffraction Data, Newtown Square, PA, 2001.
- [19] JCPDS-ICDD Card No. 6-452. International Centre for Diffraction Data, Newtown Square, PA, 2002.
- [20] C.E. Baumgartner, J. Am. Ceram. Soc. 71 (1988) C-350.
- [21] J. Ryu, J.J. Choi, H.E. Kim, J. Am. Ceram. Soc. 84 (2001) 902.
- [22] G. Shirane, S. Hoshino, K. Suzuki, Phys. Rev. 80 (1950) 1105.
- [23] C.R. Peterson, E.B. Slamovich, J. Am. Ceram. Soc. 82 (1999) 1702.







materials letters

Materials Letters 60 (2006) 1447-1452

www.elsevier.com/locate/matlet

## Effect of vibro-milling time on phase formation and particle size of lead titanate nanopowders

R. Wongmaneerung, R. Yimnirun, S. Ananta \*

Department of Physics, Faculty of Science, Chiang Mai University, Chiang Mai 50200, Thailand

Received 5 August 2005; accepted 14 November 2005

Available online 1 December 2005

#### Abstract

A perovskite-like phase of lead titanate,  $PbTiO_3$ , nanopowder was synthesized by a solid-state reaction via a rapid vibro-milling technique. The effect of milling time on the phase formation and particle size of  $PbTiO_3$  powder was investigated. Powder samples were characterized using TG-DTA, XRD, SEM and laser diffraction techniques. It was found that an average particle size of 17 nm was achieved at 25 h of vibro-milling after which a higher degree of particle agglomeration was observed on continuation of milling to 35 h. In addition, by employing an appropriate choice of the milling time, a narrow particle size distribution curve was also observed. © 2005 Elsevier B.V. All rights reserved.

Keywords: Lead titanate; Milling; Nanopowders; Phase formation; Particle size

#### 1. Introduction

Lead titanate, PbTiO<sub>3</sub> (PT), is one of the ferroelectric materials which exhibits a perovskite structure. It has a Curie temperature ~490 °C. The unique properties of the PT, i.e. the high transition temperature, pyroelectric coefficient and spontaneous polarization, make it useful for high frequency and high temperature applications in electronic devices [1,2]. When combined with other oxides, lead titanate can form a series of solid solutions such as  $Pb(Zr_{1-x},Ti_x)O_3$  (PZT),  $Pb(Mg_{1/3}Nb_{2/3})$  $O_3$ -PbTi $O_3$  (PMNT) and Pb( $Zn_{1/3}Nb_{2/3}$ ) $O_3$ -PbTi $O_3$  (PZN-PT) [2-4]. These ferroelectric alloys are widely used in ultrasonic transducers, nonvolatile memories, microactuators, multilayer capacitors and electro-optic devices [1,2]. To fabricate them, a fine powder of perovskite phase with a minimal degree of particle agglomeration is needed as the starting material in order to achieve a dense and uniform microstructure at a given sintering temperature. In order to improve the sintering behaviour of PT ceramics, a crucial focus of powder synthesis in recent years has been the formation of uniform-sized, single

morphology particulates ranging in size from nanometer to micrometers [5-7].

The development of a method to produce nanopowders of precise stoichiometry and desired properties is complex, depending on a number of variables such as nature and purity of starting materials, processing history, temperature, etc. To obtain nanosized PT powders, many investigations have focused on several chemistry-based preparation routes, such as sol-gel [5], co-precipitation [6], hydrothermal reaction [7], besides the more conventional solid-state reaction of mixed oxides [8,9]. All these techniques are aimed at reducing the particle size and temperature of preparation of the compound even though they are more involved and complicated in approach than the solid-state reaction. Moreover, high-purity PT nanopowders are still not available in bulk quantity and also very expensive. The advantage of using mechanical milling for preparation of nanosized powders lies in its ability to produce mass quantities of powders in the solid state using simple equipment and low cost starting precursors [8,9]. Although some research has been done in the preparation of PT powders via a vibro-milling technique [10,11], to our knowledge a systematic study regarding the influence of milling time on the preparation of PT powders has not yet been reported.

<sup>\*</sup> Corresponding author. Tel.: +66 53 943367; fax: +66 53 357512. *E-mail address*: supon@chiangmai.ac.th (S. Ananta).